CLONING, EXPRESSION AND PURIFICATION OF *MYCOBACTERIUM TUBERCULOSIS RV0309* ADHESIN PROTEIN

by

NIKITA DEYAL

Submitted in fulfilment of the requirements for the degree of

Masters in Medical Science (Medical Microbiology)

Discipline of Medical Microbiology

School of Laboratory Medicine and Medical Sciences

College of Health Sciences

University of KwaZulu-Natal

South Africa

2023

As the candidate's supervisor I have/~~have not~~ approved this thesis for submission.

Signed: [redacted] Name: Manormoney Pillay Date: 5 March 2024

DECLARATION

I, Nikita Deyal, declare that

(i) The research reported in this dissertation, except where otherwise indicated, is my original work.

(ii) This dissertation has not been submitted for any degree or examination at any other university.

(iii) This dissertation does not contain other persons' data, pictures, graphs or other information, unless specifically acknowledged as being sourced from other persons.

(iv) This dissertation does not contain other persons' writing, unless specifically acknowledged as being sourced from other researchers. Where other written sources have been quoted, then:

a) their words have been re-written but the general information attributed to them has been referenced;

b) where their exact words have been used, their writing has been placed inside quotation marks, and referenced.

(v) Where I have reproduced a publication of which I am an author, co-author or editor, I have indicated in detail which part of the publication was actually written by myself alone and have fully referenced such publications.

(vi) This dissertation does not contain text, graphics or tables copied and pasted from the Internet, unless specifically acknowledged, and the source being detailed in the dissertation and in the References sections.

Candidate:

Signed:  Name: Ms. Nikita Deyal Date: 04/12/23

As the candidate's supervisor, I have approved this dissertation for submission.

Signed:  Name: Prof. Manormoney Pillay Date: 5 March 2024

PRESENTATIONS

Oral Poster presentation

School of Laboratory Medicine and Medical Sciences Research Day, Durban, South Africa.

4th of October 2023

CLONING, EXPRESSION AND PURIFICATION OF *MYCOBACTERIUM TUBERCULOSIS RV0309* ADHESIN PROTEIN

Deyal, N.*, Pillay, K.*, Pillay, M.*

*Discipline of Medical Microbiology, School of Laboratory Medicine and Medical Sciences, College of Health Sciences, University of KwaZulu-Natal, 1st floor Doris Duke Medical Research Institute, Congella, Private Bag 7, Durban 4013, South Africa.

ACKNOWLEDGEMENTS

I would like to express my heartfelt gratitude to my remarkable supervisor Prof. Manormoney Pillay. Your guidance, patience, unwavering support and expertise were invaluable throughout my postgraduate journey. You have provided me with great insights, constructive feedback and care that every student should have the opportunity to receive. I am very grateful for the financial assistance you graciously provided through bursary awards and your support in various funding applications throughout my postgraduate years.

I extend my sincere appreciation to my lab supervisor and mentor Ms. Koobashnee Pillay. Your mentorship, dedication, thorough work ethic and encouragement has made such a significant impact on me. A sense of calm would always overcome me when I would see your office light on, just knowing you were around helped with any research anxiety I may have had. I will always wish the best for you and will miss our incubation chats about an array of interesting subjects. I know you will make everyone you know proud.

I also want to extend great thanks to Mr. Rivesh Maharajh for his valuable input and positive critique with respect to my work. I learnt so much from your advice, tips and motivation. Our lab chats were always entertaining and I felt at ease knowing you were also around to clarify any questions I had.

To the researchers who played a key role in assisting me with my troubles faced with project, Prof. Theresa Coetzer, Dr. Sibusiso Senzani, Dr. Raymond Hewer, Prof. Balakrishna Pillay and Dr. Sanjiv Kumar. Thank you for affording me your time, effort and expert input.

A huge thank you to Dr Ajit Kumar, your kindness, willingness to always help and share your exceptional knowledge along with research items meant so much. I am so grateful for your selfless support and have learnt so much from you. May you be blessed for all the good work that you do.

To Dr. Ofentse Pooe and his team, Lindiwe Zuma and Nothando Gasa, thank you for your great assistance and for going out of your way to help me overcome my challenges. I appreciate all your assistance with purification and PEPPI-MS sequencing preparation. I wish you success on your journeys.

To the Medical Microbiology family (in no particular order): Zareena Solwa, Inga Elson, Kiara Ramchunder, Shinese Ashokcoomar, Tarien Jael Naidoo, Johannes Mthembu, Nonhle Mkhwanazi, Tashnika Gajoo, Kynesha Moopanar, Nosipho Ndlovu, Asanda Nyide, Teniel Ramkhelawan, Dr Refilwe Molatlhegi, our support staff and other colleagues. Thank you for

creating such a positive and healthy work space. It was delightful interacting with all of you. I wish you all the best in your journeys.

To the Microbiology and Biochemistry students and staff, thank you for accommodating me and being helpful whenever I required use of your equipment and other lab items.

I want to express my deepest gratitude to my parents, Naren and Pria Deyal. Your unwavering love, support, sacrifices, prayers, encouragement and constant belief in my abilities have made it possible for me to pursue my goals and accomplish them. I am profoundly grateful that you are my parents. You both inspire me so much and are living examples of rising stronger no matter what you are confronted with. I am because you are. I hope to always make you as proud as you make me.

To my guardian angels, my grandparents and all those who bless me from above, thank you for watching over and protecting me on this journey. I know I am living in your blessings every day.

To all my friends and more especially my closest, Sahil, Arisha, Kiara as well as my wonderful family… your love, moral support, well wishes and prayers mean the world to me. Thank you for always checking in, trying to keep me motivated with all your positive energy and lifting my spirits whenever I felt low.

I would like to acknowledge and express my gratitude for the scholarship award received from UKZN College of Health Sciences. Thank you for supporting students in continuing their dreams.

Most importantly, I want to acknowledge my greatest power and strength, almighty God. It is through your grace and blessings that I am able to get through challenging yet rewarding parts of my life. I will forever be grateful for your presence, protection and unconditional love.

TABLE OF CONTENTS

LIST OF ABBREVIATIONS AND ACRONYMS

Ag85b	Antigen 85 b
AIDS	Acquired immunodeficiency syndrome
Amp	Ampicillin
AmpR	Ampicillin resistance
Apa	Alanine- proline-rich antigen
ARVs	Antiretrovirals
B-PER	Bacterial protein extraction reagent
BCG	Bacillus Calmette-Guérin
BLAST	Basic local alignment search tool
bp	Base pairs
BPaL	Bedaquiline, Pretomanid and Linezolid
BREC	Biomedical Research Ethics Committee
$CaCl_2$	Calcium chloride
CD	Circular dichroism
CDC	Centers for Disease Control and Prevention
CFP-10	Culture filtrate protein-10
CHAPS	3 - [(3-cholamidopropyl) dimethylammonio] -1- propanesulfonate
COVID-19	Coronavirus disease of 2019
CSIR	Council for Scientific and Industrial Research
CTAB	Cetyl trimethylammonium bromide
dH_2O	Distilled water
DNA	Deoxyribonucleic acid
DTT	Dithiothreitol

ECM	Extracellular matrix
E. coli	*Escherichia coli*
EDTA	Ethylenediaminetetraacetic acid
ELISA	Enzyme-linked immunosorbent assay
ELISPOT	Enzyme-linked immunospot
ESAT-6	Early secreted antigenic target 6 kDa
GST	Glutathione S-transferase
GRAVY	Grand average of hydropathy
HBHA	Heparin-binding haemagglutinin adhesin
His-tag	Polyhistidine tag
HIV	Human immunodeficiency virus
HRP	Horse-radish peroxidase
IGRA	Interferon-gamma release assay
IPTG	Isopropyl β-D-1-thiogalactopyranoside
Kan	Kanamycin
KanR	Kanamycin resistance
KCl	Potassium chloride
LAM	Lipoarabinomannan
LB	Lysogeny broth
LDt	L-D transpeptidase
LTBI	Latent tuberculosis infection
MCS	Multiple cloning site
MDR/RR-TB	Multidrug-resistant tuberculosis / rifampicin-resistant tuberculosis
MDR-TB	Multidrug-resistant tuberculosis
MS	Malate synthase

Mtb	*Mycobacterium tuberculosis*
MTBC	*Mycobacterium tuberculosis* complex
NCBI	National Center for Biotechnology Information
NEB	New England Biolabs
Ni-NTA	Nickel-nitrilotriacetic acid
OD	Optical density
PBS	Phosphate buffered saline
PBST	Phosphate buffered saline with Tween20
PCR	Polymerase chain reaction
pDNA	Plasmid DNA
pET	Polyhistidine tag expression vector
pGEX	Glutathione S-transferase expression vector
PMN	Polymorphonuclear neutrophil migration
PMSF	Phenylmethylsulfonyl fluoride
POC	Point-of-care
PstS1	Phosphate-binding protein PstS1
RD1	Region of difference 1
Rec	Recombinant
rpm	Revolutions per minute
SARS-CoV-2	Severe acute respiratory syndrome coronavirus type 2
SDS-PAGE	Sodium dodecyl sulphate-polyacrylamide gel electrophoresis
SPAAN	Software program for prediction of adhesins and adhesin-like proteins using neural networks
SRM/MRM	Selective reaction monitoring / Multiple reaction monitoring
TAE	Buffer containing Tris base, acetic acid and EDTA

TB	Tuberculosis
TDR-TB	Totally drug-resistant TB
TMB	3,3’5,5’tetramethylbenzidine
TST	Tuberculin skin test
UKZN	University of KwaZulu-Natal
WHO	World Health Organization
XDR-TB	Extensively drug-resistant TB

LIST OF FIGURES

LIST OF TABLES

ABSTRACT

Tuberculosis (TB) remains a global burden despite major advances in the design of rapid diagnostics and therapeutics. *Mycobacterium tuberculosis* (Mtb) adhesin proteins are key in the pathogenicity and virulence of *Mtb* and are potential biomarkers for diagnostics, drug targets or vaccine candidates. Numerous adhesin proteins have been considered; however, they have not proven to be both highly sensitive and specific in point-of-care tests. The increased emergence of drug-resistant strains, lack of suitable treatment regimens and poor compliance to treatments demonstrate the need for novel targets for therapeutic intervention. Research has shown that the relatively unknown Mtb *Rv0309* adhesin membrane protein is essential in the growth, biofilm development, and cellular morphology of Mtb. The *Rv0309* gene also enhances mycobacterial intracellular survival after infection, and deletion of the gene may decrease the infecting potential of the resultant mutant strain. Hence, the *Rv0309* adhesin encoding L-D transpeptidase was investigated in the current study for its ability to be cloned in glutathione S-transferase (GST)- and polyhistidine- tagged (His-tag) vectors, expressed and purified efficiently for future downstream processing.

The *Rv0309* gene was amplified using polymerase chain reaction (PCR). The plasmid DNA of pGEX-6P-1 (GST-tagged) and pET28a (His-tagged) vectors was extracted. The *Rv0309* DNA and vector DNA were restricted with the appropriate restriction endonucleases, ligated and transformed into *E. coli* BL21 cells. Transformants were confirmed by colony PCR and plasmid DNA sequencing. Recombinant protein expression was optimised using various isopropyl β-D-1-thiogalactopyranoside (IPTG) concentrations, time intervals and visualised using sodium dodecyl sulphate-polyacrylamide gel electrophoresis (SDS-PAGE) and Western blotting. Protein lysis and purification trials were performed and visualised using SDS-PAGE and Western blotting. The target band found in eluent was excised and sent for peptide mass fingerprinting for protein confirmation.

The *Rv0309* gene was successfully cloned into both vectors and optimally expressed in *Escherichia coli (E. coli)*. Despite employing an array of lysis and purification techniques, obtaining a pure form of the recombinant protein remained elusive. There was some success with pure protein being obtained during the study; however, the concentration was low and results were not reproducible. The main problems were sub-optimal lysis of the Rec-protein and ineffective binding to the purification column. Based on the bioinformatics analysis performed and information from GenScript, the reason for these problems was the high hydrophobicity of this protein. The insights gained from the lysis, purification and bioinformatic analysis of *Rv0309* in this study contribute to the understanding of membrane protein biochemistry and the intricacies associated with Mtb protein purification.

CHAPTER ONE: REVIEW OF LITERATURE

1.1 Introduction

In 2021, approximately 10.6 million people were infected with *Mycobacterium tuberculosis* (Mtb), the causative agent of tuberculosis (TB) and one of the world's leading causes of death (World Health Organization [WHO], 2021a; Bagcchi, 2023). Despite access to the latest diagnostics and therapeutic agents, TB remains a major burden globally. In addition, TB is responsible for being a leading cause of death in human immunodeficiency virus (HIV)-infected individuals. South Africa features in the top three countries for new TB cases and HIV-TB co-infection (Abdool Karim & Baxter, 2022). The low number of reported TB cases (a difference of 1.3 million between 2019 and 2020) suggested an increase in undiagnosed and untreated cases (Alene et al., 2020). Such cases are proposed to have led to further spread of TB infection in communities and increased TB mortality during the pandemic (Abdool Karim & Baxter, 2022; WHO, 2022; Bagcchi, 2023). The Coronavirus Disease of 2019 (COVID-19) pandemic has delayed the progress made by the WHO End TB strategies. Therefore, urgent attention and intervention are required, as most goals have not, and may not be achieved by 2030 (Chakaya et al., 2022; Pai et al., 2022).

An individual can present with either active or latent TB upon infection. Infection occurs when respiratory droplets containing Mtb are expelled into the atmosphere, and a healthy individual inhales these aerosolised droplets (Forrellad et al., 2013). The aerosolised bacilli are phagocytosed by alveolar macrophages (Algood et al., 2003; Smith, 2003). However, if the bacteria overcome this defence mechanism, they can start replicating in macrophages, spread to surrounding cells and grow exponentially, known as active TB, and can spread to other individuals (Dubnau & Smith, 2003; Long et al., 2022). An individual harbours Mtb in latent infection but is non-contagious and shows no signs of active illness (Centers for Disease Control and Prevention (CDC), 2020). However, latent TB can progress into active TB when an individual becomes immunocompromised (Dubnau & Smith, 2003). Globally, 25% of people are infected with Mtb, and an estimated 5-10% have a risk of latent TB progressing to active TB disease (Gill et al., 2022).

Active TB is treatable, and treatment can be effective upon early detection of the disease, especially for drug-resistant Mtb. Sputum smear microscopy, Mantoux tuberculin skin test (TST), interferon gamma release assay (IGRA) blood test, lipoarabinomannan (LAM) assays, line-probe assays, culture-based assays, chest radiography, and PCR-based assays such as Gene Xpert are currently available for TB diagnosis. However, the limitations include that they

are costly, tedious, inaccurate and have lower sensitivity (Gill et al., 2022); hence, the need to optimise existing diagnostics and develop effective novel tools. The Bacille Calmette-Guérin (BCG) vaccine is the only licensed vaccine for TB; however, only offers moderate protection against severe illness in children and is ineffective for adults or those with co-morbidities (Gopalaswamy & Subbian, 2022; Martinez et al., 2022). Current TB drug therapy can be ineffective due to poor compliance with the regimen, long-term treatment that may have poor efficacy and tolerability, and escalating drug resistance (Verma et al., 2022).

One of the challenges in designing a satisfactory and accurate point-of-care (POC) test is the lack of suitable, accurate biomarkers. Studies have shown that Mtb adhesins may be potential targets for this purpose (Kumar et al., 2013; Govender et al., 2014; Vinod et al., 2020). A critical stage of TB pathogenesis occurs when Mtb adhesin proteins attach to the host receptors to gain entry into the cell (Kumar et al., 2013). Much progress has been reported in identifying and characterising many of the Mtb adhesins (Kumar et al., 2013; Vinod et al., 2020). However, these potential biomarkers have yet to be proven as sufficiently sensitive or specific diagnostic, vaccine or drug candidates (Kline et al., 2009; Bisht & Meena, 2019). The potential vaccine and diagnostic adhesins include, Antigen 85 (Ag85) complex (Phunpae et al., 2013; Sriruan et al., 2022), early secreted antigenic target 6 kDa (ESAT-6) & 10 kDa culture filtrate protein (CFP-10) (Pinxteren et al., 2000; Lu et al., 2023), heparin-binding hemagglutinin (HBHA) (He et al., 2011; De Maio et al., 2019; Dirix et al., 2022), lipoarabinomannan carrier protein LprG (Zheng et al., 2022) and phosphate-binding protein PstS1 (PstS1) (Shahrear & Islam, 2023). Thus, continued research is required to investigate current and novel adhesins to improve TB diagnostics and therapeutics.

One of the lesser-known adhesin proteins is the conserved *Rv0309* adhesin (Kumar *et al*., 2013). The *Rv0309* protein is important in the growth, biofilm development, and cellular morphology of Mtb, thereby contributing to the pathogen's virulence and pathogenicity (Muniram, 2018). In addition, the high ratio of non-synonymous to synonymous substitutions value suggests *Rv0309* can adapt to evade host immunity (Jiang et al., 2017). Peng et al. (2022) reported that *Rv0309* was localised in the cell wall and enhanced mycobacterial intracellular survival after infection. This survival is likely due to inhibition of the pro-inflammatory response and decreased bacterial cell wall permeability, thereby contributing to mycobacterial pathogenesis (Peng et al., 2022). The deletion of the *Rv0309* gene was suggested to have decreased the infecting potential of the deletion mutant strain and that the gene is key in the virulence of Mtb (Mthembu, 2022). The average antigenic propensity for *Rv0309* is 1.0446 indicating highly antigenic sites that may evoke a significant immune response (Reche, 2023). However, no studies have tested the sensitivity and specificity of

Rv0309 as a potential biomarker. This study aims to clone, express and purify recombinant *Rv0309* protein sufficiently and with maximum purity so that future work can evaluate this protein's ability to detect *Rv0309* antibodies in patients' sera, as well as further downstream applications.

1.2 Incidence and Distribution of Tuberculosis Disease

The WHO reported that approximately 1,5 million people succumb to TB caused by Mtb annually (WHO, 2023). Despite improvements in treatment availability and healthcare services over six decades (Zumla et al., 2021), TB remains one of the top ten causes of death worldwide and is the second leading cause of death from a single infectious agent in the world, after severe acute respiratory syndrome coronavirus type 2 (SARS-CoV-2) (WHO, 2022). The unprecedented emergence of SARS-CoV-2 had adverse effects on worldwide End TB strategies with the disruption of access to health services (Cilloni et al., 2020; Sahu et al., 2021). Around 10.6 million people were diagnosed with TB in 2021 (WHO, 2022). Approximately six million of these individuals reported having access to healthcare, a decline from the 7.1 million in 2019. An estimated four million cases remained undiagnosed and unreported (WHO, 2021a), while an approximately 15% decrease in treatment for drug-resistant cases was noted as a result of the pandemic (Pai et al., 2022). Tuberculosis infection numbers have consistently declined over the years; however, the rate of decline is inadequate to achieve the original WHO End TB Strategy goals set within the stipulated time (Kim et al., 2020). The challenges caused by COVID-19 led to an increase in TB deaths, from 1.4 million deaths in 2019 to 1.6 million in 2021 (WHO, 2022). Human immunodeficiency virus-positive cases accounted for 187 000 TB deaths in 2021 (WHO, 2022).

Tuberculosis is especially prevalent in developing countries, some of which represent two-thirds of the global total. South Africa contributed 5,3% to the global total in 2021 and, hence featured in the WHO high burden country list (WHO, 2022). The reported TB incidence for South Africa was approximately 304 000 cases in 2021, with a rate of 513 cases per 100 000 population (WHO, 2022).

1.3 Tuberculosis co-infection

Tuberculosis-HIV co-infection has also seriously challenged TB control. Most HIV-infected patients die due to TB (WHO, 2019). Human immunodeficiency virus is one of the five risk factors for TB. In 2021, HIV was the second highest risk factor in the world, being accountable for approximately 860 000 TB cases (WHO, 2022). Undernourishment represents the highest

risk factor for TB as of 2021, followed by alcohol use disorders, smoking and diabetes (WHO, 2022). In South Africa, HIV-positive TB incidence increased to 163 000 cases, a rate of 274 cases per 100 000 population in 2021 (WHO, 2022). The mortality of people with TB-HIV co-infection was 33 000 cases at a rate of 55 cases per 100 000 population in the year 2021 (WHO, 2022). A study also revealed that TB-COVID coinfected patients suffered higher fatality risks compared to patients with COVID only (Quan et al., 2022).

1.4 Drug resistance

Drug-resistant TB poses a major public health threat. Drug resistance in Mtb occurs through various mechanisms, including compensatory evolution, epistasis, clonal interference, cell envelope impermeability, efflux pumps, drug degradation and modification, target mimicry and phenotypic drug tolerance (Al-Saeedi & Al-Hajoj, 2017; Rojas Echenique et al., 2019; Singh et al., 2020). The occurrence of mutations and sequential chromosomal accumulation of such mutations promote resistance of bacteria to antibiotics (Singh et al., 2020). Thus, despite the discovery and design of new anti-TB drug efforts, there is always a constant threat arising from the emergence of drug-resistant strains (Singh et al., 2020).

The currently available drugs are not effective against the escalation of drug resistance, including multidrug-resistant TB (MDR-TB), extensively drug-resistant TB (XDR-TB) and totally drug-resistant TB (TDR-TB) strains (Günther, 2014). Multidrug-resistant TB is caused by Mtb resistance to at least two first-line drugs, isoniazid and rifampicin (Monde et al., 2023). Extensively drug-resistant tuberculosis (XDR-TB) has recently been redefined by WHO (WHO, 2021b). The updated definition of XDR-TB is TB caused by Mtb strains that fulfil the definition of multidrug-resistant/rifampicin-resistant tuberculosis (MDR/RR-TB). Additionally, XDR-TB is resistant to any fluoroquinolone and at least one additional Group A drug. The Group A drugs comprise levofloxacin, moxifloxacin, bedaquiline and linezolid. These drugs represent the strongest second-line drug regimen for the long-term treatment of drug-resistant forms of TB (WHO, 2021b). Pre-XDR-TB is caused by Mtb drug resistant strains that fulfil the definition of MDR/RR-TB and that are also resistant to any fluoroquinolone (WHO, 2021b). Totally drug-resistant TB (TDR-TB) is caused by Mtb that is resistant to all first-line drugs and second-line drugs that have been tested (Velayati et al., 2013). Drug-resistant TB cases take longer to treat in comparison to drug-susceptible TB. Second-line drugs are more costly and can have more side effects which include gastrointestinal intolerance, hypothyroidism, rashes, dizziness, headache, renal toxicity, vomiting and anorexia (Jnawali & Ryoo, 2013). If Mtb is detectable in sputum, diagnosis may take one or two days. Patients may face difficulty with nausea, headache, tachycardia and dyspnea (Ugarte-Gil et al., 2015). Challenges also include

producing the sputum volume that is required (Mathebula et al., 2020) during the sputum induction procedure. When sputum is collected, samples are tested for presence of acid-fast bacillus using smear and culture tests. Culture results may only be released after eight weeks depending on bacterial growth and, hence, the delay. Extensively drug-resistant TB diagnosis takes longer, from six to sixteen weeks due to weak sterilising activity of second-line drugs and access to second-line drug susceptibility testing (Seung et al., 2015). Delays in diagnosis also vary depending on the socio-economic state of the country, with more significant delays experienced by lower-income countries and rural communities (Sreeramareddy et al., 2009; Yimer et al., 2014).

Globally, 69% of people diagnosed with bacteriologically confirmed pulmonary TB were tested for rifampicin resistance in 2021, up from 61% in 2019 and 50% in 2018 (WHO, 2022). There were 167 100 lab-confirmed cases of MDR/RR-TB, and 25 100 cases of lab-confirmed pre-XDR-TB/XDR-TB detected. This figure reflects a great fall (22%) from 201 997 people detected with drug-resistant TB in 2019. South Africa remains a TB burdened country with a high number of drug resistance cases (WHO, 2022).

Extensively drug-resistant tuberculosis was reported in 72 countries, with 967 cases in South Africa alone in 2016 (WHO, 2017). In South Africa, 100% of people diagnosed with bacteriologically confirmed pulmonary TB were tested for rifampicin resistance in 2021 (WHO, 2022). All 725 new cases of pre-XDR/XDR-TB initiated treatment (WHO, 2022). Shibabaw et al. (2020) researched the burden of pre-extensively and extensively drug-resistant tuberculosis among MDR-TB patients in Ethiopia from 2016 to 2018. The study found that many MDR-TB participants were resistant to at least one-second line drug (Shibabaw et al., 2020). This was a cause for concern as these patients were likely to develop XDR-TB. Totally drug-resistant TB was suggested when 93% of atypical XDR-TB were resistant to several anti-TB drugs in a South African study during 2008-2009 (Klopper et al., 2013).

1.5 Tuberculosis treatment

Drug-sensitive TB is treated with a six-month course consisting of first-line drugs, such as isoniazid, rifampicin, pyrazinamide and ethambutol for the first two months and second-line drugs for the remainder four months (Zumla et al., 2015). The standard treatment includes twelve weeks of isoniazid and rifapentine once a week for patients with latent infection and HIV-infected patients on antiretrovirals (ARVs). Some TB treatment courses include four months of rifampicin daily.

However, rifampicin is not used with HIV patients due to its harmful effects in conjunction with ARVs (Maartens et al., 2009). In this case, a substitute is used, such as rifabutin. If there are negative drug interactions with rifapentine or rifampicin, nine months of isoniazid is used daily (Sterling et al., 2020). Second-line drugs are used when drug resistance occurs but are less accessible, more toxic, and more costly than first-line drugs (Jnawali & Ryoo, 2013). Tuberculosis usually takes six to twelve months to cure; however, drug-resistant TB may take over 24 months. Hence, rapid detection and treatment of TB disease are crucial in preventing the increase of MDR-TB and XDR-TB cases (Jnawali & Ryoo, 2013).

Updated drug-resistant TB treatment guidelines were released by WHO (2022). One new recommendation was the use of a six-month bedaquiline, pretomanid, linezolid and moxifloxacin (BPaLM) regimen in MDR/RR-TB patients and those with additional resistance to fluoroquinolones (pre-XDR-TB). Another recommendation was a nine-month all oral regimen in patients with MDR/RR-TB and in whom resistance to fluoroquinolones had been excluded. The proposed anti-TB drug pipeline is shown in Figure 1.1.

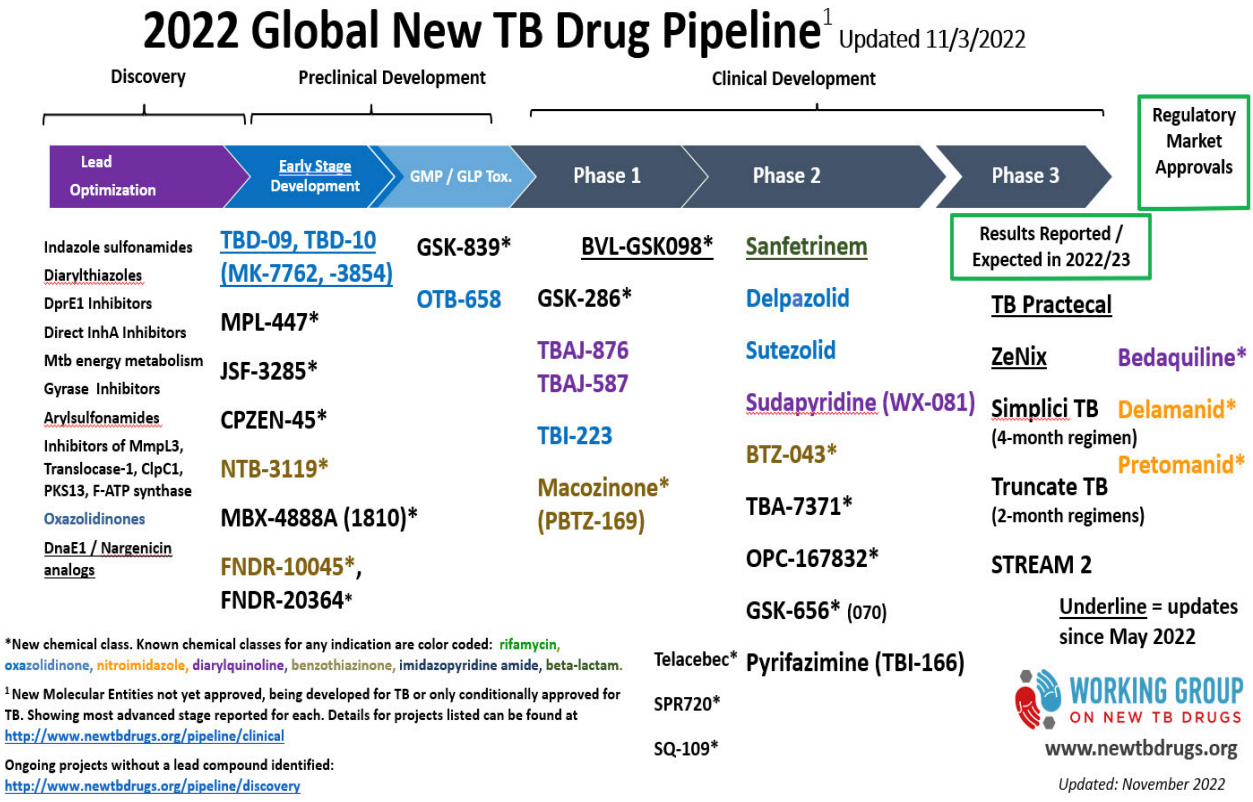

Figure 1.1: Pipeline for new anti-TB drugs and drug regimens for TB treatment (Stop TB Partnership, 2022)

Anti-TB drug development is necessary to discover novel TB treatments that are more effective by introducing shorter regimens, decreasing side effects or combating drug resistant strains. A randomised controlled trial, TB-PRACTECAL, evaluated short treatment regimens containing bedaquiline and pretomanid in combination with existing and repurposed anti-TB drugs (e.g., linezolid and clofazimine) for the treatment of microbiologically confirmed pulmonary MDR/RR-TB (Berry et al., 2022).

Furthermore, the ZeNix Phase 3 trial assessed the safety and efficacy of various doses and treatment durations of linezolid with bedaquiline and pretomanid in individuals with pulmonary MDR/RR-TB and additional resistance to fluoroquinolones (with or without resistance to injectable agents) or those with treatment intolerant or nonresponsive MDR/RR-TB. The bedaquiline, pretomanid, and linezolid (BPaL) regimen only uses three drugs that lasts 26 weeks as opposed to the conventional DR-TB regimen that includes around eight or nine tablets daily for 18 months (Haley et al., 2021). The use of 26 weeks of 600 mg linezolid over 26 weeks of 1 200 mg linezolid was also suggested as part of the BPaL regimen in adults with MDR/RR-TB or pre-XDR-TB (WHO, 2022).

Rifampicin (high dose) has been in trials examining the safety and benefit of increased doses of rifampicin (Garcia-Prats et al., 2021). Bedaquiline is used to treat MDR-TB for 24 weeks; however, the disadvantage is that it may have adverse effects on the liver and heart; hence, electrocardiograms and liver tests are monitored regularly (Tiberi et al., 2018).

1.6 Challenges associated with tuberculosis treatment and diagnosis

Data reflected an 85% success rate of treatment for drug-susceptible TB and a 57% success rate for MDR/RR-TB (WHO, 2020). The challenges that arose were the duration and complexity of drug regimens that influence adherence and toxicity. Additional challenges were the limited availability of second-line drug formulations for children due to minimal market forces, hesitance with the inclusion of children and pregnant females in clinical trials and a lack of funding (WHO, 2020). Tuberculosis-HIV co-infection treatment remains a challenge with complications of drug-to-drug interactions of anti-TB drugs and antiretroviral therapeutics.

Improvements are needed to increase TB detection and coverage. Tuberculosis treatment coverage was 71% worldwide in 2019 but decreased to 61% in 2021 (WHO, 2022). There was a distinct gap of 2.9 million cases from the 7.1 million new and relapse cases and the estimated 10 million incident cases in 2019. These gaps could be due to underreporting of detected cases or underdiagnosis. Underdiagnosis may be due to limited geographical or financial access to healthcare, delay in testing and attaining treatment, or diagnostic tests not being

sensitive or specific enough to accurately identify TB infection (WHO, 2020). Nigeria had a major challenge with underdiagnosis (Figure 1.2). The 2012 national survey showed that 75% of individuals with pulmonary TB (smear-positive) had symptoms that fulfilled screening requirements yet did not receive a prior diagnosis (WHO, 2020).

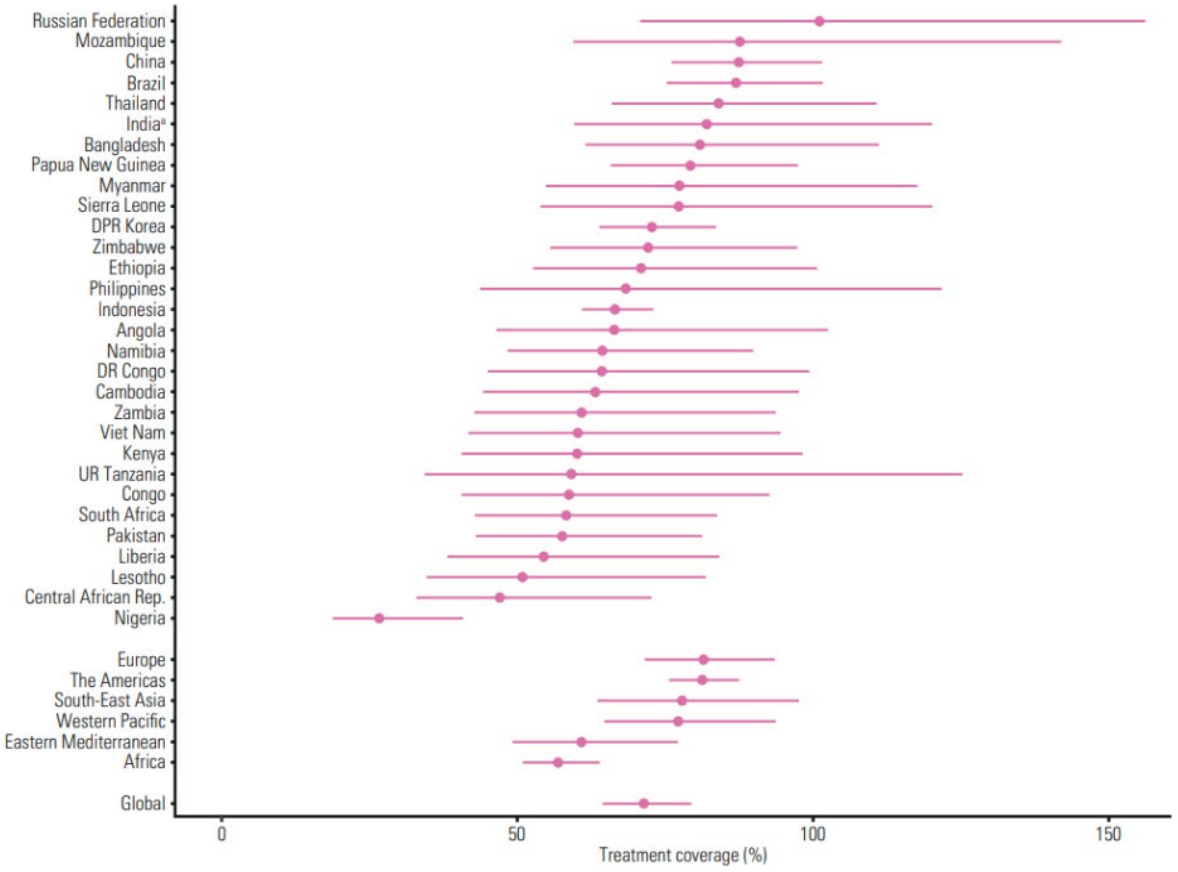

Figure 1.2 : Tuberculosis treatment coverage (new and relapse patients as a percentage of estimated TB incidence) in the 30 high TB burden countries, WHO regions and globally, 2019 (WHO, 2020).

The WHO (2020) highlighted the need for more effective, inexpensive and safe treatments that decrease treatment time, particularly with drug-resistant TB.

A cardiac and blood pressure drug, verapamil is currently under investigation (by Professor L Ramakrishnan and colleagues from the University of Cambridge and Medical Research Council Laboratory of Molecular Biology) to determine whether the drug can block the bacterial cell membrane pump (United Kingdom Research and Innovation, 2023). This followed a discovery by a student, Alex Lake, who screened and noted how verapamil stopped bacteria from ejecting rifampicin (United Kingdom Research and Innovation, 2023). These findings

show a potential for repurposing attainable and affordable drugs; however, more trials will need to be performed.

The effectiveness of TB treatment is highly dependent on rapid TB diagnosis and recognition of drug resistance; educating patients and the public on the importance of regimen adherence; contact tracing and prophylactic treatment of those contacts; and TB screening in high-risk communities (Gill et al., 2022).

1.7 Characteristics of Mycobacterium tuberculosis

Mycobacterium tuberculosis belongs to the *Mycobacterium tuberculosis complex (*MTBC*)*, that includes species, such as *M. decipiens, M. africanum, M. bovis, M. canettii, M. caprae, M. microti,* and *M. pinnipedii* (Rabinowitz & Conti, 2010; Brown-Elliott et al., 2018). Morphologically, Mtb is a rod-shaped, non-motile and facultative anaerobic bacillus (Percival et al., 2012) that is slow growing with a generation rate of approximately 12-24 hours (Voskuil et al., 2011).

Mycobacterium species contain a bilayer as their outer membrane, which is rich in lipids and contributes to its structural resilience (Bansal-Mutalik & Nikaido, 2014). The high lipid and mycolic acid content results in the bacterium staining either weak Gram-positive or not retaining dye during Gram staining (Tietze, 2012). *Mycobacterium tuberculosis* is resistant to weak disinfectants and can withstand dry environments (Bansal-Mutalik & Nikaido, 2014). The cell wall is said to be a protective layer against some antibiotics and osmotic shock (Alderwick et al., 2015). The bacterium can grow intracellularly and be cultured in laboratory media.

The bacterium's cell wall contains several complex layers (Figure 1.3) with significant amounts of various lipids and peptidoglycan (Asano et al., 1993; Belisle et al., 1997; Brennan, 2003; Fratti et al., 2003; Alderwick et al., 2007; Meena & Rajni, 2010; Rajni & Meena, 2010; Rajni & Meena, 2011; Jacobo-Delgado et al., 2023). All these above components interfere in the host defence pathways and facilitate survival within phagosomes (Asano et al., 1993; Belisle et al., 1997; Kartmann et al., 1999; Brennan, 2003; Fratti et al., 2003; Alderwick et al., 2007; Meena & Rajni, 2010; Rajni & Meena, 2010; Rajni & Meena, 2011).

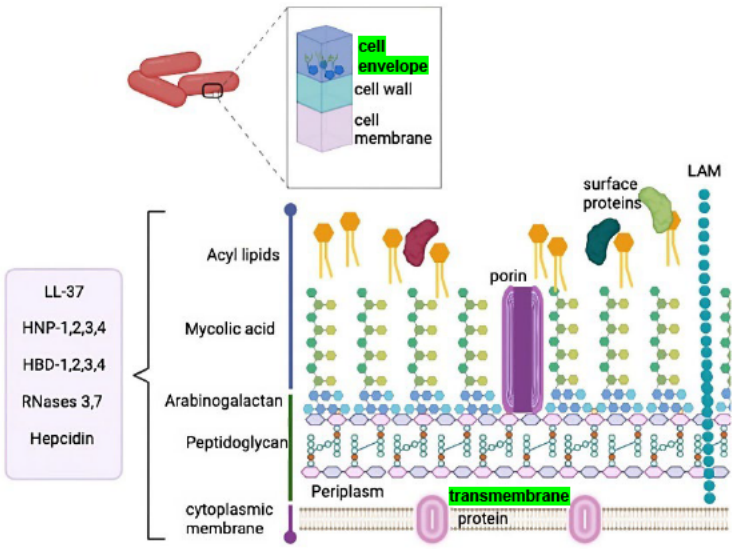

Figure 1.3: *Mycobacterium tuberculosis* cell wall components (Jacobo-Delgado et al., 2023).

Mycolic acid, cord factor and wax-D are key role-players in the Mtb cell wall. Mycolic acids influence the permeability of the cell wall due to its highly hydrophobic nature. These bacterial components provide defence against host proteins, enzymes and radicals in phagocytic granules and complement deposition in serum (Alderwick et al., 2007; Rajni & Meena, 2011).

Cord factor is a glycolipid found on the Mtb surface that causes serpentine cord formation during *in vitro* growth. Virulent strains of Mtb contain cord factor in abundance; however, avirulent strains do not (Asano et al., 1993). This factor is also an inhibitor of polymorphonuclear neutrophil (PMN) migration.

Polymorphonuclear neutrophil migrations are the first-line defence against infection and are potent effectors of inflammation (Di Carlo et al., 2001). Cord factor is toxic to mammalian cells (Rajni & Meena, 2011). The lipid wax-D is a key component of Freud's complete adjuvant and prevents oxidation burst inside the phagosome (Belisle et al., 1997; Brennan, 2003; Rajni & Meena, 2011).

1.8 Active and latent tuberculosis infection

In 2014, the global burden of latent tuberculosis infection (LTBI) was 23.0%, equating to an estimated 1.7 billion people (Houben & Dodd, 2016). Latent tuberculosis infection may be harboured in an individual for a lifetime. In individuals with LTBI, there is an estimated 5-15% chance of reactivation occurring, where latent TB transitions into active TB (Kiazyk & Ball, 2017). Active TB is described as TB disease when an infected individual's immune system is unable to defend against Mtb infection leading to illness and being able to transmit infection (Churchyard et al., 2017). Transmission occurs when an individual with TB disease expels

airborne droplets containing the bacteria into the air, which is inhaled by other individuals (Forrellad et al., 2013). Hence, TB is infectious. Post-infection, Mtb spreads to the lungs and begins to reproduce, after which the bacteria can move to other parts of the body, such as the spine or brain. During latent TB infection, Mtb can survive without replicating and progressing to disease, particularly in individuals that are not immunodeficient. These individuals display no clinical symptoms and cannot spread the disease to others but could reactivate infection if they become immunosuppressed (Forrellad et al., 2013).

1.9 Current diagnostic assays for the detection of TB

Initially, an individual can be clinically diagnosed by screening for pulmonary TB symptoms such as a cough that lasts three weeks or longer, chest pain or coughing up blood (CDC, 2020). Other physical symptoms include fatigue, weight loss, loss of appetite, chills and fever (CDC, 2020; Gill et al., 2022). It is estimated that one in four people globally produce an immunological response to Mtb infection. This infection can either stay dormant (Latent TB) or progress to active TB disease (Gill et al., 2022; WHO, 2022). Both forms of TB can be detected by a range of diagnostic tests described below.

Latent TB diagnostic tests

The Mantoux TST can identify latent TB infection. The disadvantages of the test are its lower specificity and sensitivity compared to other assays such as IGRA or enzyme-linked immunospot (ELISPOT) assay, especially when testing patients with weak immune systems (Dunn et al., 2016).

The IGRA is an alternative assay for latent TB (CDC, 2020). There are two different approaches to this method: the enzyme-linked immunosorbent assay (ELISA) – based whole-blood method, as well as the ELISPOT assay (Mazurek et al., 2010). The ELISA-based whole-blood test utilises the Mtb region of difference (RD1) antigens peptides, ESAT-6 and CFP-10. Peptides such as antigen TB7.7 are also included (Mazurek et al., 2010). The assays measure interferon-gamma levels (CDC, 2020). The ELISPOT assay is executed by separating and counting peripheral blood mononuclear cells that contain antigens ESAT-6 and CFP-10 that have been incubated for 16 to 24 hours (Mazurek et al., 2010). The number of interferon-gamma-producing T cells determines the outcome. Interferon-gamma release assays are not affected by BCG vaccination status (CDC, 2020). This is helpful when viewing latent TB infection in vaccinated patients. The downfalls of IGRAs are that they are expensive, need specialised kits, qualified personnel and an accredited laboratory. Tuberculin skin tests and IGRA tests depend on cell-mediated immunity, but neither test can differentiate between active

and latent TB infection (CDC, 2020). Novel skin-based TB detection methods, such as the C-TB skin and Diaskin test, are currently being studied to improve diagnosis and treatment of latent TB infection (Shingadia, 2012). Both these tests use recombinant Mtb ESAT-6 and CFP-10 antigens and are more specific than TST. The tests are also more accurate and cheaper than IGRA (CDC, 2020). Another simplified test developed by Qiagen uses ESAT-6 and CFP-10 in a lateral flow detection system that offers detection of both $CD4^+$ and $CD8^+$ T cell responses and was designed to improve latent TB infection among immunocompromised patients (Huang et al., 2022). However, sensitivity and specificity of the test needed to be improved as differentiation between latent and active TB was not optimal (Ndzi et al., 2016).

Active TB diagnostic tests

Active TB can be diagnosed by chest radiography or diagnostic microbiology using a sputum sample. Chest radiography is performed by obtaining a posterior-anterior X-ray image to detect chest abnormalities (Shingadia, 2012). The presence of lesions may point to TB infection; however, this cannot be used to definitively categorise the type of infection, i.e., latent or active TB. This test can eliminate the possibility of pulmonary TB in an individual with positive TST tests or TB blood tests (IGRAs), but no disease symptoms. Sputum smear microscopy is used to identify the presence of acid-fast bacilli, which indicates presumptive TB disease (Desikan, 2013; Gill et al., 2022). The method is easy and fast but can show inaccuracies as acid-fast bacilli shown may not be Mtb but rather non-tuberculous mycobacteria (Caulfield & Wengenack, 2016). The efficacy of smear microscopy is also operator dependent and the sensitivity is limited to detection of samples with bacterial loads that contain 10 000 bacilli per millilitre of sputum or higher (Lawn, 2015). Deng et al., (2021) reported that smear microscopy had the lowest sensitivity and specificity rate compared to loop-mediated isothermal amplification, GeneXpert, culture, TSPOT.TB and ratio of TB-specific antigen to phytohemagglutinin tests. Hence, culture and biochemical tests are required on all isolates to confirm Mtb. Although most culture-based assays have a high sensitivity and relatively rapid detection, Asmar & Drancourt (2015) reported that negative factors include the high cost, high hazard risk, frequent equipment maintenance, technical expertise required and high contamination rate. This may be a challenge in developing countries where resources and budgets are limited (Asmar & Drancourt, 2015). Line probe assays can be used for detecting Mtb and drug resistance in acid-fast bacilli smear-positive sputum or Mtb cultures (Desikan et al., 2017). A disadvantage seen with line probe assays is the identification of the most frequent mutations and relying on negative hybridisation results when not every mutation implies drug resistance (Mäkinen et al., 2006). The XpertMTB/RIF

and XpertUltra are used as preliminary diagnostics for TB and rifampicin resistance and have high sensitivity and specificity results (Deng et al., 2021).

South Africa uses XpertMTB/RIF as a diagnostic test for TB, and developments have been made on the Cepheid close-to-care platform – GeneXpert® Omni® (WHO, 2019). The XpertMTB/RIF test cannot be regarded as a point-of-care test as specialised equipment and personnel are often needed for its use and this can be costly for low-income countries (Andrea et al., 2013; Lawn et al., 2013; Pooran et al., 2019). The GeneXpert Omni is shown to be a promising global candidate for diagnostic testing but can be more expensive as shown by a study assessing cost effectiveness of the test (Ejalu et al., 2022). Cepheid is also designing an MTB/XDR assay to detect resistance to isoniazid, fluoroquinolone, ethionamide and second-line injectable drugs (Sohn et al., 2019). During the 2021 virtual Conference on Retroviruses and Opportunistic Infections, it was reported that using XpertUltra MTB/RIF testing as the preliminary test for TB, as opposed to a confirmatory test after the screening, has great potential to improve TB diagnosis, including all high-risk individuals (Lebina et al., 2021) . These tests broaden access to fast molecular testing for TB identification as well as antibiotic resistance. The Truenat MTB assay® is an alternative to the GeneXpert. Both Truenat MTB assay and GeneXpert make use of real-time PCR technology (Hashmi et al., 2020; Gopalaswamy et al., 2023). The limitations include having a lower sensitivity for smear-negative samples (WHO, 2019).

The WHO TB report emphasised the need for improvement of the availability and use of sensitive diagnostic tests for TB following reports of incorrect diagnoses, resulting in an increase in the number of confirmed cases (WHO, 2020). Two million new and relapse TB cases were identified using a WHO-recommended rapid diagnostic test (WHO, 2020). Although there are 48 high-burden countries, only 18 used these rapid diagnostics as an initial test for more than 50% of notified cases. It is therefore crucial to improve the efficiency and accuracy of TB diagnostic tests and supply more high-burden countries with these tests to influence treatment efficacy (Gill et al., 2022).

1.10 Current status of vaccine development

The BCG vaccine has been available to public for close to 100 years since its commercialisation in 1928 (Luca & Mihaescu, 2013). The BCG vaccine is currently the only licensed and effective vaccine for TB prevention in the world and is included in national vaccination programs (Li et al., 2022). This accessible vaccine is often given to children and prevents possible complications such as TB meningitis. The efficacy of infant BCG vaccination has been reported to be 70-80% effective against childhood TB such as meningitis and miliary

tuberculosis (Trunz et al., 2006; Katelaris et al., 2020). However, it does not prevent pulmonary disease; neither does it control latent TB progression to active disease (Hatherill & Cobelens, 2022). Additionally, it only has an immune-protective effect lasting 10-15 years and has been ineffective in stopping the spread of disease in adults and adolescents (Mustafa, 2012; Torres-Sangiao et al., 2016; Barberis et al., 2017; Gong et al., 2018; WHO, 2022). The WHO END TB Strategy target for 2035 requires a 95% reduction in the absolute number of TB deaths annually; hence, it is key to design an effective vaccine for adults and one that offers greater lasting immunity in children (Morrison & McShane, 2021; Saramago et al., 2021; WHO, 2022). Novel TB vaccines can be categorised by vaccine type. Examples are subunit, recombinant live vaccines, attenuated live vaccines, inactivated vaccines, and DNA vaccines (Figure 1.4).

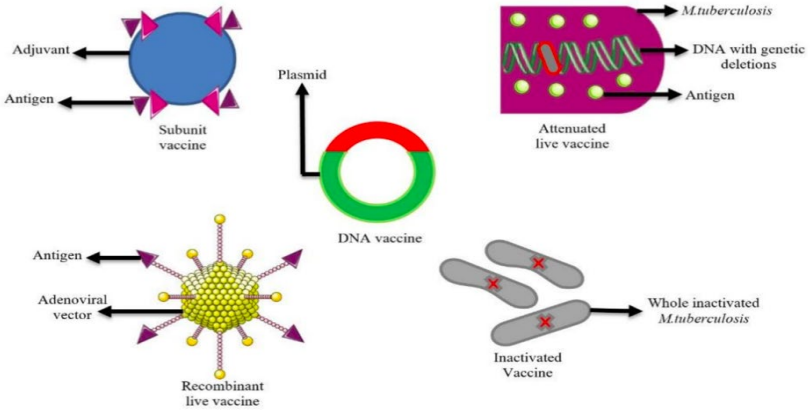

Figure 1.4: Types of vaccines (Saramago et al., 2021)

Figure 1.5 depicts the latest TB vaccine pipeline. South Africa plays a significant role in developing novel TB vaccines and facilitating clinical trials.

Clinical trials have shown that the VPM1002 vaccine has been safe for either HIV-negative or HIV-positive newborns and, more importantly, has fewer side effects compared to the current BCG vaccine (Cotton et al., 2022).

The MTBVAC vaccine is made of an attenuated Mtb clinical isolate of the Euro-American lineage. Preclinical trials in various animal models depicted that the MTBVAC is safe and is able to induce further protection when compared to the BCG vaccine. Phase 1 studies have also shown that the MTBVAC was safe and immunogenic in naïve adults and infants. The vaccine also evoked an immune response greater than BCG-induced immune responses (Martín et al., 2021).

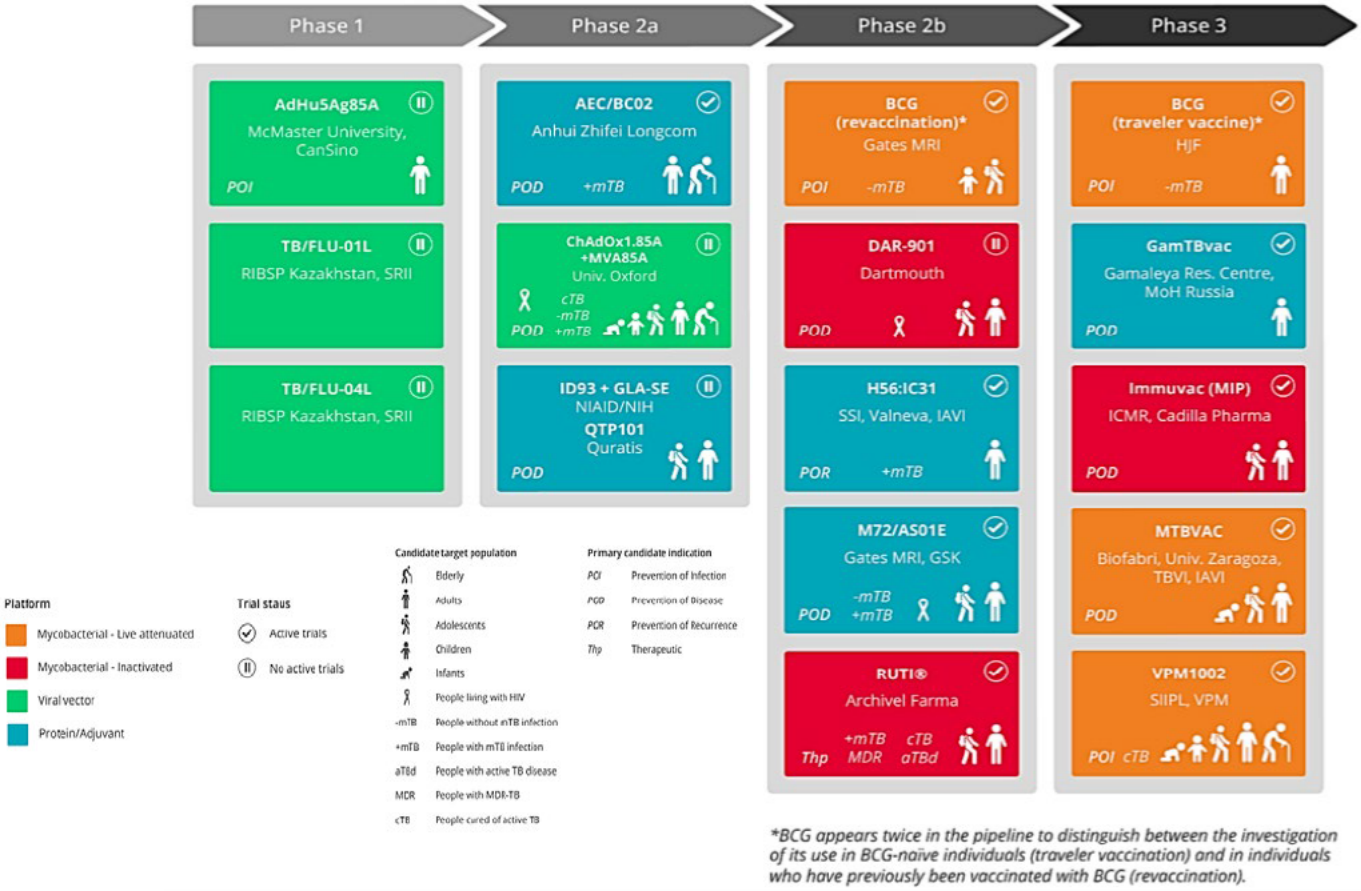

Figure 1.5: TB vaccine pipeline (Stop TB Partnership, 2022)

The Immuvac vaccine was initially designed to prevent leprosy. *Mycobacterium indicus pranii* is the agent used to produce the vaccine and contains antigens similar to those found in Mtb (Faujdar et al., 2011). These antigens evoke an immune response that assists in clearing TB from an infected individual and, when combined with treatment, can cure drug-resistant individuals through first-line therapies (Sharma et al., 2017). The GamTBvac vaccine contains three Mtb antigens, which are Ag85a and ESAT6-CFP10 fusion protein, fused with a dextran-binding domain. The vaccine induced a specific and durable Th1 and humoral immune response in trials. The efficacy and vaccine protection against Mtb was going to be tested in further studies in Phase III trial (Tkachuk et al., 2020). The subunit candidate vaccine M72/AS01E comprises immunogenic fusion protein (M72) obtained from Mtb antigens and adjuvant AS01E (Van Der Meeren et al., 2018; WHO, 2020). The vaccine was administered to participants in two doses. It was revealed to reduce the progression of latent infection to active TB with 50% efficacy in HIV-negative adults with latent TB after three years of follow-up (WHO, 2020). The vaccine's effectiveness against drug resistance needs further investigation; however, is likely to decrease drug resistance by reducing transmission and preventing the need for antibiotics. BCG revaccination (Gates MRI-TBV01-201) aims to confirm that revaccinating with BCG provides protection against a sustained infection by assessing the effectiveness after 48 months after revaccination. It also aims to explore biomarkers that remained throughout Mtb infection measured using the QuantiFERON-TB

Gold Plus assay. The H56: IC31 vaccine is an adjuvanted subunit vaccine that comprises three Mtb antigens with the IC31© adjuvant. This trial was found to be safe and immunogenic (Jenum et al., 2021).

Nanoparticles have been widely used in recent years to develop novel vaccines. These vaccines use biological or artificial particles smaller than 1000 nm and antigens specific to the pathogen (Torres-Sangiao et al., 2016). This practice prevents many infectious diseases, including HIV/AIDS and TB. Nanovaccines can induce cell-mediated and antibody-mediated immunity as well as regulate antigen presentation, making them a popular choice for anti-TB strategies (Saramago et al., 2021). However, this has disadvantages, such as possible nanomedicine toxicity or lack of regulatory guidelines.

1.11 *Mycobacterium tuberculosis* adhesins as biomarkers

Biomarkers serve as an indicator of the presence or severity of a disease or illness (Kumar et al., 2013). Biomarkers are necessary for TB as they can, firstly, detect active disease and determine whether treatment is successful. Secondly, individuals with latent TB can be diagnosed, and reoccurrence risk, as well as the success of treatment, can be assessed. Thirdly, biomarkers can determine the efficiency of TB vaccines in protecting individuals from becoming infected (Walzl et al., 2008).

Biomarkers can be identified during TB pathogenesis studies. Microbes need adhesins to attach to host cells to facilitate pathogenesis (Govender et al., 2014; Bisht & Meena, 2019). This interaction is host specific and dependent on tissue tropism. The location of these adhesins is also vital in triggering the host cell immune response. Adhesins play a crucial role in allowing close contact between host cell surface receptors and Mtb (Kline et al., 2009; Kumar et al., 2013; Bisht & Meena, 2019) and mediate attachment of the aetiological agent to host cells (Govender et al., 2014).

Adhesins also play a crucial role in bacterial aggregation and biofilm formation. Mtb express novel adhesins that assist in binding to the surface of the host cell. The host cell has receptor molecules such as integrins, glycosaminoglycans and certain sugar residues that have been depicted to interact with microbial adhesins (Delogu & Brennan, 1999; Dersch & Isberg, 2000; Brennan et al., 2001). Adhesins usually interact with particular components, such as fibronectin and laminin. These trigger signal transduction events that lead to bacterial invasion. When the mechanism behind the binding of adhesins is studied, a greater understanding of the early stages of TB infection can be gained. This knowledge can assist in developing tools for TB control, such as identifying inhibitors, vaccine development and diagnostic tool development (Govender et al., 2014).

Even though several Mtb adhesins have been characterised (Figure 1.6.) (Table 1.1), there are still other putative adherence components that contribute significantly to virulence and pathogenicity. The well-characterised Mtb adhesins include, amongst others, heparin-binding hemagglutinin adhesin (HBHA), alanine-proline-rich antigen (Apa), malate synthase (MS) (Kumar et al., 2013). Examples of membrane proteins classified as novel Mtb adhesins include *Rv2599*, *Rv0309* and *Rv3717* (Kumar et al., 2013).

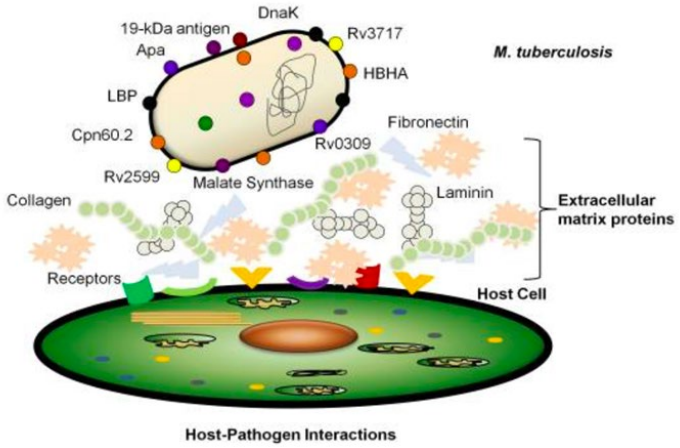

Figure 1.6: The interaction of various adhesive molecules on *Mycobacterium tuberculosis* with a host cell (Kumar et al., 2013)

Table 1.1: Summary of known *Mycobacterium tuberculosis* adhesins (Ramsugit & Pillay, 2016)

Adhesin	*Gene (s)*	Mediates adhesion to
19-kDa antigen	*Rv3763*	Monocytes and macrophages
Alanine- and proline-rich antigen (Apa)	*Rv1860*	Pulmonary surfactant protein A and macrophages
Antigen 85 complex	*Rv0129c, Rv1886c, Rv3803c, and Rv3804c*	Fibronectin and macrophages
Cpn60.2 molecular chaperone	*Rv0440*	Macrophages
Curli pili	*Rv3312A*	Laminin, *M. tuberculosis*, macrophages, and epithelial cells
DnaK molecular chaperone	*Rv0350*	Macrophages
Early secreted antigen ESAT-6	*Rv3875*	Laminin
Glutamine synthetase A1	*Rv2220*	Fibronectin
Glyceraldehyde-3-phosphate dehydrogenase	*Rv1436*	Possibly fibronectin (as occurs in group A streptococci)
Heparin-binding hemagglutinin adhesin	*Rv0475*	*M. tuberculosis* and epithelial cells
Laminin-binding protein	*Rv2986c*	Laminin
L,D-transpeptidase	*Rv0309*	Fibronectin and laminin
Malate synthase	*Rv1837c*	Fibronectin, laminin, and epithelial cells
Membrane protein	*Rv2599*	Collagen, fibronectin, and laminin
Mycobacterium cell entry-1 protein	*Rv0169*	Epithelial cells
N-acetylmuramoyl-L-alanine amidase	*Rv3717*	Fibronectin and laminin
PE-PGRS proteins	*Rv1759c*	Fibronectin
	Rv1818c	*M. tuberculosis* and macrophages
Protein kinase D	*Rv0931c*	Brain endothelia and laminin
PstS-1 (38-kDa antigen)	*Rv0934*	Macrophages
Type IV pili	*Rv3654c-Rv3660c*	Possibly macrophages and epithelial cells

1.12 Membrane protein *Rv0309*

The *Rv0309* gene is 657 base pairs (bp) in length and is part of a YkuD superfamily domain (Kumar et al., 2013). According to the National Center for Biotechnology Information (NCBI), "YkuD are a family of proteins that are found in a range of bacteria. This domain can act as an L, D – transpeptidase that gives rise to an alternative pathway for peptidoglycan cross-linking. This gives bacteria resistance to beta-lactam antibiotics that inhibit penicillin-binding proteins (PBPs) which usually carry out the cross-linking reaction". It is made up of two beta-sheets that form a cradle capped by an alpha helix. The region has a conserved histidine and cysteine (active site residue). The circular dichroism (CD) spectrum relies on differential absorption of left and right circularly polarized light and is particularly sensitive to the secondary structure of proteins enabling this spectrum to be a valuable tool when evaluating structure, folding and binding properties of a protein (Greenfield, 2006). The *Rv0309* protein depicts a typical beta-sheet-rich structure, with a presence of 5% alpha helices, 47% beta sheet and 48% random coils (Kumar et al., 2013). The structures are formed by hydrogen bonding and hydrophobic interactions and can influence the binding of protein to other substrates or molecules. The *Rv0309* was identified through an integrated computational approach using a software program for prediction of adhesins and adhesin-like proteins using neural networks (SPAAN) for adhesin prediction, PSORTb, SubLoc and LocTree for extracellular localization, and basic local alignment search tool (BLAST) for verifying non-similarity to human proteins (Kumar et al., 2013).

The *Rv0309* binds strongly to two crucial host extracellular matrix (ECM) components, fibronectin and laminin (Kumar et al., 2013) (Figure: 1.6) (Figure 1.7) which suggests there may be a strong antigenic stimulus. Fibronectin plays a fundamental role in cell adhesion and is arranged into a mesh of fibrils and linked to receptors found on the cell surface (Kular et al., 2014). Laminin has a trimeric structure and assists in cell adhesion as well as contributes to structure of ECM (Kular et al., 2014).

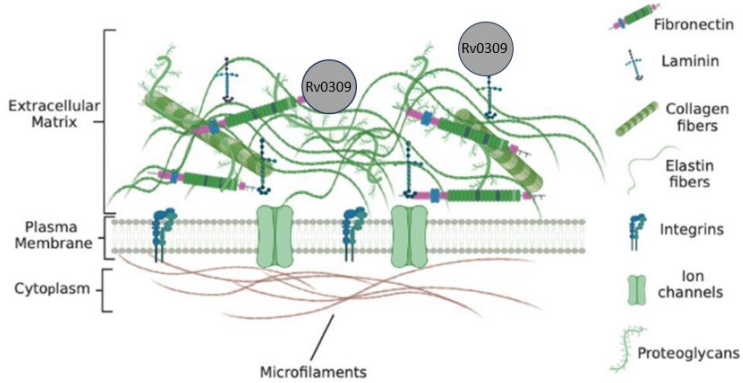

Figure 1.7: The *Rv0309* binds to extracellular matrix molecules, fibronectin and laminin. Adapted from (Dzobo & Dandara, 2023).

The *Rv0309* also encodes an L, D-transpeptidase (Ldt) found in many bacterial species. In the Mtb H37Rv chromosome, there are five Ldt variations (Gupta et al., 2010; Lavollay et al., 2011). The structure of Ldt variations differ. An example of LdtMt1 is shown in Figure 1.8.

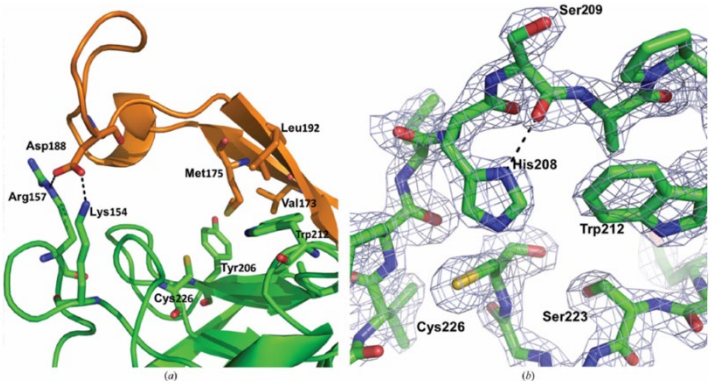

Figure 1.8: Details of the LdtMt1 structure. (a) The LdtMt1pincer. Hydrophobic/aromatic residues involved in interactions of the two-stranded β-sheet of the cap and residues involved in salt-bridge formation are shown in stick representation. Cys226 is also shown for identification of the catalytic pocket. (b) (2Fo - Fc) electron-density map of the LdtMt1catalytic site contoured at 2.0σ (Correale et al., 2013).

The L, D-transpeptidases function in cross-linking (Sanders et al., 2014) and attachment of lipoproteins to peptidoglycan *in vivo*. Studies have shown that Ldts are associated with virulence in an acute infection of a mouse model and involved in the adjustment to the non-replicative state of Mtb. The L, D-transpeptidase cross-link glycan chains by producing 4 →3 peptide bonds joining residues at the fourth and third locations of peptides (Lavollay et al., 2011). These cross-links are found in 20% of mycobacteria (Lavollay et al., 2011). *Mycobacterium tuberculosis* at the stationary phase has an elevated amount of 80% of Ldt cross-links. L, D-transpeptidases are also known as the only enzymes that can speed up the construction of novel cross-links in the absence of *de novo* synthesis of precursors. This function is essential, as mature peptidoglycan does not contain pentapeptide stems needed for the D, D transpeptidation (Goffin & Ghuysen, 2002). This cross-link also allows the peptidoglycan to be resistant to endopeptidases through hydrolytic action. These cross links appeared to strengthen the peptidoglycan layer under stress conditions (Morè et al., 2019). These cross-links also provide lysozyme resistance in organisms such as *Caulobacter crescentus* (Woldemeskel & Goley, 2017; Stankeviciute et al., 2019) and *A. tumefaciens* (Stankeviciute et al., 2019).

The *Rv0309* protein has been shown to promote Mtb growth and biofilm formation, allowing the pathogen Mtb to be more resistant to harsh conditions or antibiotics (Muniram, 2018). Another study reported that *Rv0309* was localised in the cell wall and enhanced mycobacterial

intracellular survival after infection, likely through inhibition of the pro-inflammatory response and decrease of bacterial cell wall permeability, thereby contributing to mycobacterial pathogenesis (Peng et al., 2022). Mthembu (2022) reported that the elimination of the *Rv0309* gene in the mutant strain may have reduced the infecting capability of the strains and that the gene is key in the virulence of Mtb. Additionally, the removal of the *Rv0309* gene along with *HBHA* induced great expression of other genes that are crucial in Mtb virulence (Mthembu, 2022).

1.13 Significance of this work

The *Rv0309* plays an essential role in TB pathogenesis eliciting Mtb intracellular survival and promoting bacterial growth. If the Rec-*Rv0309* protein can be purified in sufficient quantity, the adhesin protein can be evaluated for its ability to induce an immune response. This would validate the protein for inclusion in the design of a vaccine candidate or diagnostic assay. Immunolocalisation of *Rv0309* can also be performed using immunofluorescent microscopy to determine binding association with host cells. The crystal structure can be determined and molecular docking studies performed to design an anti-TB drug that targets *Rv0309*. Increased knowledge on the *Rv0309* adhesin protein may lead to a potential rapid POC test, anti-TB drug or vaccine candidate that can decrease TB incidence, prevalence and mortality rates.

1.14 Research Design

Aim: To clone, express and purify Mtb *Rv0309* adhesin protein

Objectives:

- Clone *Rv0309* gene into vector using PCR, agarose gel electrophoresis, restriction digestion, ligation and transformation
- Confirm the viability of recombinant clones by colony PCR and DNA sequencing
- Express recombinant *Rv0309* protein using *Escherichia coli* BL21 cells
- Confirm the integrity of the recombinant *Rv0309* protein by SDS-PAGE and Western blotting
- Purify recombinant *Rv0309* proteins using affinity chromatography and sequence eluent band using peptide mass fingerprinting

CHAPTER TWO: METHODOLOGY

2.1 Cloning, expression & purification of *Mycobacterium tuberculosis Rv0309* protein

The overview of the workflow for cloning, expression and purification for both GST and His-tagged vectors are described below with further details being provided later in this section. The *Mycobacterium tuberculosis (*Mtb*) Rv0309* gene was amplified using the polymerase chain reaction (PCR). Plasmid deoxyribonucleic acid (DNA) of pGEX-6P-1 containing a glutathione S-transferase (GST) tag and pET28a containing a polyhistidine tag (His-tag) was purified from stock cultures. The *Rv0309* and pGEX-6P-1 plasmid DNA (pDNA) were restricted with the appropriate restriction endonucleases (BamHI and EcoRI), ligated and transformed into *Escherichia coli (E. coli)* BL21 cells. Transformants were confirmed by colony PCR and plasmid DNA sequencing. Recombinant protein expression was optimised using various isopropyl β-D-1-thiogalactopyranoside (IPTG) concentrations, time intervals and, thereafter, visualised using sodium dodecyl sulphate-polyacrylamide gel electrophoresis (SDS-PAGE) and Western blotting. Protein lysis and purification trials were performed and visualised using SDS-PAGE and Western blotting. Challenges were encountered with the purification of the GST-tagged protein; hence, cloning was repeated with a pET28a vector containing His-tag, followed by expression and purification of the His-tagged protein.

2.1.1 Ethical clearance

Ethics approval was granted (BREC/00002801/2021) by the Biomedical Research Ethics Committee (BREC) at the University of KwaZulu-Natal (UKZN).

2.1.2 Bacterial strains and culture conditions

The bacterial (*E. coli*) strains and plasmid (vector) used in the study are listed in Table 2.1. A loopful of the pure vector was used to inoculate lysogeny broth (LB) media and cultured overnight at 37°C with shaking at 200 revolutions per minute (rpm). The culture was aliquoted by adding 750 µL into a centrifuge tube containing 250 µL 50% glycerol and stored at -80°C.

Table 2.1: Bacterial strains used in this study

Bacteria/Vector/ Strain	Reference
E. coli BL21	Pillay, K (Medical Microbiology, UKZN)
E. coli DH5α	Pillay, K (Medical Microbiology, UKZN)
pGEX-6P-1	National Bioproducts Institute (Durban, South Africa)
pET28a	Kumar, A (Microbiology, UKZN)
pGEX-6P-1 with *Rv0309*	This study
pET28a with *Rv0309*	This study

2.1.3 Mycobacterium tuberculosis DNA

Mycobacterium tuberculosis genomic DNA was supplied by the Discipline of Medical Microbiology, UKZN. The DNA had been isolated using the laboratory strain, Mtb H37Rv, according to the cetyl-trimethylammonium bromide (CTAB)- sodium chloride (NaCl) method (Larsen *et al.,* 2007).

2.1.4 Vectors used in the study

The pGEX-6P-1 vector

The pGEX-6P-1 (Figure 2.1) vector stock was donated by the National Bioproducts Institute and propagated at UKZN. The pGEX-6P-1 vector is commonly used to express and purify Rec-proteins in bacterial systems such as *E. coli (*Fang et al., 2016). The vector contains a GST- tag necessary for affinity purification of Rec-protein using glutathione agarose and a strong T7 promoter for enhanced expression. A multiple cloning site (MCS) is present to efficiently insert the gene of interest. The ampicillin resistance (AmpR) is used as a selectable marker.

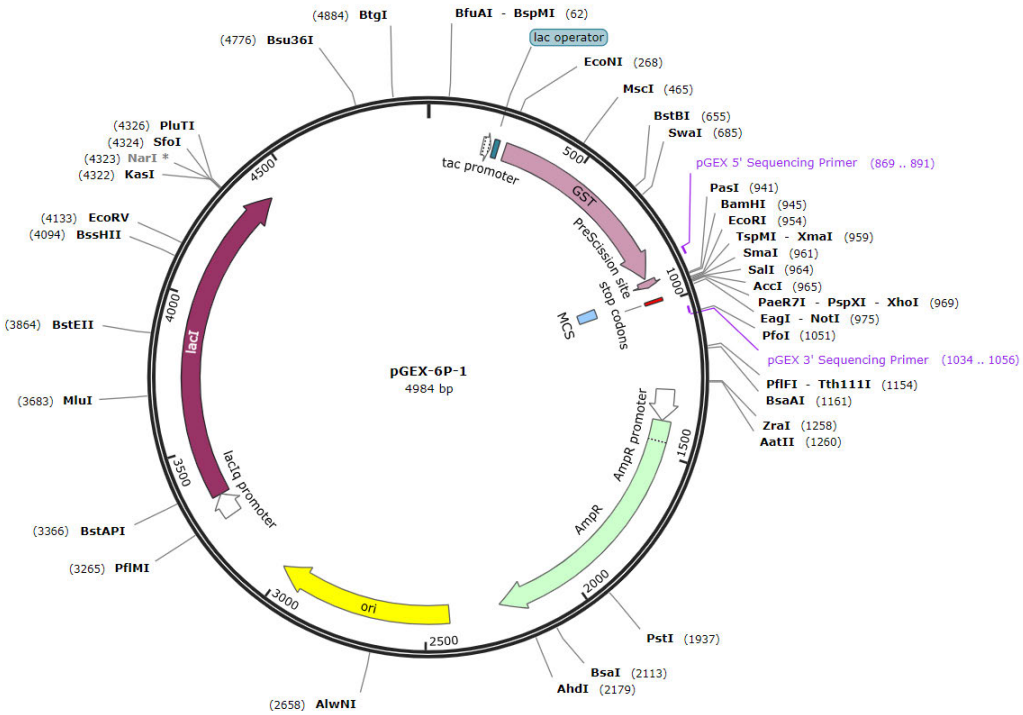

Figure 2.1: Plasmid map of pGEX-6P-1 and vector restriction sites created by SnapGene software. The pGEX-6P-1 vector contains a gene encoding AmpR that allows for the selection of cells that can grow in media containing ampicillin, leading to their rapid identification. In addition, the pGEX vector contains a 26 kDa GST-tag. The vector contains a range of restriction sites available for effective cloning.

The pET28a vector

The pET28a (Figure 2.2) vector was donated by Microbiology, Westville Campus, UKZN. The pET28a is designed to express and purify Rec-proteins in bacterial systems. The vector contains a His-tag that allows for affinity purification with nickel-nitrilotriacetic acid (Ni-NTA) resin (Fang et al., 2016). Similar to pGEX-6P-1, pET28a contains a MCS for easy insertion of the gene of interest. The vector contains kanamycin resistance (KanR) as a selectable marker and has a strong T7 promoter for high-level gene expression.

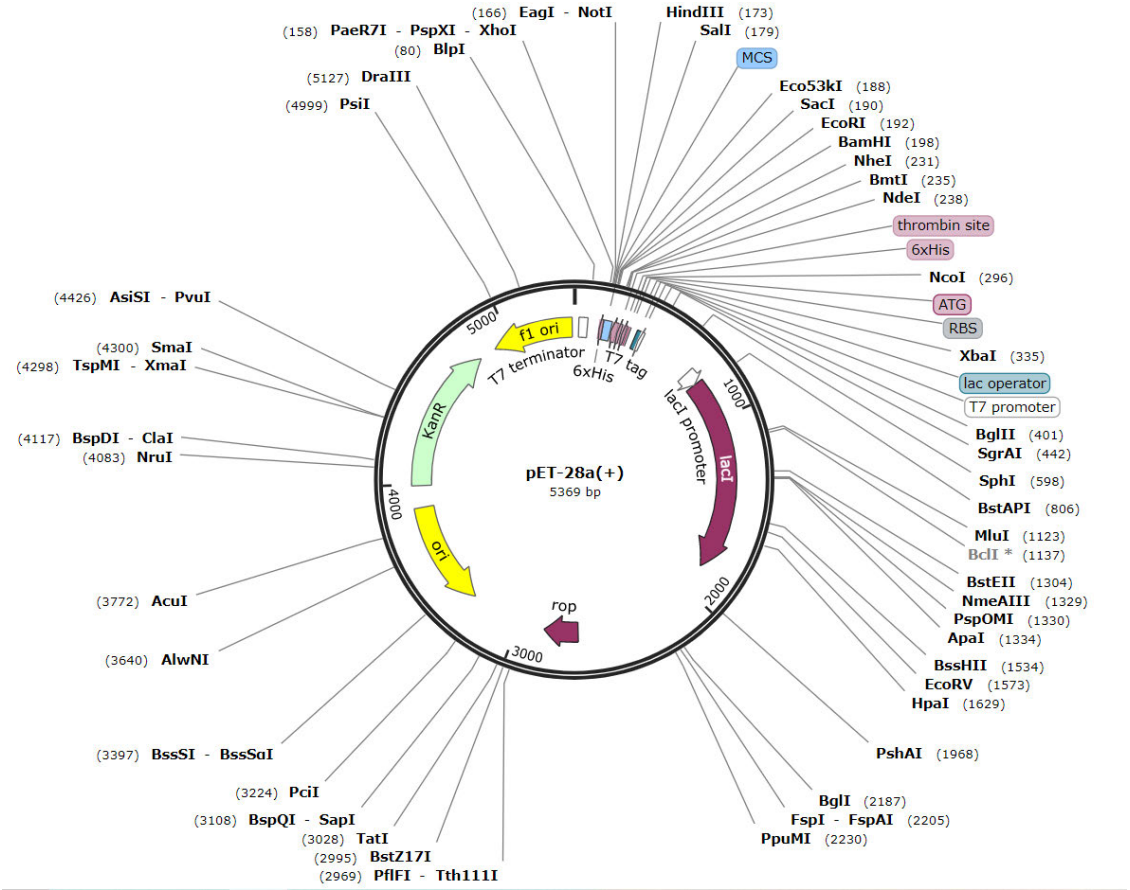

Figure 2.2: Plasmid map of pET28a and vector restriction sites created by SnapGene software. The pET28a contains a gene encoding KanR that allows for the selection of cells that can grow in media containing kanamycin, leading to their rapid identification. In addition, the pET vector contains a ± 0.8 kDa His-tag. Like pGEX-6P-1, this vector contains many restriction sites for efficient cloning.

2.1.4.1 Isolation of plasmid DNA

The GeneJET Plasmid Miniprep Kit (ThermoFisher Scientific™, Massachusetts, United States of America [USA]) was used to isolate plasmid DNA for pGEX-6P-1, pET28a and Rec-*Rv0309* plasmid DNA. Briefly, one mL of culture was centrifuged (Sigma Zentrifugen, Osterode, Germany) at 24 000 x g for one minute, and the supernatant was discarded. After repeating

four times, the pellet was resuspended with 250 µL of the Resuspension Solution and vortexed (Boeco, Hamburg, Germany) well. Lysis solution (250 µL) was added and mixed thoroughly by inverting the tube four to six times until the solution became viscous and slightly clear. Neutralisation solution (350 µL) was added and mixed immediately and thoroughly by inverting the tube four to six times, followed by centrifugation for five minutes at 12 000 x g to pellet cell debris and chromosomal DNA. The supernatant was pipetted into a GeneJET spin column and centrifuged (Sigma Zentrifugen, Osterode, Germany) for one minute at 12 000 x g. The flow-through was discarded, and the column was placed back into the collection tube. Wash solution (500 µL) was added to the spin column, centrifuged (Sigma Zentrifugen, Osterode, Germany) for one minute, and the flow-through was discarded. The wash step was repeated once, after which the spin column was centrifuged (Sigma Zentrifugen, Osterode, Germany) for one minute to remove residual ethanol. The column was placed into a clean microcentrifuge tube, and 30 µL elution buffer was added to the centre of the column membrane. After incubation for two minutes at room temperature (range 20°C – 25°C), the column was centrifuged (Sigma Zentrifugen, Osterode, Germany) for two minutes to elute the plasmid DNA, which was stored at -20°C.

2.1.4.2 Analysis of the Plasmid DNA

The purity and concentration of the purified plasmid DNA were determined using a NanoDrop 2000 Spectrophotometer (ThermoFisher Scientific™, Massachusetts, USA), viewed using agarose gel electrophoresis, and documented by G:BOX gel documentation system (Syngene, Cambridge, United Kingdom).

2.1.5 Amplification of Rv0309 gene

2.1.5.1 Primer Design

Prior to primer design, the *Rv0309* sequence was analysed using SignalP 6.0 programme to identify and remove any signal peptides present. A signal peptide cleavage site was present on the protein sequence between positions 15 and 16. Hence, 15 amino acids were removed as they form part of the hydrophobic transmembrane region of the sequence. The SnapGene software (Version 6.2) was used to perform virtual cloning that predicted the sequence of the recombinant vector with the truncated gene (Figure 2.3 and Figure 2.4). The gene and the designed primers, excluding the signal peptide, were selected in the software program, resulting in the amplification of the gene harbouring the desired restriction sites. Restriction sites for BamHI and EcoRI were chosen as they are common endonucleases and could be used for other vectors, ensuring recognition sequences are present in the correct orientation

for vectors (Table 2.2). In this study, the insert required BamHI at the 5'-end and EcoRI at the 3'-end.

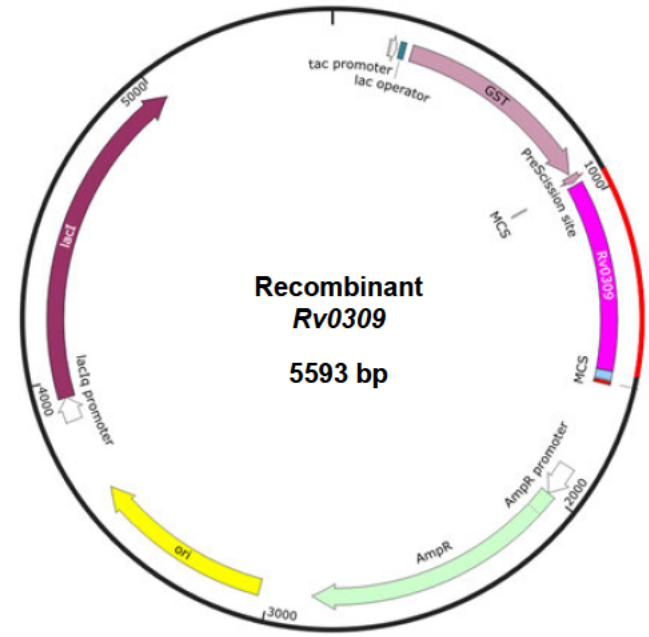

Figure 2.3: Plasmid map of *Rv0309* virtually cloned in pGEX-6P-1 created with SnapGene software (from Dotmatics; available at snapgene.com)

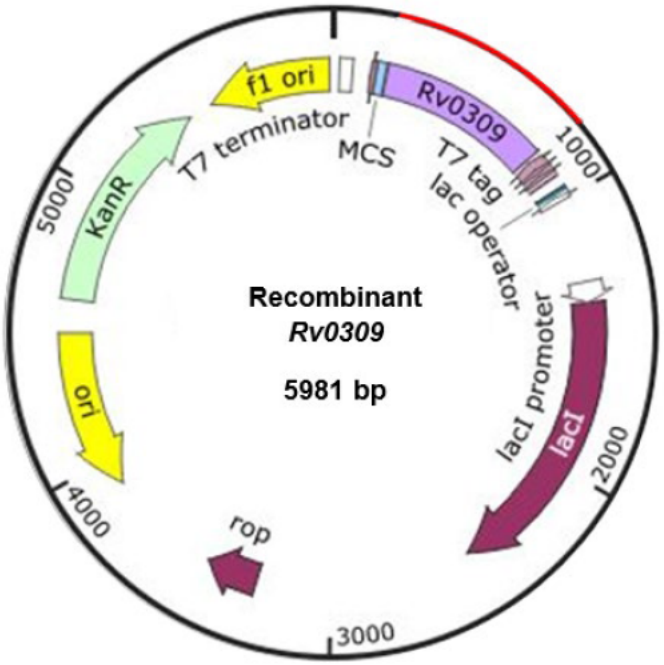

Figure 2.4: Plasmid map of *Rv0309* virtually cloned in pET28a created with SnapGene software (from Dotmatics; available at snapgene.com)

Table 2.2: Primers for the amplification of *Rv0309* cloned into pGEX-6P-1 and pET28a

Sequence	Number of bases	Restriction enzyme	PCR product size
5' AATCTC**GGATCC**ATGGTTGCTGTGGTTCTCGCGCCAG 3'	37	**BamHI**	~611 bp
5' AGTGCC**GAATTC**TTACTTGGCGATCGCGATCACCGCACC 3'	39	**EcoRI**	

2.1.5.2 Polymerase chain reaction

The Mtb H37Rv DNA was supplied by the Discipline of Medical Microbiology, UKZN. The reaction for gene amplification (Table 2.3) was set up as per the New England Biolabs (NEB) protocol with optimised thermal cycling conditions (Table 2.4). A Bio-Rad T100 Thermal Cycler (Bio-Rad, California, USA) was used to perform PCR.

The reagents used for PCR included Q5 Hot Start High-Fidelity 2X Master Mix (NEB, Massachusetts, USA), forward and reverse primers designed for *Rv0309* amplification (Inqaba Biotec, Pretoria, South Africa), and Nuclease Free Water (NEB, Massachusetts, USA).

Table 2.3: PCR set-up for *Rv0309*

Reagent	Volume (µL)	Final Concentration
Q5 Hot Start High – Fidelity 2X Master Mix	12.5	1 X
Forward Primer (10 µM stock)	1.25	0.5 µM
Reverse Primer (10 µM stock)	1.25	0.5 µM
Nuclease-Free Water	9	
Mtb H37Rv DNA	1	50 ng

Table 2.4: PCR conditions

Step		Temperature (°C)	Duration (seconds)
Initial denaturation		98	30
Denaturation	30 cycles	98	10
Annealing		72	30
Extension		72	60
Final extension		72	120

The annealing temperature of 72°C was obtained from the NEB T_m Calculator site (available at: https://tmcalculator.neb.com/#!/main). Once the PCR run was completed, 5 µL of PCR product was added to 3 µL of 6X DNA loading dye (ThermoFisher Scientific™, Massachusetts, USA) containing GelRed (Sigma-Aldrich, Massachusetts, USA). The amplified products were then electrophoresed in a 1.5% agarose gel in 1 X Tris-acetate-EDTA (TAE) buffer at 90 volts (V) for one hour (Sambrook and Russell, 2001). Once bands of the expected size were observed using a G:BOX gel documentation system (Syngene, Cambridge, United Kingdom), PCR was repeated to bulk up on product for purification.

2.1.5.3 Purification of PCR products

The PCR products were purified with the PureLink™ PCR Purification Kit (Invitrogen™, California, USA). Briefly, four volumes of PureLink™ Binding Buffer (B2) containing isopropanol were added to one volume of the PCR product (50–100 µL). The sample was mixed well and then added to the PureLink™ Spin Column and centrifuged (Sigma Zentrifugen, Osterode, Germany) at 10,000 × g for one minute at room temperature (range 20°C – 25°C). The flow-through was discarded, and the column was washed with 650 µL of Wash Buffer containing ethanol. The column was centrifuged (10,000 × g, one minute, room temperature). The flow-through was discarded, and the column was centrifuged (Sigma Zentrifugen, Osterode, Germany) again (maximum speed, two minutes, room temperature) to remove residual Wash Buffer. The spin column was placed in a 1.7 mL PureLink™ Elution Tube supplied with the kit. The purified PCR products were eluted by adding 30 uL of Elution Buffer (10 mM Tris-HCl, pH 8.5) to the centre of the column, incubating the column for one minute at room temperature and centrifuging the column (maximum speed, two minutes, room temperature). The purified PCR product was quantified using a NanoDrop 2000

Spectrophotometer (ThermoFisher Scientific™, Massachusetts, USA) and then stored at –20°C.

2.1.6 Restriction Digestion of amplified Rv0309, pGEX-6P-1 and pET28a plasmid DNA

When designing primers, the restriction sites of the restriction enzymes, EcoRI (ThermoFisher Scientific™, Massachusetts, USA) and BamHI (ThermoFisher Scientific™, Massachusetts, USA) were added to produce "sticky" or ends containing overhangs that are compatible with pGEX-6P-1 and pET28a vectors (Sambrook and Russell, 2001). The ThermoFisher Scientific™ Fast Digest enzymes were used because they are able to cleave target bases more rapidly than conventional enzymes. Table 2.5, Table 2.6, and Table 2.7 reflect the double digest reaction set-up for the insert and both vectors, respectively.

Table 2.5: Reaction set-up for the restriction digestion of amplified *Rv0309*

Reagent	Volume (µL)
Pure PCR product	8.48
Fast Digest Buffer	2
Fast Digest EcoRI enzyme	1
Fast Digest BamHI enzyme	1
Nuclease Free Water	7.52
Total	20

Table 2.6: Reaction set-up for the restriction digestion of pGEX-6P-1

Reagent	Volume (µL)
pGEX-6P-1 pDNA	12
Fast Digest Buffer	4
Fast Digest EcoRI enzyme	1
Fast Digest BamHI enzyme	1
Nuclease Free Water	2
Total	20

Table 2.7: Reaction set-up for the restriction digestion of pET28a

Reagent	Volume (µL)
pET28a pDNA	10
Fast Digest Buffer	2
Fast Digest EcoRI enzyme	1
Fast Digest BamHI enzyme	1
Nuclease Free Water	6
Total	20

The reaction tubes were incubated for 30 minutes in a water bath (FMH Instruments, Cape Town, South Africa) set at 37°C (per manufacturer's sheet). Thereafter, the samples were immediately heat-inactivated in a water bath (FMH Instruments, Cape Town, South Africa) set at 80˚C for 5 minutes. The restricted products were visualised by electrophoresis for one hour at 90 V in a 0.8% gel in 1 X TAE buffer. The sample contained loading dye made from TriTrack DNA loading dye (6X) added to GelRed. The Thermo Scientific™ GeneRuler 1 kb DNA ladder was used as molecular weight marker. Once the target bands of the expected molecular weights were observed, the samples were quantified using a NanoDrop 2000 Spectrophotometer (ThermoFisher Scientific™, Massachusetts, USA) and stored at -20°C.

2.1.7 Ligation reaction between restricted vectors and Rv0309 gene

The ligation of the vector and *Rv0309* gene was accomplished with the Rapid DNA Ligation Kit (ThermoFisher Scientific™, Massachusetts, USA), as per the manufacturer's insert, using the reactions shown in Table 2.8 and Table 2.9 (for pGEX-6P-1 with *Rv0309*) and Table 2.10 and Table 2.11 (for pET28a with *Rv0309*). Ratios of 1:3 and 1:5 of vector to insert were used to produce recombinant vectors. The amounts of restricted insert and vector were concentration-dependent. To calculate the volume of restricted products required in the ligation reaction, the *in silico* ligation calculator was used and divided by the concentration of restricted products (Appendix C). The tubes were vortexed (Boeco, Hamburg, Germany) briefly. The ligation mixes were incubated at 22°C for 20 minutes and then stored at 8°C. The kit allowed for rapid ligation; hence, incubation time was faster than conventional ligation reactions.

Table 2.8: Reaction set-up for rapid ligation reaction (1:3) between pGEX-6P-1 and *Rv0309*

Reagent	Volume (µL)
Restricted insert	0.24
Restricted vector	0.64
Ligase buffer	4
Ligase	1
Nuclease Free Water	14.12
Total	20

Table 2.9: Reaction set-up for rapid ligation reaction (1:5) between pGEX-6P-1 and *Rv0309*

Reagent	Volume (µL)
Restricted insert	0.39
Restricted vector	0.64
Ligase buffer	4
Ligase	1
Nuclease Free Water	13.97
Total	20

Table 2.10: Reaction set-up for rapid ligation reaction (1:3) between pET28a and *Rv0309*

Reagent	Volume (µL)
Restricted insert	0.7
Restricted vector	1.46
Ligase buffer	4
Ligase	1
Nuclease Free Water	2.84
Total	10

Table 2.11: Reaction set-up for rapid ligation reaction (1:5) between pET28a and *Rv0309*

Reagent	Volume (µL)
Restricted insert	1.16
Restricted vector	1.46
Ligase buffer	4
Ligase	1
Nuclease Free Water	2.38
Total	10

2.1.8 Transformation into E. coli DH5α cells

A vial of competent *E. coli* DH5α cells (donated by Pillay, K from UKZN) and the stored ligation mixes were thawed on ice. Thereafter, 50 µL of cells and 5 µL of ligation mix were aliquoted into a sterile centrifuge tube and incubated on ice for 30 minutes (Sambrook and Russell, 2001). The sample was heat shocked in a 42.5°C water bath (FMH Instruments, Cape Town, South Africa) for 45 seconds and then placed on ice for two minutes. Thereafter, 950 µL of super optimal broth with catabolite repression (S.O.C) media (ThermoFisher Scientific™, Massachusetts, USA) was added to the tube and then transferred into a flask, which was incubated (Apex Scientific, KZN, South Africa) at 37°C with agitation for one hour. A total of 150 µL of the culture was spread onto LB agar containing ampicillin (100 mg/mL), that allowed

for the growth of clones containing the selective marker for ampicillin resistance for GST-tagged clones. LB agar plates containing kanamycin (50 mg/mL) were used to grow clones containing the selective marker for kanamycin resistance for His-tagged clones. The remainder of the culture was centrifuged (ThermoFisher Scientific™, Massachusetts, USA), and the pellet was resuspended in approximately 150 µL of supernatant and plated out on LB/Kan agar plates. The plates were incubated (Apex Scientific, KZN, South Africa) overnight at 37°C.

2.1.9 Confirmation of viable clones by colony PCR

Colony PCR (Sambrook and Russell, 2001) was performed to determine if the *Rv0309* gene was present within clones grown on the agar plates.

One colony per plate was transferred into 10 µL of a PCR Mastermix in a PCR tube. Two 'master plates' containing the selected colonies on LB/Amp and LB/Kan plates were incubated (Apex Scientific, KZN, South Africa) at 37°C overnight. Colony PCR was set up as shown in Table 2.12 and Table 2.13.

Table 2.12: Colony PCR set-up for *Rv0309*

Reagent	Volume (µL)	Final Concentration
Q5 Hot Start High – Fidelity 2X Master Mix	5	1 X
Forward Primer (10 µM stock)	1.25	0.5 µM
Reverse Primer (10 µM stock)	1.25	0.5 µM
Nuclease-Free Water	3	

Table 2.13: Thermal cycling conditions

Step		Temperature (°C)	Duration (seconds)
Initial denaturation		98	30
Denaturation	30 cycles	98	10
Annealing		72	30
Extension		72	60
Final extension		72	120

The PCR products were viewed using agarose gel electrophoresis, as described in section 2.1.5.2. Once the expected molecular weight bands were obtained, selected clones were taken forward to make glycerol stocks and for pDNA isolation for transformation into *E. coli* BL21 cells.

2.1.10 Preparation of Rec-Rv0309 glycerol stock culture of clones from E. coli DH5α

A loopful of a colony was used to inoculate LB media and grown overnight at 37°C with shaking at 200 rpm. Aliquots of 750 µL culture were added to 250 µL 50% glycerol and stored (-80 °C).

2.1.11 Isolation of Rec-Rv0309 plasmid DNA

The GeneJET Plasmid Miniprep Kit (ThermoFisher Scientific™, Massachusetts, USA) was used for the isolation of plasmid DNA as described in section 2.1.4.1. and which was stored at -20°C, and used to transform *E. coli* BL21 cells (donated by Pillay, K from UKZN).

2.1.12 Transformation of pDNA into E. coli BL21 cells

Since pET28a is a low-copy plasmid, transformation into *E. coli DH5α* cells was required due to its high transformation efficiency. Once colony PCR was performed, the pDNA isolated from positive transformants was used for transformation into *E. coli* BL21 cells. The *E. coli* BL21 cells are known for producing high-level expression of Rec-proteins. Hence, competent *E. coli* BL21 cells were transformed with pDNA as described for *E. coli DH5α* in section 2.1.8.

2.1.13 Confirmation of viable clones

Colony PCR was performed as described in section 2.1.9 and set up using Tables 2.12 and 2.13 to determine if the *Rv0309* gene was present within clones grown on the plate.

Once bands were reflected the correct fragment size, glycerol stocks were made for the positive clones and stored at -80°C. Positive clones were taken forward to small-scale expression.

2.1.14 Expression of recombinant Rv0309 protein

A small-scale expression of Rec-*Rv0309* protein was performed to determine the optimum isopropyl β-D-1-thiogalactopyranoside (IPTG) (Sigma-Aldrich, California, USA) concentration and duration of induction. The temperature chosen for induction was 25°C as the literature previously stated that Rec-*Rv0309* has a propensity to aggregate and form inclusion bodies (Vasina & Baneyx, 1996; Sahdev et al., 2008; Francis & Page, 2010; San-Miguel et al., 2013; So et al., 2023). A lower induction temperature (25°C) was recommended to prevent aggregation. A loopful of the glycerol stock of the *Rv0309* clone was added to 5 mL LB/Amp media and incubated (Apex Scientific, KZN, South Africa) overnight at 37°C with agitation (180

rpm). The next day, 100 µL of the overnight culture was added to four tubes containing 10 mL of LB/Amp media and incubated (Apex Scientific, KZN, South Africa) at 37°C with agitation (180 rpm) until an optical density $(OD)_{600nm}$ of 0.6 was reached. Thereafter, the flask was placed in a water bath (FMH Instruments, Cape Town, South Africa) set at 16°C for one hour, and 1 mL of culture was collected as T0, centrifuged (Sigma Zentrifugen, Osterode, Germany) at 24 000 x g for five minutes, and the pellet was resuspended in 150 µL of 0.5 M Tris-Cl, pH 6.8 for SDS-PAGE analysis. Four concentrations of IPTG were tested, 0.25, 0.5, 0.75 and 1 mM, and the cultures were induced for five hours (T1-T5). Every hour, 1 mL of the sample was collected from each of the tubes, the OD_{600nm} reading was recorded, and the sample was centrifuged (Sigma Zentrifugen, Osterode, Germany) (24 000 x g, five minutes, room temperature) and the pellet resuspended in 150 µL 0.5 M Tris-Cl, pH 6.8. The optimal time-point was selected when SDS-PAGE reflected the sample with the highest level of expression. The samples were quantified using a NanoDrop 2000 Spectrophotometer (ThermoFisher Scientific™, Massachusetts, USA) for standardisation during SDS-PAGE. The optimal IPTG concentration (0.5 mM IPTG for GST-tagged protein and 0.25 mM IPTG for His-tagged protein) and induction period (3 hours of induction for GST-tagged protein and 4 hours of induction for His-tagged protein) were applied to a large-scale expression that was performed by transferring 10 mL of culture to 1 L of media. After centrifugation at maximum speed for 8 minutes at 4°C, the pellet was stored at 20°C (Sambrook & Russell, 2001).

2.1.15 Analysis of recombinant Rv0309 protein using SDS-PAGE

Two Tris-glycine acrylamide gels were prepared, one for SDS-PAGE and the other for Western blotting (Sambrook & Russell, 2001). The percentage of resolving gels used was based on the size of Rec-proteins. The samples were thawed, and protein concentration was measured using a NanoDrop 2000 Spectrophotometer (ThermoFisher Scientific™, Massachusetts, USA). The samples were normalised to ensure that equivalent concentrations of total protein were loaded into gels to make accurate comparisons. The sample with middle-value concentration was used as a standard for others. The samples were diluted using loading buffer or increased by adding more sample volume using $C_1V_1 = C_2V_2$ calculations. The calculated amounts were added to a centrifuge tube containing a calculated amount of 5X SDS loading dye. The samples were vortexed (Boeco, Hamburg, Germany) and denatured at 95°C using a heat block (FMH Instruments, Cape Town, South Africa) for 10 minutes with occasional vortexing. An amount of 12,5 µL was loaded into the wells into the duplicate gels. Protein sizes were estimated by loading 5 µL of Spectra™ Multicolour Broad Range Protein Ladder (ThermoFisher Scientific™, Massachusetts, USA) into one of the wells. The samples

were electrophoresed at 90 V for two hours and thirty minutes. One gel was stained in a plastic tray containing Coomassie Brilliant Blue (ThermoFisher Scientific™, Massachusetts, USA) while shaking at room temperature for 30 minutes. Thereafter, the gel was destained on a shaker with destaining solution (containing 50% distilled water, 40% methanol and 10% acetic acid) at room temperature (range 20°C-25°C) for one hour, followed by overnight in fresh solution. The gel was viewed and documented using a cell phone camera the next day.

2.1.16 Western blotting

Blotting paper was added to the Bio-Rad Transblot Turbo anode tray (Bio-Rad, California, USA) and hydrated with towbin buffer (Appendix). Nitrocellulose membrane (Bio-Rad, California, USA), cut to size, was placed on top of the wet stack. Towbin buffer was added to the wet membrane. The second SDS-PAGE gel was placed onto the membrane with two additional pieces of blotting paper over the gel. A roller was used to dislodge all the air bubbles. The cathode lid was placed on top of the stack, and the mini turbo protocol (as per manufacturer's sheet) was used to transfer the protein to the nitrocellulose membrane. The nitrocellulose membrane was removed and placed in a clean box.

2.1.16.1 GST-tagged protein

Primary blocking buffer was made with 5% skim milk diluted in phosphate buffered saline (PBS) (Sigma-Aldrich, California, USA) containing Tween-20 (T) (ThermoFisher Scientific™, Massachusetts, USA) and 30 µL GST-Tag Monoclonal Antibody (ThermoFisher Scientific™, Massachusetts, USA). Primary blocking buffer was added to the membrane and incubated at 4ºC overnight.

The membrane was washed with phosphate buffered saline with Tween-20 (PBST) four times for fifteen minutes with shaking, with a buffer change at each interval. The membrane was then submerged in a secondary blocking buffer comprising 30 mL PBST containing 5% skim milk and 6 µL Goat Anti-Mouse IgG Antibody- Horse-radish peroxidase (HRP)-conjugate (Sigma-Aldrich, California, USA) for one hour with shaking. The membrane was washed four times with PBST for fifteen minutes with shaking. The substrate 3,3',5,5' – Tetramethylbenzidine (TMB) (ThermoFisher Scientific™, Massachusetts, USA) was added to the membrane and placed in the dark for 15 minutes. Once the colour developed, the membrane was rinsed in distilled water, viewed and documented using a cell phone camera.

2.1.16.2 His-tagged protein

A blocking buffer prepared with 5% skim milk diluted in PBST (ThermoFisher Scientific™, Massachusetts, USA) was added to the membrane and kept overnight at 4°C. The membrane was washed with PBST three times for five minutes while shaking on ice, with a buffer change at each interval. The membrane was then submerged in a buffer comprising 30 mL PBST with 5% skim milk and 15 µL anti-HIS-peroxidase antibody (Sigma-Aldrich, Darmstadt, Germany). The membrane was incubated for two hours on ice with shaking, followed by washing three times for five minutes with a wash buffer change at each interval. The wash buffer was discarded, and substrate TMB (ThermoFisher Scientific™, Massachusetts, USA) was added to the membrane and placed in the dark for 15 minutes. Once colour developed, the membrane was rinsed in distilled water and documented.

2.1.17 Purification of expressed proteins

When the presence and integrity of protein were confirmed, protein lysis and purification were performed. Prior to purification, protein lysis plays a fundamental role in disrupting the integrity of the cell membrane, allowing the target components within the cell to be accessible during purification.

2.1.17.1 *GST expressed protein*

Purifying the rec-*Rv0309* protein containing a GST-tag was attempted using Pierce™ Glutathione Agarose (ThermoFisher Scientific™, Massachusetts, USA) as per the manufacturer's instructions. Many challenges were encountered during the lysis/purification process, and several optimisation strategies were employed to improve product yield, as highlighted in Table 2.14. These included increasing culture volume to obtain a more highly concentrated pellet, attempting various lysis methods and reagents to optimise the lysate that was taken forward to purification, experimenting with the temperature and pH of buffers, testing different types of purification systems, adjusting the binding time between protein and columns and introducing reagents such as sodium lauroyl sarcosinate (also known as sarkosyl) and 3-((3-cholamidopropyl) dimethylammonio)-1-propanesulfonate (CHAPS) to maintain solubility during the purification process.

Table 2.14: Modified methods for lysis, solubilization and purification of recombinant *Rv0309* protein containing a GST-tag

Original method (Soluble protein preparation)	Method 1 (Soluble protein preparation)	Method 2 (Inclusion body preparation)	Method 3	Method 4	Method 5	Method 6	Method 7
A pellet resulting from a 10 mL culture was used.	A pellet resulting from a 20 mL culture was used.	A pellet resulting from a 50 mL culture was used.	A pellet resulting from a 50 mL culture was used.	2 x pellets resulting from 50 mL cultures were used (one stored at -20°C and other at -80°C).	A pellet resulting from a 50 mL culture was used.	A pellet resulting from a 50 mL culture was used.	16 x pellets resulting from 1 mL cultures were used. (One pellet will be subject to sonication and chemical lysis and the other will be subject to sonication only). Sonication was tested at different durations for optimisation.
PBS lysis was prepared.	Remained the same as original method.	Remained the same as original method.	Remained the same as original method.	Remained the same as original method.	Remained the same as original method.	Remained the same as original method.	Remained the same as original method.
Pellet was thawed on ice and 5 mL PBS Lysis buffer was added and vortexed.	Remained the same as original method.	Remained the same as original method.	Pellet thawed on ice and 2.5 mL PBS Lysis buffer added and vortexed.	2.5 mL PBS Lysis buffer added.	Remained the same as original method.	Remained the same as original method.	PBS was added to one pellet, PBS lysis buffer was added to the other pellet.
Resuspended pellet was incubated on end- over-end rotator for 30 minutes.	Remained the same as original method.	Sample was freeze-thawed three times (freeze -80°C for 3 minutes and thawed at 42°C for 30 seconds) and then vortexed. Centrifuged at 4000 rpm for 15 minutes at 4°C. Supernatant was discarded. The pellet was washed thrice with 1% Triton X-100 (5 mL) and centrifuged at 4000rpm for 15 minutes at 4°C. Final pellet was resuspended in 5 mL solubilization buffer (containing Urea). The solution was incubated at 30°C for one hour.	Volumes of 1% Triton X-100 and Solubilisation buffer added were decreased from 5 mL to 2.5 mL.	For freeze-thaw step, sample thawed at room temperature. 2.5 mL of 1% Triton X-100 and Solubilisation buffer added. Solution incubated on ice not 30°C for one hour.	Sample was freeze-thawed three times (freeze at -80°C for 3 minutes and thawed at 42°C for 30 seconds) and then vortexed. Centrifuged at 4000 rpm for 15 minutes at 4°C. Supernatant was stored not discarded to be analysed on SDS-PAGE.	Sample was freeze-thawed three times (freeze at -80°C for 3 minutes and thawed at 42°C for 30 seconds) and then vortexed. Centrifuged at 4000 rpm for 15 minutes at 4°C. Supernatant was used for purification.	Added 100 µL of PBS (mechanical lysis) / PBS lysis buffer (mechanical and chemical lysis) to resuspend pellet. Placed microcentrifuge tubes on ice for 1 minute. Sonicate for 10 seconds, 20 seconds, 30 seconds, 40 seconds, 50 seconds, 1 minute, 5 minutes and 10 minutes Place microcentrifuge tubes on ice for 2 minutes. Added Triton X-100 and mix gently at room temperature for 30 minutes to solubilise proteins. Sonication performed using ultrasonic water bath.

Table 2.14: Modified methods for lysis, solubilization and purification of recombinant *Rv0309* protein containing a GST-tag (continued)

Original method (Soluble protein preparation)	Method 1 (Soluble protein preparation)	Method 2 (Inclusion body preparation)	Method 3	Method 4	Method 5	Method 6	Method 7
100 µL was taken for analysis as "total lysate" for visualization of SDS-PAGE.	Remained the same as original method.	Remained the same as original method.	Remained the same as original method.	Remained the same as original method.	Remained the same as original method.	Remained the same as original method.	Remained the same as original method.
Total lysate was centrifuged at 4000 rpm at room temperature for 30 minutes.	Remained the same as original method.	Remained the same as original method.	Remained the same as original method.	Remained the same as original method.	N/A	N/A	Centrifuge crude extract at 10 000 x g for 5 minutes at 4°C.
Supernatant was carefully collected and stored at -20°C as "clear lysate".	Remained the same as original method.	Supernatant was carefully collected and stored at -20°C as "solubilized protein" The supernatant (5 mL) was then loaded into ThermoScientific™Snake Skin™ Dialysis Tubing and dialysed for one hour at room temperature in 1500 mL of Tris-NaCl buffer on a stirrer. The buffer was discarded and fresh buffer of 1500 mL was added and dialysed for another hour. Thereafter, the buffer was discarded, and fresh buffer added again (1500 mL) and incubated at 4°C for four hours with magnetic stirrer. Once incubation was completed, the solution was aspirated and stored as "dialysed protein" at -20°C. An amount of 100 µL was collected for SDS analysis.	Remained the same as original method.	Supernatant was carefully collected and stored at -20°C as "solubilized protein". No dialysis was done.	Supernatant that was not discarded in steps above was concentrated using Amicon®Ultra15 Centrifugal Filter Units (as per manufacturer's sheet).	N/A	Remained the same as original method.
Purification as per Pierce protocol.	Remained the same as original method.	Remained the same as original method.	Remained the same as original method.	Remained the same as original method.	Remained the same as original method.	Binding time increased from two hours to four hours.	Binding time increased to six hours.

Table 2.14: Modified methods for lysis, solubilization and purification of recombinant *Rv0309* protein containing a GST-tag (continued)

Original method (Soluble protein preparation)	Method 8 (Purifying vector on its own to see if agarose column is functioning well) alongside rec-protein	Method 9 (Adjusting pH of buffers during purification based on pI of protein)	Method 10 (ÄKTA purification trial)	Method 11 (Ion-Exchange trial)	Method 12 (Size-Exclusion trial)	Method 13 (Overnight binding)	Method 14 (CHAPS & Sarkosyl)
A pellet resulting from a 50 mL culture was used.	A pellet resulting from a 50 mL culture (pGEX-6P-1) was used.	A pellet resulting from a 50 mL culture was used.	A pellet resulting from a 50 mL culture was used.	A pellet resulting from a 1 mL cultures were used.	A pellet resulting from a 50 mL culture was used.	A pellet resulting from a 50 mL culture was used.	A pellet resulting from a 50 mL culture was used.
PBS lysis was prepared.	Remained the same as original method.	Remained the same as original method.	Substituted DTT for β-mercaptoethanol.	Tried both PBS-Lysis buffer and Tris-NaCl.	Remained the same as original method.	Remained the same as original method.	Remained the same as original method with an addition of CHAPS and DNase I.
Pellet was thawed on ice and 5 mL PBS Lysis buffer was added and vortexed.	Remained the same as original method.	Remained the same as original method.	Remained the same as original method.	Added 400 µL of each buffer into different pellet microcentrifuge tubes. Sonicated using sonicator OMNI SONIC RUPTOR 400. Pulsed 5 times each x 5 rounds.	15 mL PBS Lysis buffer was added.	Remained the same as original method.	Remained the same as original method.
Resuspended pellet was incubated on end-over-end rotator for 30 minutes.	Placed tubes on ice for 1 minute. Sonicated for 5 minutes. Placed tubes on ice for 2 minutes. Added Triton X-100 and mixed gently at room temperature for 30 minutes to solubilise proteins.	Placed tubes on ice for 1 minute. Sonicated using ultrasonic water bath for 5 minutes. Placed tubes on ice for 2 minutes. Added Triton X-100 and mixed gently at room temperature for 30 minutes to solubilise proteins.	Placed tubes on ice for 1 minute. Sonicated using probe sonicator for 5 minutes. Placed tubes on ice for 2 minutes. Added Triton X-100 and mixed gently at room temperature for 30 minutes to solubilise proteins.	N/A	Tubes were sonicated for three minutes.	Placed tubes on ice for 1 minute. Sonicated using probe sonicator for 5 minutes. Placed tubes on ice for 2 minutes. Added Triton X-100 and mixed gently at room temperature for 30 minutes to solubilise proteins.	Resuspended pellet on end-over-end rotator for 30 minutes. Aliquoted into microcentrifuge tubes. Sonicated using Precellys on the lowest setting and then incubated on ice for 30 minutes.

Table 2.14: Modified methods for lysis, solubilization and purification of recombinant *Rv0309* protein containing a GST-tag (continued)

Original method (Soluble protein preparation)	Method 8 (Purifying vector on its own to see if agarose column is functioning well)	Method 9 (Adjusting pH of buffers during purification based on pI of protein)	Method 10 (ÄKTA purification trial)	Method 11 (Ion-Exchange trial)	Method 12 (Size-Exclusion trial)	Method 13 (Overnight binding)	Method 14 (CHAPS & Sarkosyl)
100 µL was taken for analysis as "total lysate" for visualization of SDS-PAGE.	Remained the same as original method.	Remained the same as original method.	Remained the same as original method.	N/A	N/A	Remained the same as original method.	Remained the same as original method.
Total lysate was centrifuged at 4000 rpm at room temperature for 30 minutes.	Centrifuged crude extract at maximum speed for 10 minutes at 4°C.	Centrifuged crude extract at maximum speed for 10 minutes at 4°C.	N/A	Centrifuged microcentrifuge tubes at 12 000 rpm at 4°C for 10 minutes.	Centrifuged microcentrifuge tubes for 10 minutes at 4°C 5000 rpm.	N/A	Centrifuged at 20 000 x g; 20 minutes at 4°C.
Supernatant was carefully collected and stored at -20°C as "clear lysate".	Remained the same as original method.	Remained the same as original method.	N/A	Collected supernatant (soluble fraction) and pellet (inclusion bodies) Pellet was solubilised using 50 µL Urea and Tris-NaCl.	Size exclusion Chromatography was performed.	N/A	Remained the same as original method.
Purification as per Pierce protocol.	Remained the same as original method.	Adjusted pH of buffers to a pH lower than pI of protein.	ÄKTA purification was performed.	Ion-Exchange Chromatography.	ÄKTA purification was performed.	As per Pierce protocol, with modification of letting protein bind overnight at 4°C.	As per Pierce protocol, with modification of lysis buffer used for wash steps, sarkosyl added to elution buffer.

Table 2.14: Modified methods for lysis, solubilization and purification of recombinant *Rv0309* protein containing a GST-tag (continued)

Original method (Soluble protein preparation)	Method 15 (Sarkosyl only)
A pellet resulting from a 10 mL culture was used.	A pellet resulting from a 50 mL culture was used.
PBS lysis buffer was prepared	Remained the same as original method with an addition of 1% SDS.
Pellet was thawed on ice and 5mL PBS lysis buffer was added and vortexed.	Remained the same as original method.
Resuspended pellet was incubated on end-over-end rotator for 30 minutes.	Resuspended pellet on end-over-end rotator for 30 minutes. Aliquoted into microcentrifuge tubes. Sonicated using Precellys on the lowest setting and then incubated on ice for 30 minutes.
100 µL was taken for analysis as "total lysate" for visualization of SDS-PAGE	Remained the same as original method.
Total lysate was centrifuged at 4000 rpm at room temperature for 30 minutes.	Centrifuged at 20 000 x g; 20 minutes at 4°C.
Supernatant was carefully collected and stored at -20°C as "clear lysate".	Remained the same as original method.
Purification as per Pierce protocol.	As per Pierce protocol, with modification of lysis buffer used for wash steps, sarkosyl added to elution buffer.

2.1.17.2 His-tag expressed protein

Purification of the Rec-*Rv0309* protein that contained a His-tag was attempted using multiple methods outlined in Table 2.15. Conventional methods were initially attempted, such as using Bacterial Protein Extraction Reagent (B-PER) as a lysis buffer and using ÄKTA start™ to purify the protein. The ÄKTA start™ is a preparative chromatography system for laboratory scale protein purification Thereafter, different strategies were attempted to improve lysis, such as harsher sonication, lysing with reagent overnight and using different reagents to make up the lysis buffer. Denaturing trials were also performed using guanidine hydrochloride (G-HCl). Thereafter, an attempt based on published success with Rec-Rv0309 was performed. Various purification systems were used to optimise purification. Additionally, a purification trial was performed in a 4°C walk-in fridge. Peptide mass fingerprinting was performed on excised target band in eluent lane to sequence protein and determine mass.

Table 2.15: Modified methods for lysis, solubilization and purification of recombinant Rv0309 protein containing a His-tag

	Method 1	Method 2	Method 3	Method 4	Method 5	Method 6
Amount of culture used to make pellet	100 mL	100 mL	100 mL	100 mL	100 mL	100 mL
Lysis buffer added	B-PER reagent	B-PER reagent	Tris, KCl, Glycerol, PMSF, Triton X-100 added to pellet and left overnight Freeze-Thaw step included the next day	Tris, KCl, Glycerol, PMSF, Triton X-100 added to pellet and left overnight Freeze-Thaw step included the next day	Lysozyme added to pellet and left overnight. Tris, KCl, Glycerol, PMSF, Triton X-100 added the next day.	Lysozyme added to pellet and left overnight. Tris, KCl, Glycerol, PMSF, Triton X-100 added the next day.
Sonication	Sonicated on ice at 30 second intervals for two minutes	Sonicated on ice using harsher mode.	Sonicated on ice at 30 second intervals for two minutes	Sonicated on ice at 30 second intervals for two minutes	Sonicated on ice at 30 second intervals for two minutes	Sonicated on ice at 30 second intervals for two minutes
Centrifugation	20 000 x g for 1 hour at 4°C	20 000 x g for 1 hour at 4°C	20 000 x g for 1 hour at 4°C	20 000 x g for 1 hour at 4°C	20 000 x g for 1 hour at 4°C	20 000 x g for 1 hour at 4°C
Supernatant collected as "clear lysate".	Clear lysate collected and used for purification steps.	Clear lysate collected and used for purification steps.	Clear lysate collected and used for purification steps.	Clear lysate collected and used for purification steps.	Clear lysate collected and used for purification steps.	Clear lysate collected and used for purification steps.
Purification methods were followed as per Manufacturer's sheet	ÄKTA™ purification using Ni-NTA cartridge	ÄKTA™ purification using Ni-NTA cartridge	ÄKTA™ purification using Ni-NTA cartridge	ÄKTA™ purification using HisPur Cobalt cartridge	Ni-NTA beads	Size Exclusion Chromatography

Table 2.15: Modified methods for lysis, solubilization and purification of recombinant Rv0309 protein containing a His-tag (continued)

	Method 7	**Method 8**	**Method 9**	**Method 10**	**Method 11**	**Method 12 (Based off Kumar *et al.*, 2013 method)**
Amount of culture used to make pellet	100 mL	100 mL	100 mL	100 mL	100 mL	100 mL
Lysis buffer added	Lysozyme added to pellet and left overnight. Tris, KCl, Glycerol, PMSF, Triton X-100 added the next day.	Equilibrium/Wash buffer (containing sodium phosphate, sodium chloride and imidazole used as lysis buffer	PBS, lysozyme, DTT, PMSF, SDS, Triton X-100 added to pellet as lysis buffer	Equilibrium/Wash buffer (containing sodium phosphate, sodium chloride and imidazole with an addition Guanidine hydrochloride to test under denaturing conditions	Lysozyme added to pellet and left overnight. Tris, KCl, Glycerol, PMSF, Triton X-100 added the next day along with Guanidine hydrochloride	Tris-HCl pH 7.9, 500 mM NaCl, 5 mM Imidazole, 1mM PMSF and lysozyme was added. Sample was left to incubate on ice for an hour. Thereafter, the sample was passed through a 0.8 mm needle syringe five times
Sonication	Sonicated on ice at 30 second intervals for two minutes	Sonicated on ice at 30 second intervals for two minutes	Sonicated on ice at 30 second intervals for two minutes	Sonicated on ice at 30 second intervals for two minutes	Sonicated on ice at 30 second intervals for two minutes	Sonicated on ice at 30 second intervals for two minutes
Centrifugation	20 000 x g for 1 hour at 4°C	20 000 x g for 1 hour at 4°C	20 000 x g for 1 hour at 4°C	20 000 x g for 1 hour at 4°C	20 000 x g for 1 hour at 4°C	20 000 x g for 1 hour at 4°C
Supernatant collected as "clear lysate"	Clear lysate collected and used for purification steps.	Clear lysate collected and used for purification steps.	Clear lysate collected and used for purification steps.	Clear lysate collected and used for purification steps.	Clear lysate collected and used for purification steps.	Clear lysate collected and used for purification steps.
Purification methods were followed as per Manufacturer's sheet	HisPur Cobalt agarose using gravity flow columns	HisPur Cobalt agarose using gravity flow columns	HisPur Cobalt agarose using gravity flow columns	HisPur Cobalt columns -denaturing	HisPur Cobalt columns - denaturing	Ni-NTA column

Table 2.15: Modified methods for lysis, solubilization and purification of recombinant Rv0309 protein containing a His-tag (continued)

	Method 13
Amount of culture used to make pellet	100 mL
Lysis buffer added	PBS, lysozyme, DTT, PMSF, SDS, Triton X-100 added to pellet as lysis buffer
Sonication	Sonicated on ice at 30 second intervals for two minutes
Centrifugation	20 000 x g for 1 hour at 4°C
Supernatant collected as "clear lysate"	Clear lysate collected and used for purification steps.
Purification methods were followed as per Manufacturer's sheet	HisPur Cobalt agarose using gravity flow columns at 4°C

2.1.18 Bioinformatics analysis

Although bioinformatics was not a part of the main objectives for this project, basic computational analysis was undertaken to determine possible reasons for the challenges with Rec-*Rv0309* protein purification. Academic experts provided their input and hydrophobicity was speculated to be the main reason. Therefore, bioinformatic tools relating to hydrophobicity were used. The tools used were the grand average of hydropathy (GRAVY) calculator, ThermoFisher Scientific peptide analysis tool and PHYRE2 software.

CHAPTER THREE: RESULTS

3.1 Cloning, expression and purification of *Rv0309* gene into pGEX-6P-1 and pET28a vectors

3.1.1. Signal peptide analysis of Rv0309 sequence

The *Rv0309* sequence was analysed using SignalP 6.0 software to determine the signal peptide region within sequence. The amino acids present in the signal peptide were removed during primer design. The cleavage site was found to be between positions 15 and 16 on the protein sequence (Figure 3.1). This indicated that 15 amino acids could be removed in the design as they formed part of hydrophobic transmembrane region of sequence.

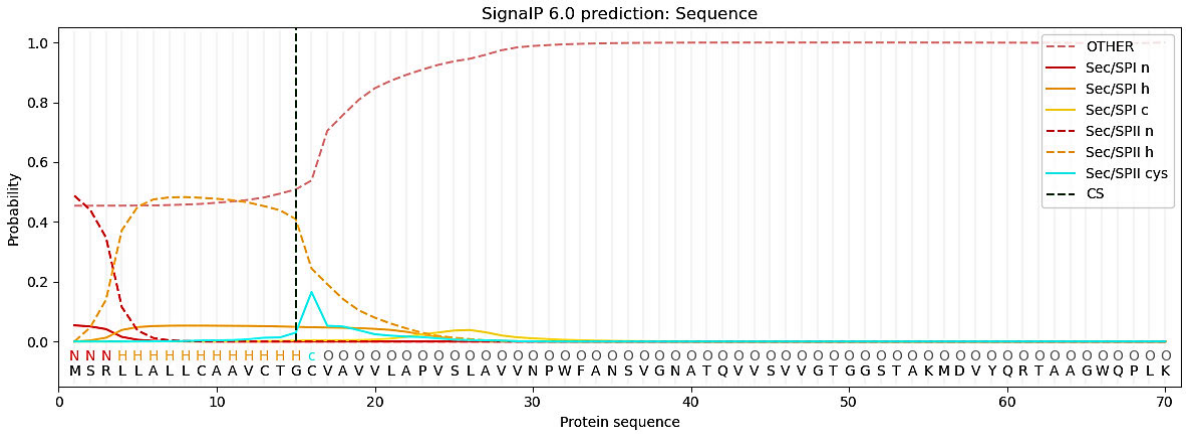

Figure 3.1: Signal peptide analysis of *Rv0309* sequence generated using SignalP 6.0 software (available at: https://services.healthtech.dtu.dk/services/SignalP-6.0/).

3.1.2 Polymerase chain reaction amplification of Rv0309 gene

The concentration of the Mtb H37Rv DNA extracted using the CTAB-NaCl protocol was measured by a Nanodrop and was calculated as 2324 ng/µL. The DNA was diluted to 50 ng/µL using nuclease-free water. Thereafter, the DNA was stored at -20°C.

Since the melting temperature (72°C) of primers was high, Q5 Hot-Start Fidelity 2 X Master Mix (NEB, Massachusetts, USA) was used as it is thermostable during the reaction. Polymerase chain reaction was performed to amplify the *Rv0309* gene without the signal peptide. A clear, concise band was observed in each test lane between 500 base pairs (bp) and 700 bp, indicating the target gene. The *Rv0309* gene without signal peptide was

approximated to be 612 bp in size (Figure 3.2). The negative control showed no bands or smears, indicating no contamination in the master mix. Since the same primers were used for both vectors, the bulked-up insert was used for cloning into pGEX-6P-1 and pET28a.

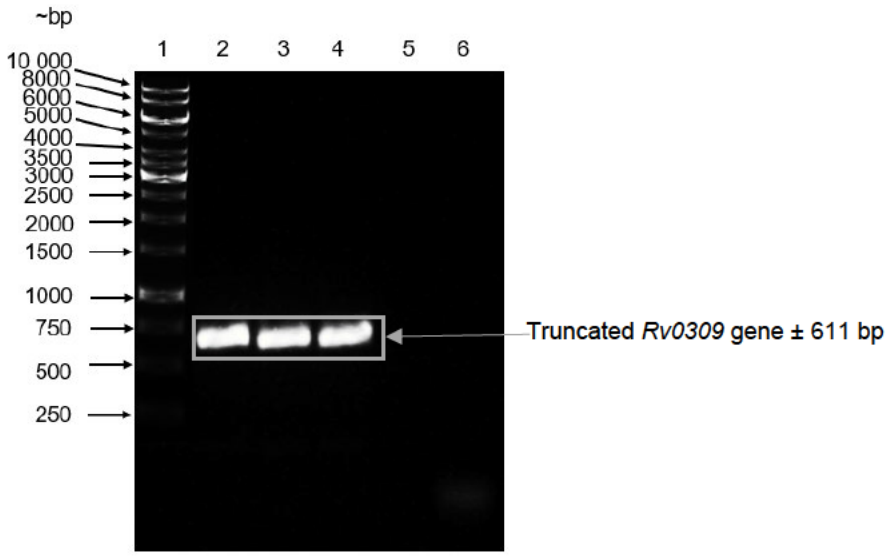

Figure 3.2: Agarose gel electrophoresis of amplified *Rv0309* truncated gene using PCR. Samples were electrophoresed and viewed using a 1.5% (w/v) agarose gel. Each sample contained loading dye made from TriTrack DNA loading dye (6X) added to GelRed. Lane 1: Thermo Scientific™ GeneRuler 1 kb DNA ladder, Lane 2 to Lane 4: amplified *Rv0309* gene, Lane 5: Blank, Lane 6: Negative control (distilled water used as template).

3.1.3 Analysis of purified Rv0309 PCR products

The pooled and purified PCR products were analysed on 1.5% agarose gel to ensure the purity of samples before restriction digestion, thus eliminating potential challenges in downstream processes. The bright and distinct band (Lane 2, Figure 3.3) confirmed integrity to be uncompromised; therefore, the pooled PCR insert product was used for cloning with pET28a.

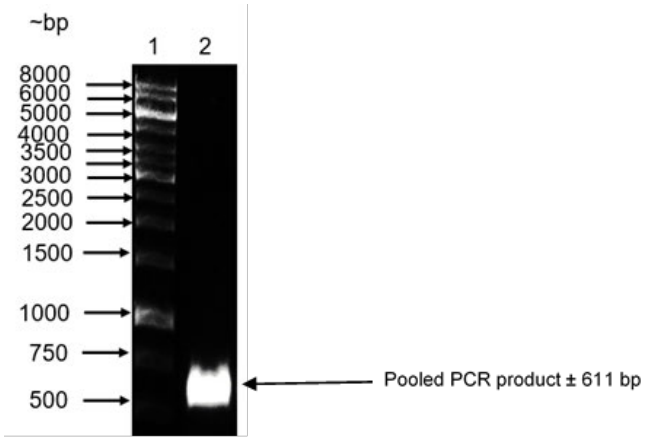

Figure 3.3: Agarose gel electrophoresis of pooled PCR product. Samples were electrophoresed and viewed using a 1.5% (w/v) agarose gel. Each sample contained loading dye made from TriTrack DNA loading dye (6X) added to GelRed**.** Lane 1: Thermo Scientific™ GeneRuler 1 kb DNA ladder, Lane 2: pooled truncated *Rv0309* PCR product.

3.1.4 Plasmid DNA preparation

The electrophoresis of the plasmid DNA of pGEX-6P-1 revealed three bands (Figure 3.4). The three bands indicate different conformations of plasmid, which are linear, nicked and supercoiled. Three distinct bands were also expected and seen for electrophoresis of pET28a pDNA (Figure 3.5).

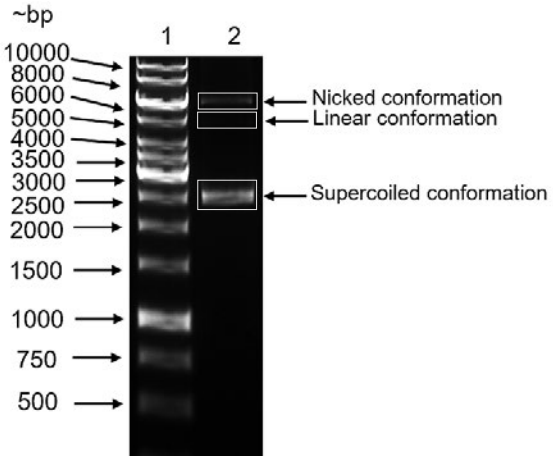

Figure 3.4: Agarose gel electrophoresis of pGEX-6P-1 plasmid DNA. Plasmid DNA was electrophoresed and viewed using a 0.8% (w/v) agarose gel. The sample contained loading dye made from TriTrack DNA loading dye (6X) added to GelRed**.** Lane 1: Thermo Scientific™ GeneRuler 1 kb DNA ladder, Lane 2: pGEX-6P-1 pDNA.

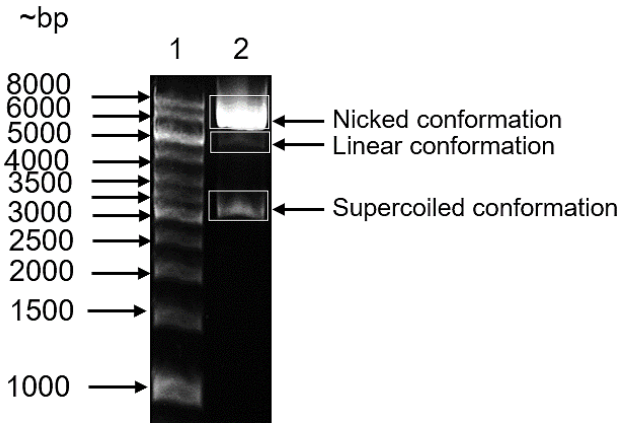

Figure 3.5: Agarose gel electrophoresis of pET28a plasmid DNA. Plasmid DNA was electrophoresed and viewed using a 0.8% (w/v) agarose gel. The sample contained loading dye made from TriTrack DNA loading dye (6X) added to GelRed. Lane 1: Thermo Scientific™ GeneRuler 1 kb DNA ladder, Lane 2: pET28a pDNA.

3.1.5 Restriction digestion of Rv0309 insert, pGEX-6P-1 and pET28a

The DNA of *Rv0309* insert and both vectors was digested by the enzymes BamHI and EcoRI (Figure 3.6 and Figure 3.7). The expected result was a single band for each restricted product. The unrestricted insert presented with one band; therefore, it is difficult to confirm whether the restriction was successful for the insert based on the gel image. The restricted insert reflected a bright single band similar to the unrestricted insert sample (Figure 3.6 and Figure 3.7). The restricted insert appeared higher up than the unrestricted insert (Figure 3.6), but both appear to have the same size (± 611 bp) in Figure 3.7. The concentration of insert DNA appeared lower for pET28a compared to pGEX-6P-1. The restricted vectors displayed a bright single band, indicating restriction was successful for both vectors.

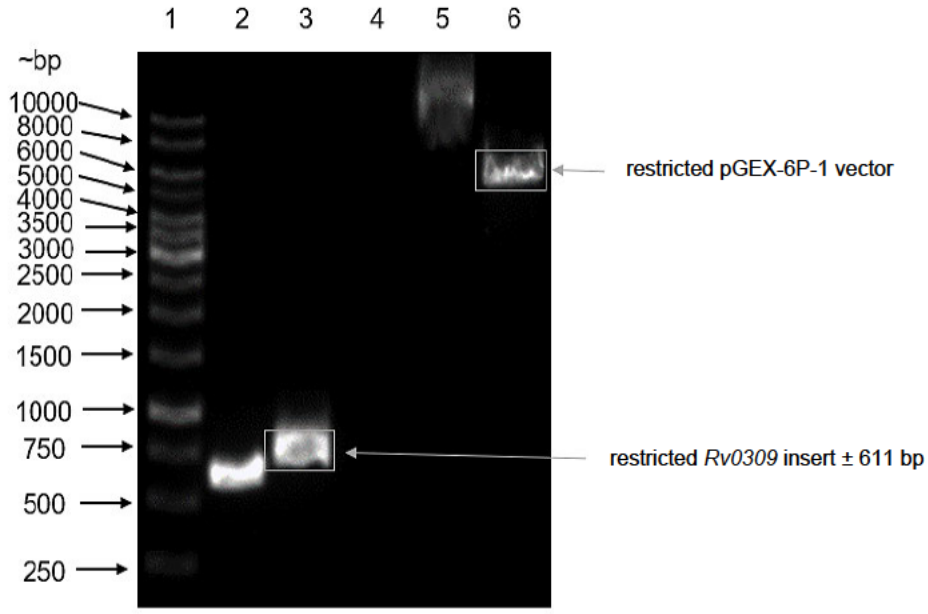

Figure 3.6: Agarose gel electrophoresis of restricted products for *Rv0309* and pGEX-6P-1. Samples were electrophoresed and viewed using a 0.8% (w/v) agarose gel. BamHI and EcoRI Fast Digest enzymes were used for the restriction digestion reaction. Lane 1: Thermo Scientific™ GeneRuler 1 kb DNA, Lane 2: unrestricted *Rv0309* insert, Lane 3: restricted *Rv0309* insert, Lane 4: Blank, Lane 5: unrestricted pGEX-6P-1 vector, Lane 6: restricted pGEX-6P-1 vector.

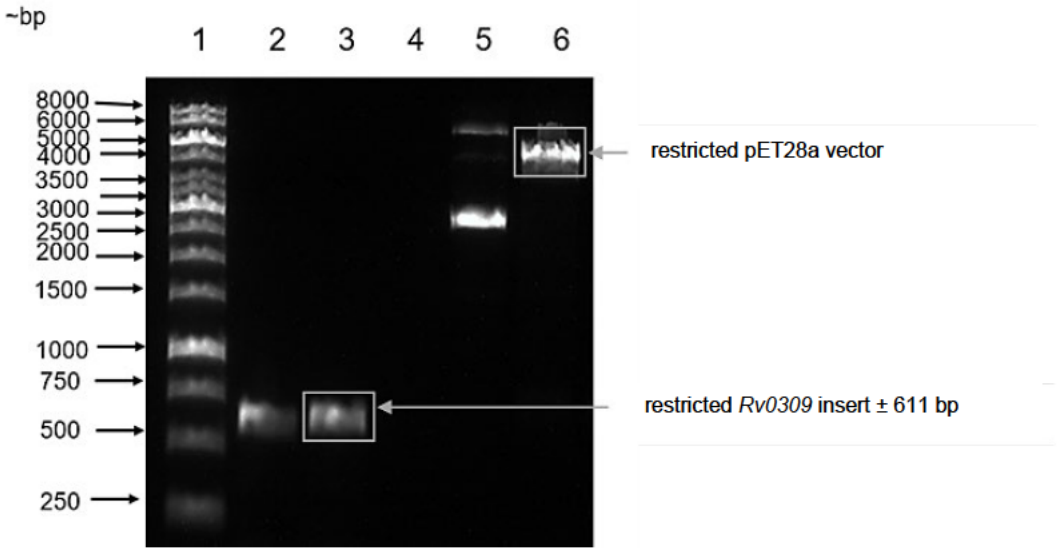

Figure 3.7: Agarose gel electrophoresis of restricted products for *Rv0309* and pET28a. Samples were electrophoresed and viewed using a 0.8% (w/v) agarose gel. BamHI and EcoRI Fast Digest enzymes were used for the restriction digestion reaction. Lane 1: Thermo Scientific™ GeneRuler 1 kb DNA, Lane 2: unrestricted *Rv0309* insert, Lane 3: restricted *Rv0309* insert, Lane 4: Blank, Lane 5: unrestricted pET28a vector, Lane 6: restricted pET28a vector.

3.1.6 Confirmation of clones post ligation and transformation

3.1.6.1 The pGEX-6P-1-Rv0309 clones

Following transformation into *E. coli* BL21 cells and plating, numerous colonies were obtained, of which six were selected for screening using colony PCR. All colonies (Lanes 3-8) screened positive for the *Rv0309* insert (Figure 3.8), confirming that the gene was cloned successfully into the pGEX-6P-1 vector. Colony 3 in Lane 5 produced the most intense bright band, and was therefore chosen to grow up as a starter culture to produce a glycerol stock, prepare a master plate, and for small-scale expression of the recombinant *Rv0309* protein.

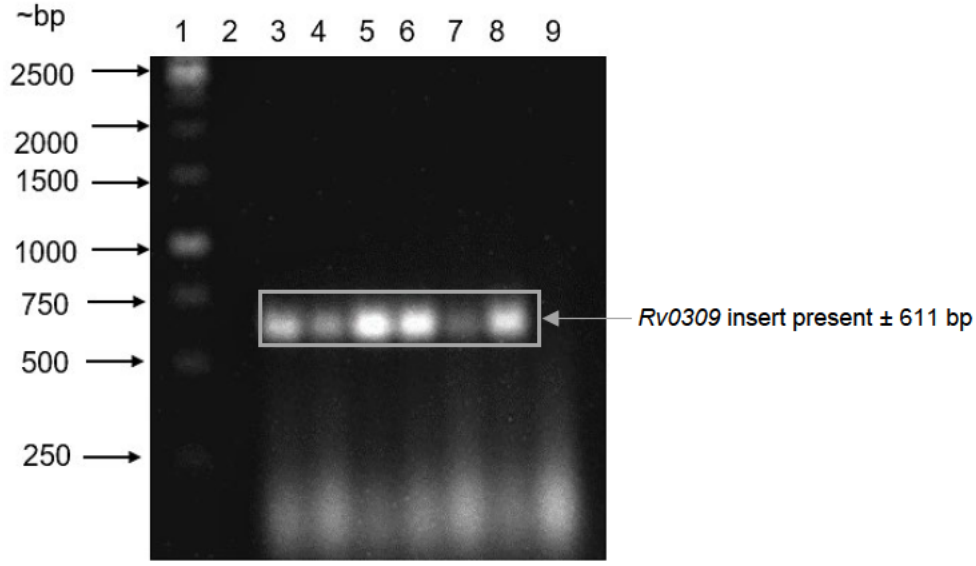

Figure 3.8: Colony PCR confirmation of positive pGEX-6P-1-*Rv0309* transformants after transformation into *E. coli* BL21 cells. Chemically competent *E. coli* BL21 cells were used during transformation to allow for high-level protein expression and better induction. Samples were electrophoresed in a 1% (w/v) agarose gel. Lane 1: Thermo Scientific™ GeneRuler 1 kb DNA ladder, Lane 2: Blank, Lane 3: colony 1, Lane 4: colony 2, Lane 5: colony 3, Lane 6: colony 4, Lane 7: colony 5, Lane 8: colony 6, Lane 9: Negative control (distilled water used as template).

3.1.6.2 The pET28a-Rv0309 clones

The colony PCR results revealed positive transformants (Figure 3.9) for seven colonies (Lanes 2,3,4,7,8,11 & 12) when transformed in *E. coli DH5α* cells. Lane 10 showed an unexpected distinct band around 400 bp region. Each positive transformant varied in band intensity and size. The colony represented in Lane 3 from the 1:3 plate with a high band concentration and expected size was used to grow the overnight culture for pDNA isolation before transforming into *E. coli* BL21 cells.

Transformation into *E. coli* BL21 cells resulted in many colonies on the lysogeny broth/kanamycin (LB/Kan) agar plate. The twelve colonies selected for screening tested positive for *Rv0309* insert by colony PCR (Figure 3.10), confirming that the *Rv0309* gene was cloned successfully into pET28a. The colony represented in Lane 2 was cultured to prepare glycerol stocks and a master plate for storage, as well as a starter culture for small-scale expression of the recombinant *Rv0309* protein.

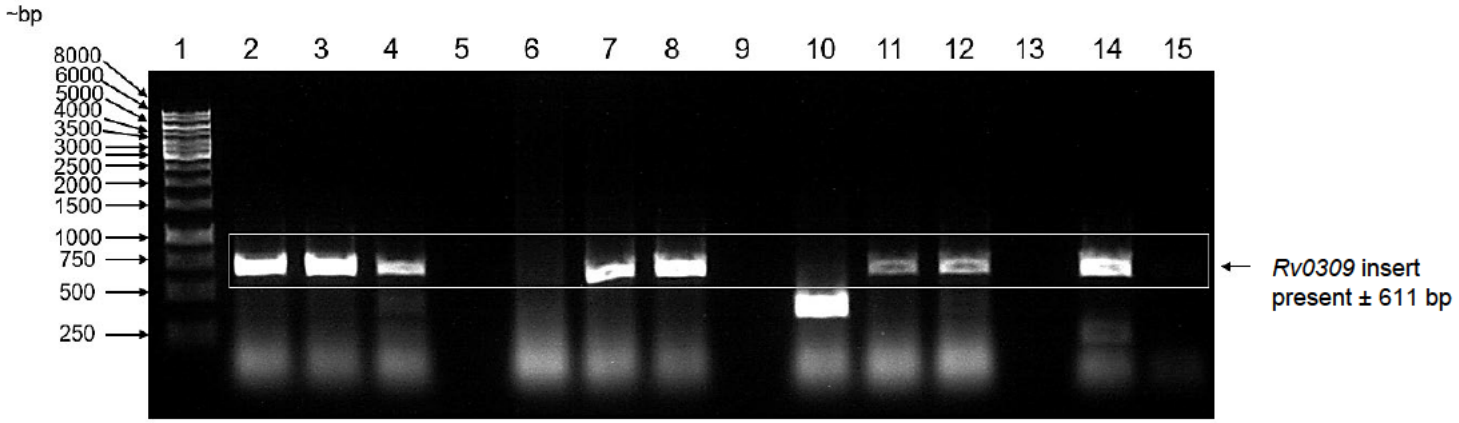

Figure 3.9: Colony PCR confirmation of *pET28a-Rv0309* positive transformants in *E. coli* DH5α cells. The pET28a-*Rv0309* ligation mixtures were transformed into chemically competent *E. coli* DH5α cells to maximise transformation efficiency. Samples were electrophoresed on a 1% (w/v) agarose gel. Lane 1: Thermo Scientific™ GeneRuler 1 kb DNA ladder, Lane 2-4: colonies from 1:3 plate, Lane 5: Blank, Lane 6-8: colonies from 1:5 plate, Lane 9: Blank, Lane 10-12: colonies from 1:3 resuspended plate, Lane 13: Blank, Lane 14: Positive control, Lane 15: Negative control (distilled water used as template).

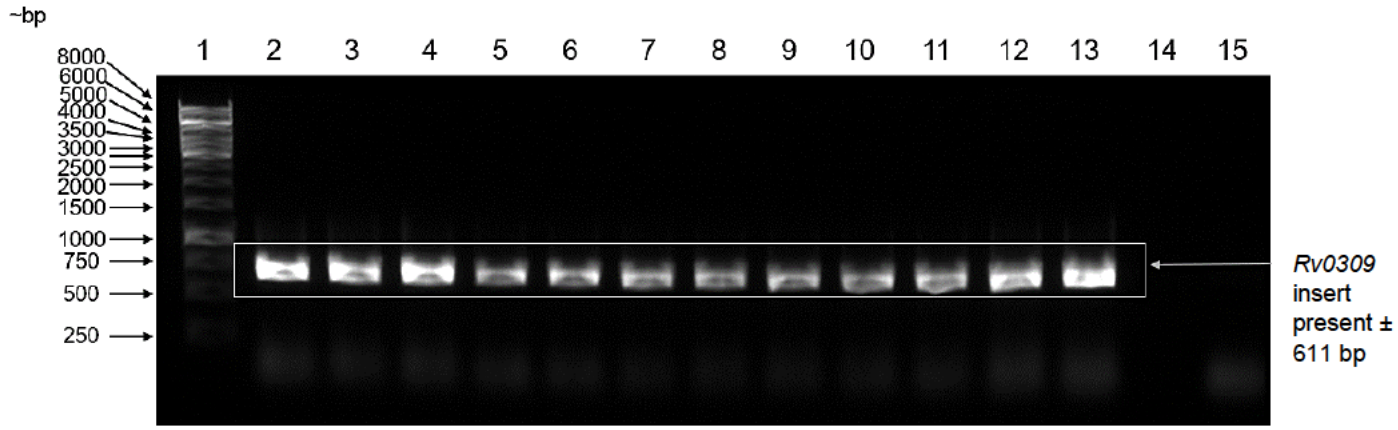

Figure 3.10: Colony PCR confirmation of pET28a-*Rv0309* positive transformants after transformation from *E. coli* DH5α into *E. coli* BL21 cells. Chemically competent *E. coli* BL21 cells were used to allow for high-level protein expression and better induction. Samples were electrophoresed on a 1% agarose gel. Lane 1: Thermo Scientific™ GeneRuler 1 kb DNA ladder, Lane 2-13: colonies from the plate, Lane 14: Blank, Lane 15: Negative control (distilled water was used as template).

3.1.7 Expression of recombinant Rv0309 proteins

The small-scale protein expression of recombinant GST-tagged protein revealed the following optimum conditions: induction temperature, 25°C; IPTG induction concentration, 0.5 mM and induction period, five hours (Figure 3.11). The induced bands were seen at ±45 kDa, whilst the expected size of the recombinant *Rv0309* combined with the GST-tag was ±48 kDa. The optimum conditions for the expression of the His-tagged-Rec-*Rv0309* protein were: induction temperature, 25°C; IPTG induction concentration; 0.25 mM and the induction period, four hours (Figure 3.12). The induced bands were present at ±25 kDa, whilst the size of the expected recombinant *Rv0309* with the His-tag was ±22 kDa. Molecular weight can vary when comparing calculated and observed values (Guan et al., 2015; Thermofisher Scientific, 2023b). This suggests that the bands were within the expected region. The expression was successful, as evidenced by a time dependent increase from T1 to T5 for both recombinant proteins (Figures 3.11 and 3.12).

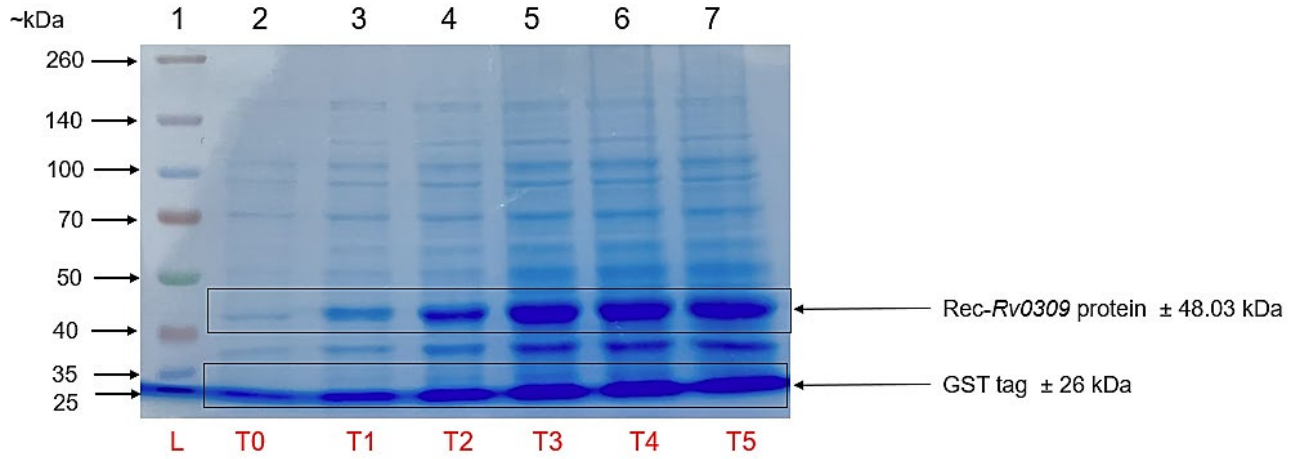

Figure 3.11: SDS-PAGE gel showing small-scale expression of recombinant *Rv0309* in pGEX-6P-1 vector. Once the OD reached ~0.6, flasks containing Lysogeny Broth/Ampicillin cultures with Rec-*Rv0309* were induced with 0.5 mM IPTG for 5 hours at 25°C. A volume of 1 mL culture was taken for analysis every hour, centrifuged, and pellet resuspended in 150 µL of 0.5 M Tris-HCl pH 6.5. Samples were normalised and then electrophoresed using a 10% reducing Tris-glycine SDS-PAGE gel stained with Coomassie blue.

Lane 1: Thermo Scientific Spectra Multicolour Broad Range Protein Ladder (L), Lane 2: Sample before IPTG induction (T0), Lane 3: Sample after one hour of IPTG induction (T1), Lane 4: Sample after two hours of IPTG induction (T2), Lane 5: Sample after three hours of IPTG induction (T3), Lane 6: Sample after four hours of IPTG induction (T4), Lane 7: Sample after five hours of IPTG induction (T5).

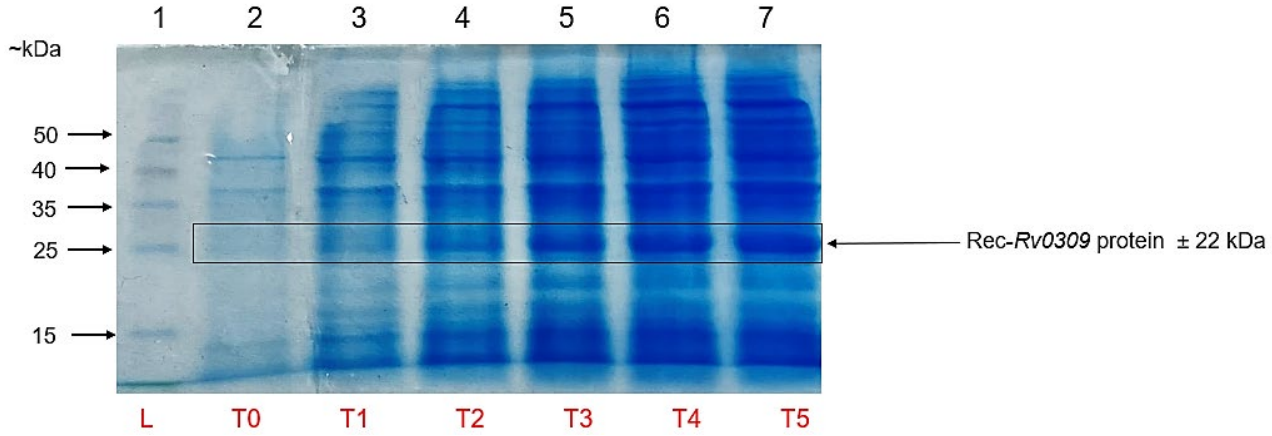

Figure 3.12: SDS-PAGE gel showing small-scale expression of recombinant *Rv0309* in pET28a vector. Once the OD reached ~0.6, flasks containing Lysogeny Broth/Kanamycin cultures with Rec-*Rv0309* were incubated on ice for one hour. Samples were then induced with 0,25 M IPTG for 5 hours at 25°C. A volume of 1 mL culture was taken for analysis every hour, centrifuged, and pellet resuspended in 150 µL of 0.5 M Tris-HCl pH 6.5. Samples were electrophoresed using an 18% reducing Tris-glycine SDS-PAGE gel stained with Coomassie blue. Lane 1: Thermo Scientific Spectra Multicolour Broad Range Protein Ladder (L), Lane 2: Sample before IPTG induction (T0), Lane 3: Sample after one hour of IPTG induction (T1), Lane 4: Sample after two hours of IPTG induction (T2), Lane 5: Sample after three hours of IPTG induction (T3), Lane 6: Sample after four hours of IPTG induction (T4), Lane 7: Sample after five hours of IPTG induction (T5).

Western blotting confirmed that the expressed bands in expected regions were that of recombinant *Rv0309* protein containing GST-tag (Figure 3.13) and His-tag (Figure 3.14), respectively.

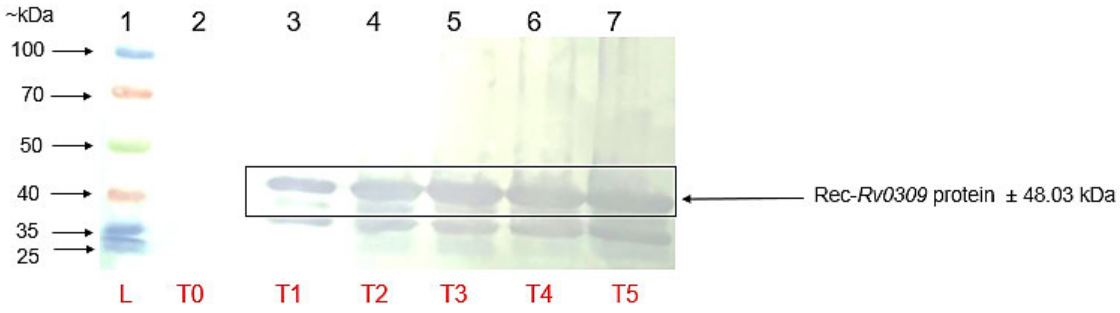

Figure 3.13: Western blot showing recombinant *Rv0309* in pGEX-6P-1 vector before purification. The nitrocellulose membrane was incubated with GST-Tag Monoclonal Antibody (1:1000) followed by secondary antibody Goat Anti-Mouse IgG Antibody, HRP conjugate (1:5000). The reaction was detected using 3,3',5,5'-tetramethylbenzidine blotting solution. Lane 1: Thermo Scientific Spectra Multicolour Broad Range Protein Ladder, Lane 2: Sample before IPTG induction (T0), Lane 3: Sample after one hour of IPTG induction (T1), Lane 4: Sample after two hours of IPTG induction (T2), Lane 5: Sample after three hours of IPTG induction (T3), Lane 6: Sample after four hours of IPTG induction (T4), Lane 7: Sample after five hours of IPTG induction (T5).

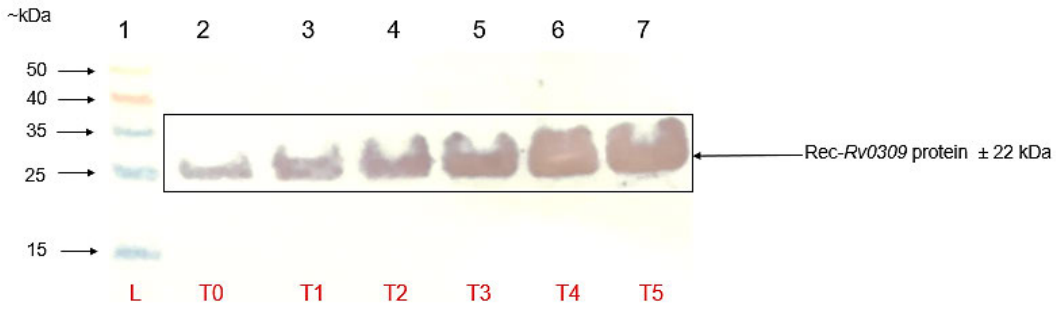

Figure 3.14: Western blot showing recombinant *Rv0309* in pET28a vector before purification. The nitrocellulose membrane was incubated with Anti-polyhistidine-peroxidase antibody, Mouse Monoclonal (1:2000). The reaction was detected using 3,3',5,5'-tetramethylbenzidine blotting solution. Lane 1: Thermo Scientific Spectra Multicolour Broad Range Protein Ladder (L), Lane 2: Sample before IPTG induction (T0), Lane 3: Sample after one hour of IPTG induction (T1), Lane 4: Sample after two hours of IPTG induction (T2), Lane 5: Sample after three hours of IPTG induction (T3), Lane 6: Sample after four hours of IPTG induction (T4), Lane 7: Sample after five hours of IPTG induction (T5).

Once the optimum conditions for protein expression were determined, expression was performed on a larger scale (100 mL culture volumes).

3.1.8 Purification of recombinant Rv0309 proteins

GST-tagged-Rv0309

The lysis and purification of the GST-tagged protein was a major challenge due to inadequate lysis and poor binding to the purification agarose/column. This was evident when observing the low band intensity of lysates and samples collected before wash/flow-through samples. Hence, multiple methods were attempted to obtain the desired pure protein and the findings are shown in this section below.

Clear lysate preparation

Prior to purification, an expressed pellet resulting from a 10 mL culture was lysed and 1 mL was taken to be analysed on an SDS-PAGE (Figure 3.15). The expressed target protein was distinct in the expected region. The total lysate indicates the pellet after lysis but before centrifugation. The total lysate was less concentrated than the expressed pellet yet still distinct, whilst the clear lysate was much fainter than both.

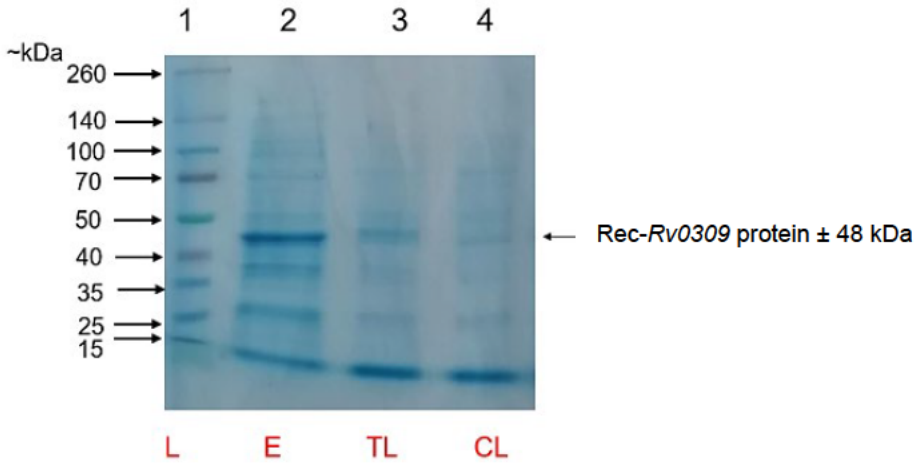

Figure 3.15: SDS-PAGE gel showing lysed recombinant *Rv0309* in pGEX-6P-1 vector prior to purification using clear lysate preparation method. A 10 mL expressed pellet was lysed, and total lysate and clear lysate (representing soluble fraction) were electrophoresed. The expressed pellet sample refers to 1 mL taken from 10 mL culture that was centrifuged and resuspended in 150 µL of 0.5 M Tris-HCl pH 6.5 after expression. Samples were analysed using a 10% reducing Tris-glycine SDS-PAGE gel stained with Coomassie blue. Lane 1: Thermo Scientific Spectra Multicolour Broad Range Protein Ladder (L), Lane 2: Expressed pellet at T5 (E), Lane 3: Total lysate (TL), Lane 4: Clear lysate (CL).

Following purification, the clear lysate sample in Lane 2 was indistinct and in low concentration (Figure 3.16). Due to the low starting concentration, it was difficult to establish whether any protein had bound to glutathione agarose or was released in elution steps. It is highly possible that the volume of pellet used was too small or that the protein was insoluble or that the sonication step was not effective. Hence, an expressed pellet resulting from a 20 mL culture was prepared to test the former possibility.

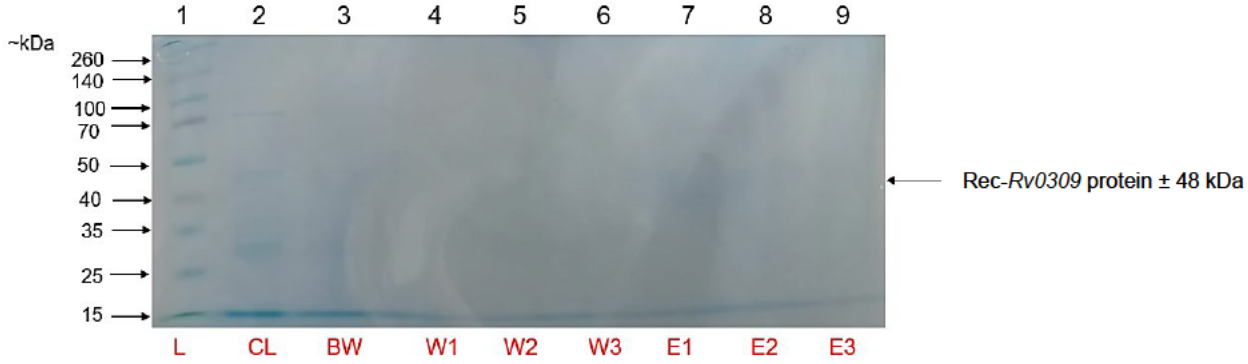

Figure 3.16: SDS-PAGE gel showing purification results of recombinant *Rv0309* in pGEX-6P-1 vector. Samples were electrophoresed on a 10% reducing Tris-glycine SDS-PAGE gel stained with Coomassie blue. Lane 1: Thermo Scientific Spectra Multicolour Broad Range Protein Ladder (L), Lane 2: Clear Lysate (CL), Lane 3: Before Wash (BW), Lane 4: Wash 1 (W1), Lane 5: Wash 2 (W2), Lane 6: Wash 3 (W3), Lane 7: Eluent 1 (E1), Lane 8: Eluent 2 (E2), Lane 9: Eluent 3 (E3).

Increased culture volume did not increase recombinant protein concentration

A pellet resulting from a 20 mL culture was lysed, and total lysate and clear lysate (representing soluble fraction) were analysed. The lysate of pellet from a larger 20 mL culture resulted in more concentrated bands, with the easily recognizable Rec-protein. However, the clear lysate was in low concentration (Figure 3.17). The ladder did not run as expected, possibly due to the electrophoretic conditions.

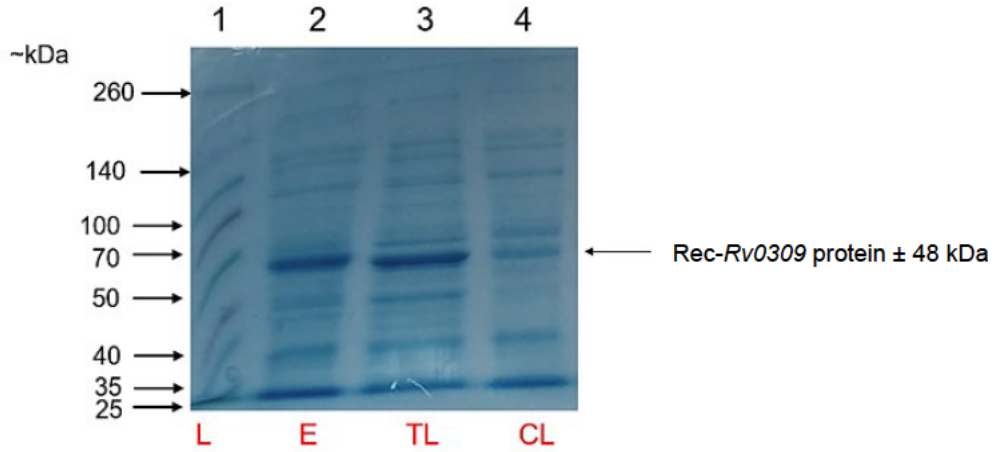

Figure 3.17: SDS-PAGE gel showing lysis of recombinant *Rv0309* in pGEX-6P-1 vector prior to purification. Expressed pellet refers to 1 mL culture taken from 20 mL culture centrifuged and resuspended in 150 µL of 0.5 M Tris-HCl pH 6.5 after expression. Samples were electrophoresed on a 10% reducing Tris-glycine SDS-PAGE gel stained with Coomassie blue. Lane 1: Thermo Scientific Spectra Multicolour Broad Range Protein Ladder (L), Lane 2: Expressed pellet at T5 (E), Lane 3: Total lysate (TL), Lane 4: Clear lysate (CL).

Purification of the clear lysate shown in Figure 3.17, resulted in the loss of the protein during the before-wash and wash steps (Figure 3.18). This indicated that the protein did not bind optimally to glutathione agarose. No bands were seen in eluents lanes (Lanes 7,8 and 9).

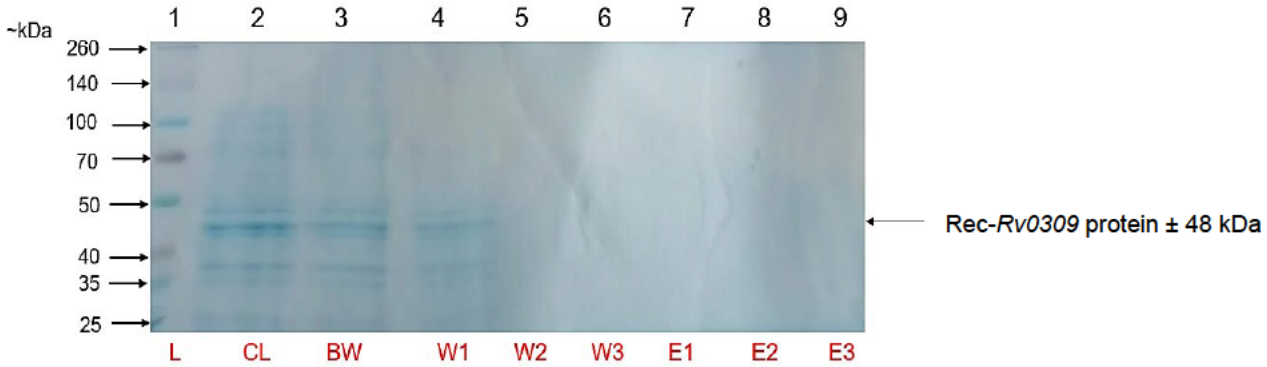

Figure 3.18: SDS-PAGE gel showing purification of recombinant *Rv0309* in pGEX-6P-1 vector. Samples were electrophoresed on a 10% reducing Tris-glycine SDS-PAGE gel stained with Coomassie blue. Lane 1: Thermo Scientific Spectra Multicolour Broad Range Protein Ladder (L), Lane 2: Clear Lysate (CL), Lane 3: Before Wash (BW), Lane 4: Wash 1 (W1), Lane 5: Wash 2 (W2), Lane 6: Wash 3 (W3), Lane 7: Eluent 1 (E1), Lane 8: Eluent 2 (E2), Lane 9: Eluent 3 (E3).

The clear lysate preparation for soluble protein did not produce the expected results despite increasing culture volume and total lysate showing an intense band. Therefore, inclusion body preparation was attempted to solubilise the insoluble fraction of protein pellet. A larger 50 mL culture volume was used to increase yield of protein.

Inclusion body preparation

The larger 50 mL volume of culture resulting in a larger pellet size was lysed using inclusion body preparation and produced a dark and concise band. However, no band was found in solubilised (Lane 3) and dialysed protein (Lane 4) samples (Figure 3.19).

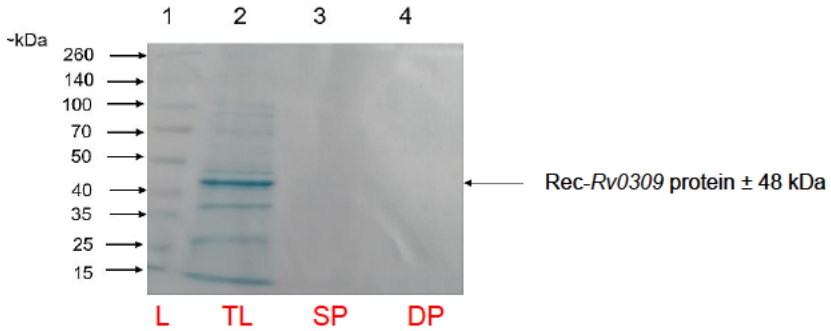

Figure 3.19: SDS-PAGE gel showing lysed recombinant *Rv0309* in pGEX-6P-1 vector prior to purification using inclusion body preparation method. Expressed pellet refers to 1 mL culture centrifuged and resuspended in 150 µL of 0.5 M Tris-HCl pH 6.5 after expression. Samples were electrophoresed using a 10% reducing Tris-glycine SDS-PAGE gel stained with Coomassie blue. Lane 1: Thermo Scientific Spectra Multicolour Broad Range Protein Ladder (L), Lane 2: Total lysate (TL), Lane 3: Solubilised protein (SP), Lane 4: Dialysed protein (DP).

Reduction of the lysis buffer, solubilisation buffer and Triton X-100 volumes added to pellet to avoid dilution of protein

The volume of lysis buffer, solubilisation buffer and Triton X-100 added was halved. Solubilised protein from inclusion body preparation in Lane 5 was slightly more intense than clear lysate sample (Figure 3.20). Lane 6 containing dialysed sample unexpectedly showed no band present, as dialysis was expected to increase concentration of sample.

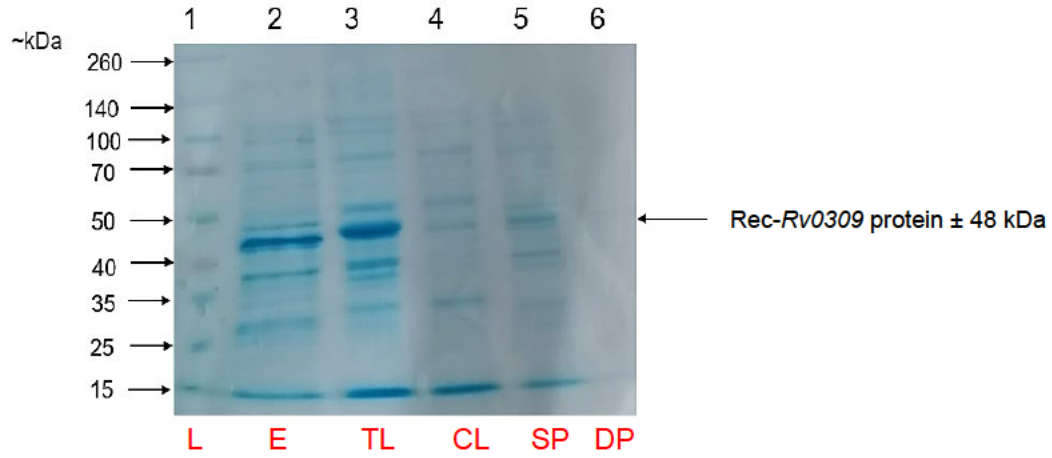

Figure 3.20: SDS-PAGE gel showing lysed recombinant *Rv0309* in pGEX-6P-1 vector prior to purification using insoluble protein preparation method with volume modifications. Expressed pellet refers to 1 mL culture centrifuged and resuspended in 150 µL of 0.5 M Tris-HCl pH 6.5 after expression. Samples were electrophoresed using a 10% reducing Tris-glycine SDS-PAGE gel stained with Coomassie blue. Lane 1: Thermo Scientific Spectra Multicolour Broad Range Protein Ladder (L), Lane 2: Expressed pellet at T5 (E), Lane 3: Total lysate (TL), Lane 4: Clear lysate (CL), Lane 5: Solubilised protein (SP), Lane 6: Dialysed protein (DP).

Concentration of supernatant with Amicon® filter

The supernatant from a previous experiment was used. Once the lysed sample was centrifuged (ThermoFisher Scientific™, Massachusetts, USA), the supernatant was collected. The remaining pellet was solubilised using urea and dialysis was performed. The volume of lysis buffer, solubilisation buffer and Triton X-100 added was halved. In order to understand at which point the protein was lost, the discarded supernatant sample from the first centrifugation step in inclusion body preparation was concentrated by Amicon® Ultra-15 centrifugal filter and further analysed. The band of the Amicon® concentrated sample (Lane

5), solubilised protein (Lane 8) and dialysed protein (Lane 9) inexplicably appeared less bright than that of the unconcentrated sample (Lane 7) (Figure 3.21).

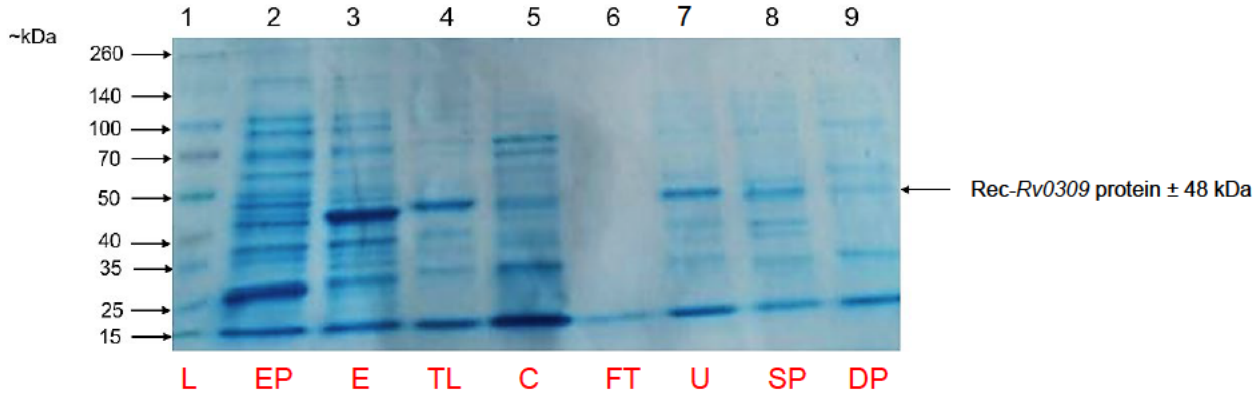

Figure 3.21: SDS-PAGE gel showing lysis of recombinant *Rv0309* in pGEX-6P-1 vector using insoluble protein preparation method and concentrating supernatant with Amicon® filters. Expressed pellet refers to 1 mL culture centrifuged and resuspended in 150 µL of 0.5 M Tris-HCl pH 6.5 after expression. Samples were electrophoresed using a 10% reducing Tris-glycine SDS-PAGE gel stained with Coomassie blue. Lane 1: Thermo Scientific Spectra Multicolour Broad Range Protein Ladder (L), Lane 2: Expressed pellet of pGEX-6P-1 (EP), Lane 3: Expressed pellet of Rec-*Rv0309* at T5 (E), Lane 4: Total lysate (TL), Lane 5: Concentrated supernatant (C), Lane 6: Flow through from filter (FT), Lane 7: Unconcentrated supernatant (U), Lane 8: Solubilised protein (SP), Lane 9: Dialysed protein (DP).

Purification of unconcentrated supernatant

Binding was performed for two hours with a before-wash sample taken before three wash steps using Tris-NaCl and eluting three times with a buffer (pH 8) containing reduced glutathione. The unconcentrated supernatant that displayed a bright band in Figure 3.21 was added to glutathione agarose column. The eluent lanes were expected to contain a single band in the region of interest (±48 kDa), indicating Rec-protein has been purified. The unconcentrated sample in Lane 2 showed a very faint band (Figure 3.21), this was unexpected as it was expected to look like sample in Lane 5 in Figure 3.20. Since such a low concentration was seen, it is clear that sample binding to column would have been low in concentration. Hence, no eluents were seen (Figure 3.22).

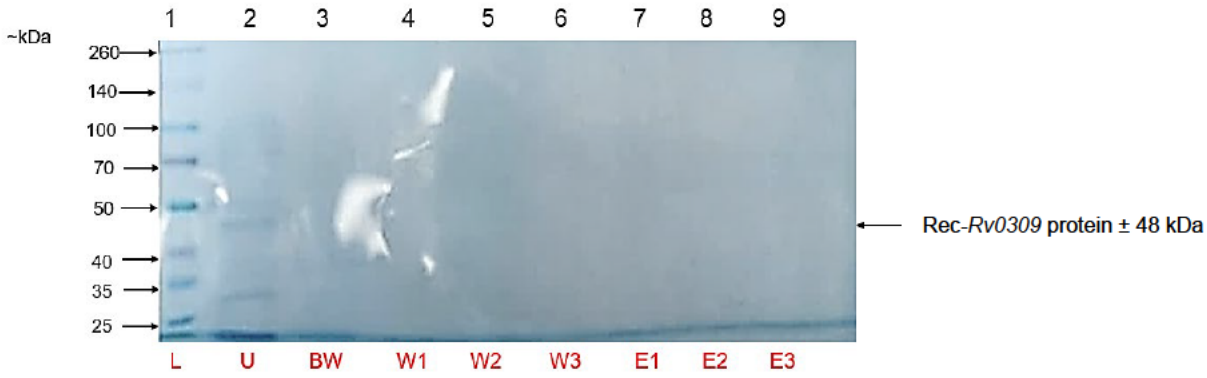

Figure 3.22: SDS-PAGE gel showing purification result of recombinant *Rv0309* in pGEX-6P-1 vector. Samples were electrophoresed using a 10% reducing Tris-glycine SDS-PAGE gel stained with Coomassie blue. Lane 1: Thermo Scientific Spectra Multicolour Broad Range Protein Ladder (L), Lane 2: Unconcentrated supernatant (U), Lane 3: Before Wash (BW), Lane 4: Wash 1 (W1), Lane 5: Wash 2 (W2), Lane 6: Wash 3 (W3), Lane 7: Eluent 1 (E1), Lane 8: Eluent 2 (E2), Lane 9: Eluent 3 (E3).

Introduction of sonication with PBS buffer to improve lysate band

Since sonication is a standard recommendation for lysis of insoluble proteins, mechanical (sonication) and chemical (lysis buffer) lysis methods were compared. The gels from Figures 3.23 to 3.27 were viewed on a gel documentation system; however, the system did not have the option to see multicolours; hence, ladder colours are not shown. When samples were subjected to mechanical lysis only (Figure 3.23), there was a clear difference between sonicated (Lanes 3 to 8) and unsonicated samples (Lane 9). The sonication duration did not seem to make a significant difference, from 40 seconds (Lane 5) onwards. The control sample in Lane 10 did not undergo sonication but contained lysis buffer.

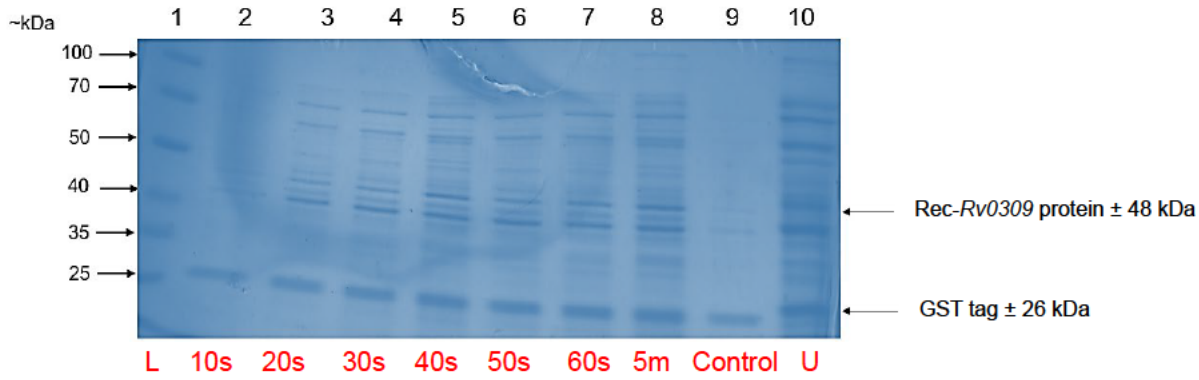

Figure 3.23: SDS-PAGE gel showing sonication duration tests for lysis of recombinant *Rv0309* in pGEX-6P-1 vector prior to purification. Pellets resulting from a 1 mL culture were lysed by adding PBS and sonication only. Samples were electrophoresed using a 10% reducing Tris-glycine SDS-PAGE gel stained with Coomassie blue. Lane 1: Thermo Scientific Spectra Multicolour Broad Range Protein Ladder (L), Lane 2: sonication for 10 seconds (10s), Lane 3: sonication for 20 seconds (20s), Lane 4: sonication for 30 seconds (30s), Lane 5: sonication for 40 seconds (40s), Lane 6: sonication for 50 seconds (50s), Lane 7: sonication for 60 seconds (60s), Lane 8: sonication for five minutes (5m), Lane 9: no sonication (Control), Lane 10: Supernatant from step 6 of original insoluble protein protocol (U).

Purification of sample lysed by mechanical lysis only

Since sonication was beneficial, purification was attempted using a sample that was sonicated for five minutes followed by insoluble protein preparation. The supernatant was collected and added to the glutathione agarose column (Figure 3.24). The flow-through was then added again to column three more times to promote binding of any unbound protein. However, the protein sample was still removed in the before wash and the wash samples, and did not bind to the column. The Rec-protein was not seen in eluent lanes.

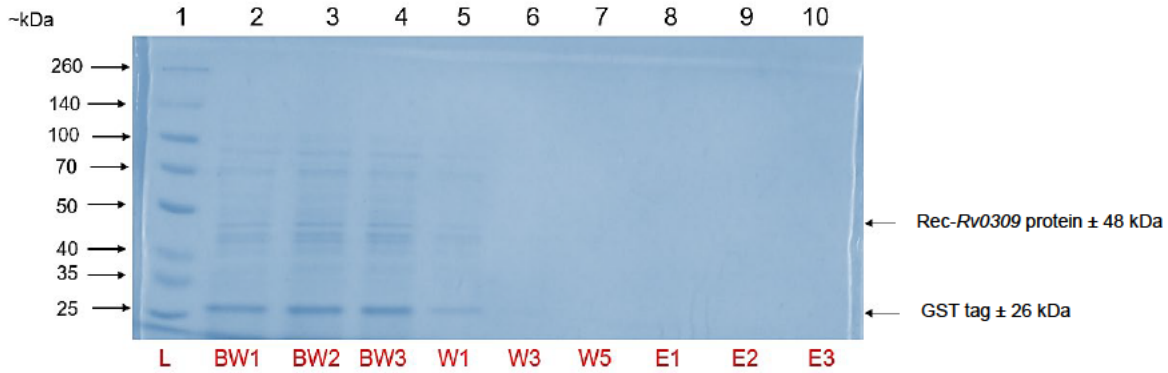

Figure 3.24: SDS-PAGE gel showing purification of recombinant *Rv0309* in pGEX-6P-1 vector after mechanical lysis only. The sample that was sonicated for five minutes was added to glutathione agarose for binding. Samples were electrophoresed using a 10% reducing Tris-glycine SDS-PAGE gel stained with Coomassie blue. Lane 1: Thermo Scientific Spectra Multicolour Broad Range Protein Ladder (L), Lane 2: Before Wash 1 (BW1), Lane 3: Before Wash 2 (BW2), Lane 4: Before Wash 3 (BW3), Lane 5: Wash 1 (W1), Lane 6: Wash 3 (W3), Lane 7: Wash 5 (W5), Lane 8: Eluent 1 (E1), Lane 9: Eluent 2 (E2), Lane 10: Eluent 3 (E3).

Use of both mechanical and chemical lysis to improve lysate

Pellets resulting from a 1 mL culture were lysed by adding PBS lysis buffer and sonication (Figure 3.25). The samples all seemed more intense than when sonicated only (Figure 3.23). The unsonicated sample containing only lysis buffer (Lane 9) appeared very similar to samples lysed with both chemical and mechanical lysis (Lanes 2 to 8, Figure 3.25).

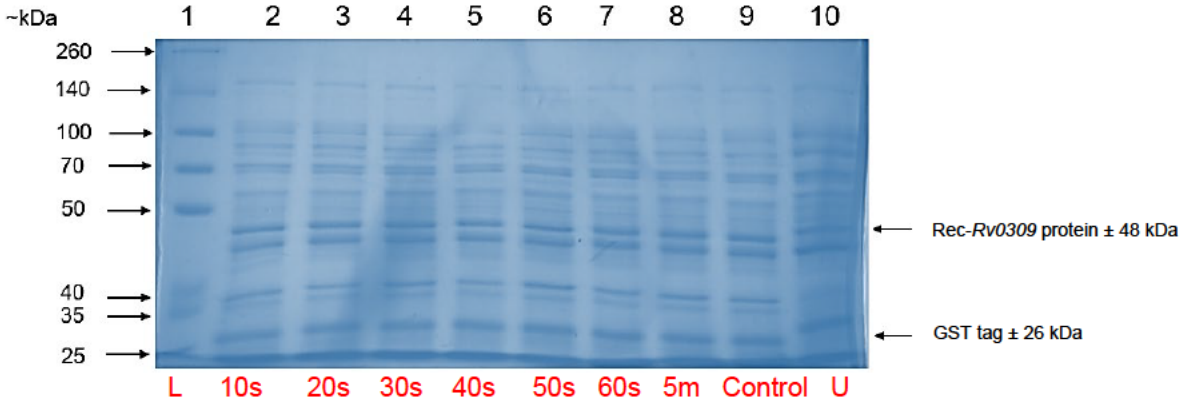

Figure 3.25: SDS-PAGE gel showing sonication duration and chemical tests for lysis of recombinant *Rv0309* in pGEX-6P-1 vector prior to purification. Samples were electrophoresed using a 10% reducing Tris-glycine SDS-PAGE gel stained with Coomassie blue. Lane 1: Thermo Scientific Spectra Multicolour Broad Range Protein Ladder (L), Lane 2: sonication for 10 seconds, Lane 3: sonication for 20 seconds, Lane 4: sonication for 30 seconds, Lane 5: sonication for 40 seconds, Lane 6: sonication for 50 seconds, Lane 7: sonication for 60 seconds, Lane 8: sonication for five minutes, Lane 9: no sonication (control), Lane 10: Supernatant from step 6 of original insoluble protein protocol.

Purification of sample subjected to mechanical and chemical lysis

Purification was performed using a sample subjected to mechanical and chemical lysis (Figure 3.26). The sample containing lysis buffer and that was sonicated for five minutes was added to glutathione agarose for binding. The binding step was repeated three times with the same sample therefore three before wash samples were collected. However, the sample was still discharged during the before-wash and the wash steps. Very faint bands were observed in the expected region in eluent lanes (Lanes 8 -10). This indicated that pure protein was eluted; however, the concentration was very low due to the loss of most of Rec-protein before the elution steps.

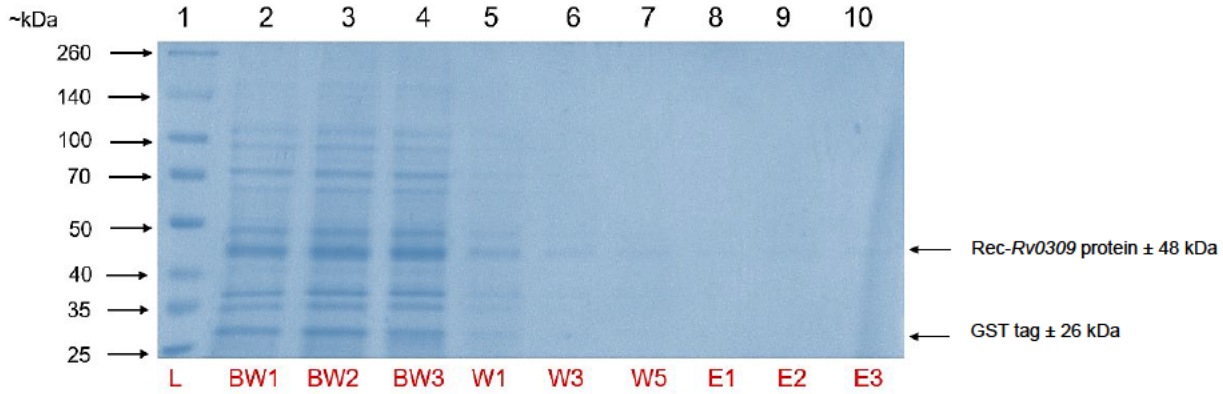

Figure 3.26: SDS-PAGE gel showing purification of recombinant *Rv0309* in pGEX-6P-1 vector after mechanical and chemical lysis. Samples were electrophoresed using a 10% reducing Tris-glycine SDS-PAGE gel stained with Coomassie blue. Lane 1: Thermo Scientific Spectra Multicolour Broad Range Protein Ladder (L), Lane 2: Before Wash 1 (BW1), Lane 3: Before Wash 2 (BW2), Lane 4: Before Wash 3 (BW3), Lane 5: Wash 1 (W1), Lane 6: Wash 3 (W3), Lane 7: Wash 5 (W5), Lane 8: Eluent 1 (E1), Lane 9: Eluent 2 (E2), Lane 10: Eluent 3 (E3).

Good binding efficacy of the glutathione agarose when purifying expressed pGEX-6P-1

The effectiveness of the agarose column was tested by purifying expressed pGEX-6P-1 to observe whether or not GST-tag would be eluted. Fresh glutathione agarose was used. Glutathione agarose can be used up to three times provided the column is regenerated before each use. Fresh glutathione agarose was used for previous experiments. The expressed pellet of pGEX-6P-1 was lysed and centrifuged, and the clear lysate was added to the glutathione agarose for binding. Binding was conducted for two hours, including with a before wash sample, followed by five wash steps using Tris-NaCl. The protein was eluted three times with a buffer (pH 8) containing reduced glutathione. Expressed pGEX-6P-1 was purified with ease using method outlined for the Rec-protein (Figure 3.27). This was evident by the presence of the three GST-tag eluents in Lanes 7 to 9.

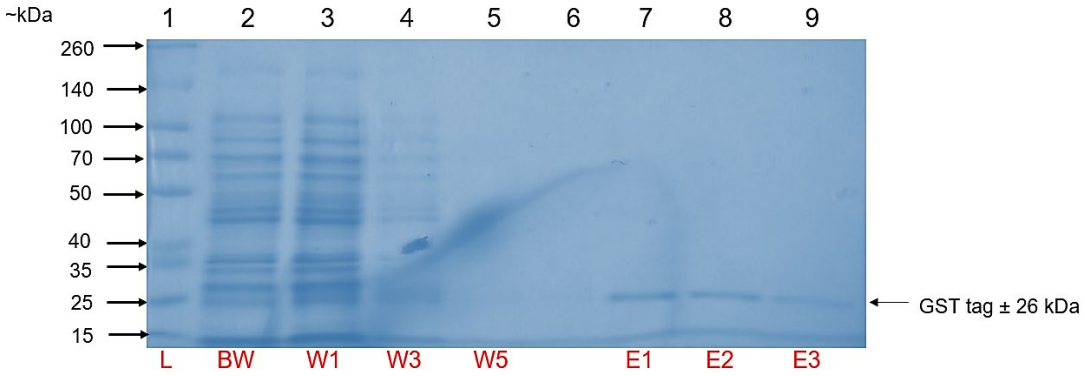

Figure 3.27: SDS-PAGE gel showing purification of pGEX-6P-1 vector to determine efficacy of column binding property. Samples were electrophoresed using a 10% reducing Tris-glycine SDS-PAGE gel stained with Coomassie blue. Lane 1: Thermo Scientific Spectra Multicolour Broad Range Protein Ladder (L), Lane 2: Before Wash (BW), Lane 3: Wash 1 (W1), Lane 4: Wash 3 (W3), Lane 5: Wash 5 (W5), Lane 6: Blank, Lane 7: Eluent 1 (E1), Lane 8: Eluent 2 (E2), Lane 9: Eluent 3 (E3).

Replacement of dithiothreitol with β-mercaptoethanol in lysis buffer did not affect purification

Dithiothreitol was replaced with β-mercaptoethanol in lysis buffer; however, ÄKTA purification reflected little to no eluent peaks on graph when purification was attempted (image not provided).

Adjustment of buffer pH to complement pI of protein did not improve purification

The expressed pellet of Rec-*Rv0309* was lysed, centrifuged (ThermoFisher Scientific™, Massachusetts, USA) and supernatant was added to glutathione agarose for binding. The isoelectric point (pI) of a protein is an important factor when performing protein purification. The pI of the protein is 8.48. Buffers that have a pH close to the pI of protein confers no charge to the protein, thus may cause aggregation or precipitation, hence a buffer (pH 6) was used. However, this made no difference as the Rec-protein was still released in the before wash steps and during washes (Figure 3.28) and no eluent bands were seen.

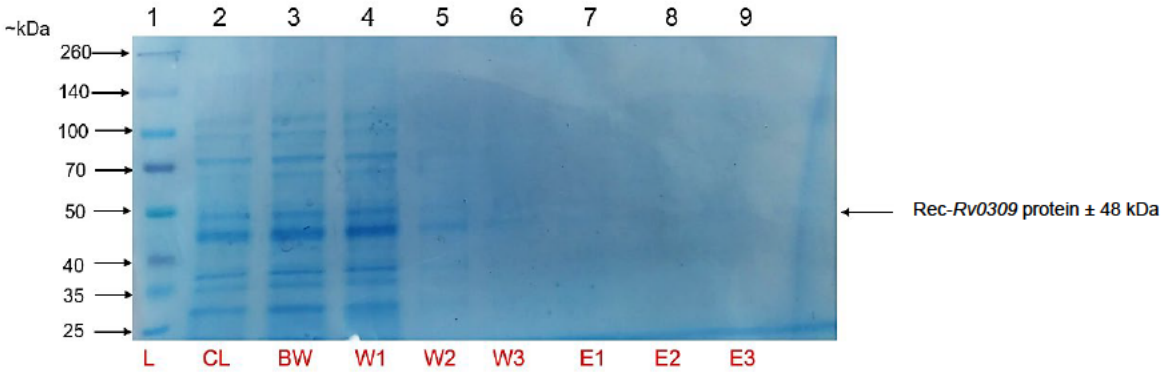

Figure 3.28: SDS-PAGE gel showing purification of recombinant *Rv0309* in pGEX-6P-1 vector with pH changes to buffer based on protein isoelectric point. Samples were electrophoresed using a 10% reducing Tris-glycine SDS-PAGE gel stained with Coomassie blue. Lane 1: Thermo Scientific Spectra Multicolour Broad Range Protein Ladder (L), Lane 2: Clear lysate (CL), Lane 3: Before Wash (BW), Lane 4: Wash 1 (W1), Lane 5: Wash 2 (W2), Lane 6: Wash 3 (W3), Lane 7: Eluent 1 (E1), Lane 8: Eluent 2 (E2), Lane 9: Eluent 3 (E3).

Solubilisation of proteins with urea

Urea is a denaturing agent and can assist in solubilisation of proteins that form inclusion bodies. After solubilisation with urea, purification was attempted using ion exchange chromatography. Although the clear lysate produced a distinct band (Lane 2), no protein was released after purification (Figure 3.29). There were other very faint, smaller protein bands in the clear lysate. An Amicon® filter was used to remove smaller proteins (Figure 3.30); however, the Rec-protein seemed lost during the process (Figure 3.30) and smaller proteins were present.

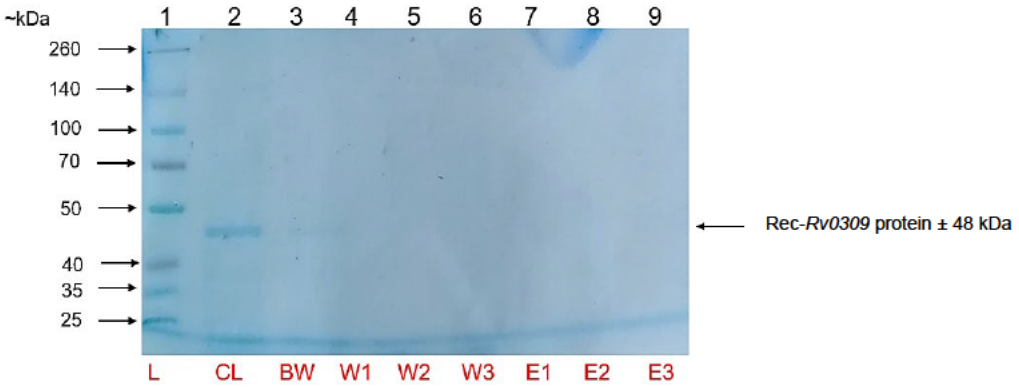

Figure 3.29: SDS-PAGE gel showing purification of recombinant *Rv0309* in pGEX-6P-1 vector using ion-exchange chromatography in small scale experiment. Samples were electrophoresed using a 10% reducing Tris-glycine SDS-PAGE gel stained with Coomassie blue. Lane 1: Thermo Scientific Spectra Multicolour Broad Range Protein Ladder (L), Lane 2: Clear lysate (CL), Lane 3: Before

Wash (BW), Lane 4: Wash 1 (W1), Lane 5: Wash 2 (W2), Lane 6: Wash 3 (W3), Lane 7: Eluent 1 (E1), Lane 8: Eluent 2 (E2), Lane 9: Eluent 3 (E3).

Loss of Rec-protein during filtration of smaller proteins using Amicon® filters

The expressed pellet of Rec-*Rv0309* was lysed with urea; thus, urea removal was performed thereafter. The sample was centrifuged (ThermoFisher Scientific™, Massachusetts, USA) and supernatant was used as solubilised protein. The sample was put through an Amicon® filter and ion-exchange purification was performed with the filtered protein. The other fainter, smaller protein bands in the clear lysate (Lane 2) in Figure 3.29 were still seen in sample after the use of the Amicon® filter (Figure 3.30). This resulted in faint bands in the gel, and the loss of the bulk of the Rec-protein (Lane 2, Figure 3.30, compared to Lane 2, Figure 3.29). No bands were seen in any washes or eluents.

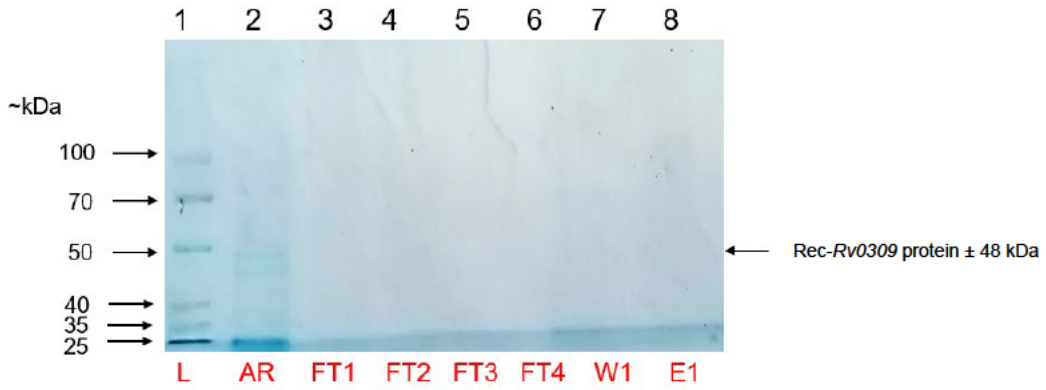

Figure 3.30: SDS-PAGE gel showing the purification of recombinant *Rv0309* in pGEX-6P-1 vector using ion exchange chromatography. Samples were analysed using a 10% reducing Tris-glycine SDS-PAGE gel stained with Coomassie blue. Lane 1: Spectra™ Multicolour Broad Range Protein Ladder (L), Lane 2: Sample after removing urea (AR), Lane 3: Ion exchange flow-through (FT1), Lane 4: Ion exchange flow-through (FT2), Lane 5: Ion exchange flow-through (FT3), Lane 6: Ion exchange flow-through (FT4), Lane 7: Wash 1 (W1), Lane 8: Eluent 1 (E1).

Size exclusion of urea depleted protein sample using Amicon® filters

The expressed pellet of Rec-*Rv0309* was lysed with urea which was removed thereafter. Size-exclusion using Amicon® filters was performed to exclude other co-purified proteins. The sample was centrifuged and supernatant was used as solubilised protein. Size-exclusion was unsuccessful, as the other proteins were not removed, and the Rec-protein concentration was lower (Lane 3) compared to the distinct bright band of the expressed pellet (Lane 4) (Figure 3.31).

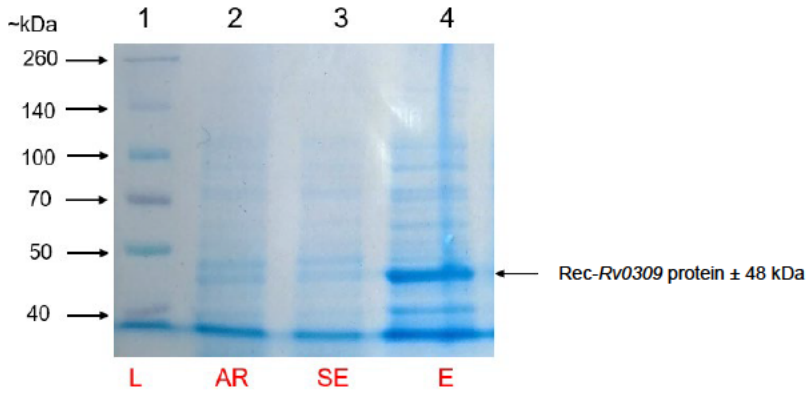

Figure 3.31: SDS-PAGE gel showing size-exclusion using Amicon® filters. Samples were analysed using a 10% reducing Tris-glycine SDS-PAGE gel stained with Coomassie blue. Lane 1: Spectra™ Multicolour Broad Range Protein Ladder (L), Lane 2: Sample after removing urea (AR), Lane 3: Size-exclusion sample (SE), Lane 4: Expressed pellet (E).

Overnight binding of Rec-protein to Pierce glutathione column at 4°C

The expressed pellet was lysed with urea, which was removed thereafter. Sample was centrifuged and supernatant was loaded onto glutathione agarose column and left to bind overnight at 4°C. There was a distinct expressed pellet sample (Figure 3.32). However, the sample in Lane 3 did not contain expected band and seemed to have lost protein. Thus, binding experiment was not successful as sample added to column was not optimal, and another method to obtain a more concentrated sample was attempted thereafter (Figure 3.33).

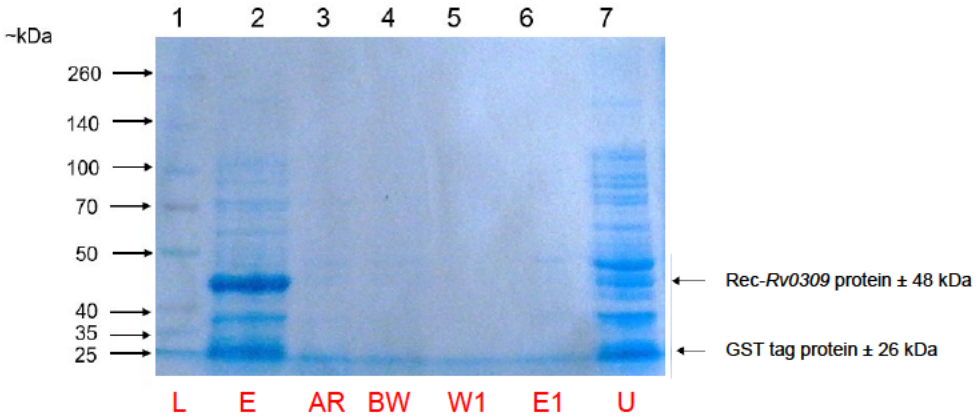

Figure 3.32: SDS-PAGE gel showing purification of recombinant *Rv0309* in pGEX-6P-1 vector by binding overnight at 4°C. Samples were analysed using a 10% reducing Tris-glycine SDS-PAGE gel stained with Coomassie blue. Lane 1: Thermo Scientific Spectra Multicolour Broad Range Protein Ladder (L), Lane 2: Expressed pellet at T5 (E), Lane 3: Sample after removing urea (AR), Lane 4: Before Wash (BW), Lane 5: Wash 1 (W1), Lane 6: Eluent 1 (E1), Lane 7: Uninduced sample at T0 (U).

Lysis and purification using combination of Triton X-100, CHAPS and RNAse I with sarkosyl in elution buffer

The expressed pellet of Rec-*Rv0309* was lysed with lysis buffer with an addition of CHAPS, Triton X-100 and RNAse I. The sample was centrifuged (ThermoFisher Scientific™, Massachusetts, USA) and the supernatant was added to glutathione agarose column and left to bind for two hours. Lysis buffer was used in wash steps and sarkosyl was added to elution buffer.

Very faint bands, indicating low concentration, were found in eluent lanes (Lanes 8 to 10) (Figure 3.33). The clear lysate sample loaded into column had an intense band. The before wash sample appeared the most intense on gel, indicating protein loss due to lack of binding; thus, resulting in faint bands of purified protein in eluent. The width of lanes 3 and other lanes may have been due to diffusion of wells before current was introduced or ionic strength of the sample being lower than that of gel. Since the well appeared to be narrower in Lane 3 this could have concentrated the before wash sample run (Figure 3.33).

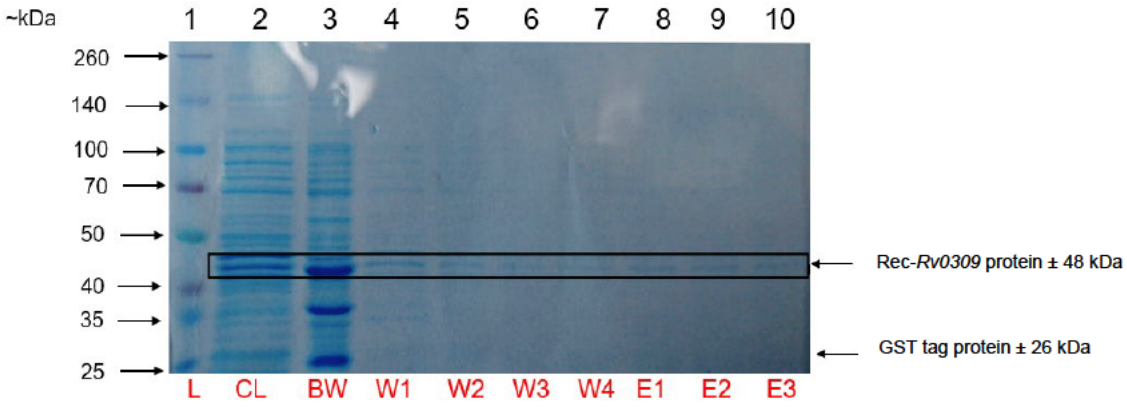

Figure 3.33: SDS-PAGE gel showing purification of recombinant *Rv0309* in pGEX-6P-1 vector using Triton X-100, CHAPS and RNAse I in lysis buffer and introducing sarkosyl to elution buffer. Samples were analysed using a 10% reducing Tris-glycine SDS-PAGE gel stained with Coomassie blue. Lane 1: Thermo Scientific Spectra Multicolour Broad Range Protein Ladder (L), Lane 2: Clear lysate (CL), Lane 3: Before Wash (BW), Lane 4: Wash 1 (W1), Lane 5: Wash 2 (W2), Lane 6: Wash 3 (W3), Lane 7: Wash 4 (W4), Lane 8: Eluent 1 (E1), Lane 9: Eluent 2 (E2), Lane 10: Eluent 3 (E3).

Lysis buffer used in wash steps and elution buffer containing sarkosyl for purification

The expressed pellet of Rec-*Rv0309* was lysed with lysis buffer containing SDS. Sample was centrifuged (ThermoFisher Scientific™, Massachusetts, USA) and supernatant was added to glutathione agarose column and left to bind. Lysis buffer was used in wash steps and sarkosyl was added to elution buffer.

Very faint bands were seen in Lanes 2 to 9 (Figure 3.34). The sample seemed to be washed out in the steps prior and during wash steps. Very faint eluent bands were seen in Lanes 7-9. Lanes 4 to 9 seemed to migrate unusually. This is also seen in the Western blot performed with identical gel (Figure 3.35). The Western blot indicates that the target protein was present and eluted as a purified protein with a molecular weight that was over 50 kDa which is higher than expected compared to the protein eluted in Figure 3.33.

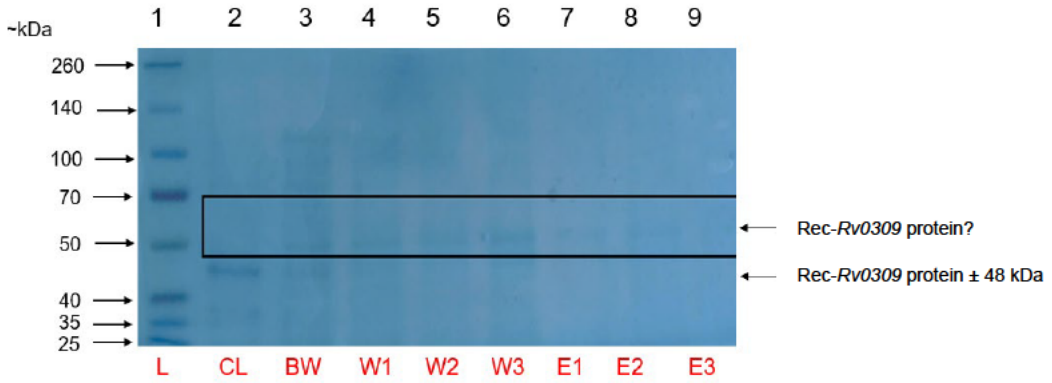

Figure 3.34: SDS-PAGE gel showing purification of recombinant *Rv0309* in pGEX-6P-1 vector using lysis buffer for wash steps and introducing sarkosyl to elution buffer. Samples were electrophoresed using a 10% reducing Tris-glycine SDS-PAGE gel stained with Coomassie blue. Lane 1: Thermo Scientific Spectra Multicolour Broad Range Protein Ladder (L), Lane 2: Clear lysate (CL), Lane 3: Before Wash (BW), Lane 4: Wash 1 (W1), Lane 5: Wash 2 (W2), Lane 6: Wash 3 (W3), Lane 7: Eluent 1 (E1), Lane 8: Eluent 2 (E2), Lane 9: Eluent 3 (E3).

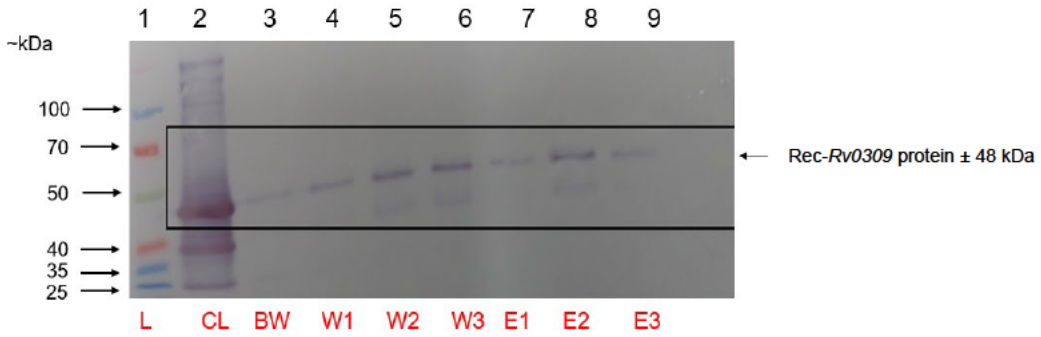

Figure 3.35: A Western blot showing the purification of recombinant *Rv0309* in pGEX-6P-1 vector using lysis buffer for wash steps and introducing sarkosyl to elution buffer. Samples were electrophoresed using a 10% reducing Tris-glycine SDS-PAGE gel. The gel was transferred onto nitrocellulose membrane that was incubated overnight with primary antibody (GST-Tag Monoclonal Antibody) and thereafter washed with buffer containing Phosphate-Buffered Saline and Tween (PBST). The membrane was incubated again with secondary antibody (Goat Anti-Mouse IgG Antibody, HRP conjugate). Colour was developed using 3,3′,5,5′-Tetramethylbenzidine (TMB). Lane 1: Thermo Scientific Spectra Multicolour Broad Range Protein Ladder (L), Lane 2: Clear lysate (CL), Lane 3: Before Wash (BW), Lane 4: Wash 1 (W1), Lane 5: Wash 2 (W2), Lane 6: Wash 3 (W3), Lane 7: Eluent 1 (E1), Lane 8: Eluent 2 (E2), Lane 9: Eluent 3 (E3).

3.1.8 Purification of recombinant His-tagged- Rv0309 protein

A pellet obtained from 100 mL expressed culture lysed with B-PER reagent and sonication, was purified with nickel-nitrilotriacetic acid (Ni-NTA) chromatography. Two SDS-PAGE gels were electrophoresed simultaneously, one for staining and viewing whilst other was for Western blot. SDS-PAGE gel analysis showed faint bands for all three eluents in the expected region (Figure 3.36). In addition, there was evidence of some unexpected bands between 55 to 130 kDa. This may be due to insufficient washing or other proteins binding to the Ni-NTA column due to its propensity of high-affinity binding of proteins with low specificity. Western blotting confirmed that the band found in eluents were that of recombinant *Rv0309* protein (Figure 3.37). The other unexpected bands seen on SDS-PAGE gel were absent on Western blot. The target band in eluent 2 (Lane 6) was excised and then sequenced using peptide mass fingerprinting and revealed 98% match with reference sequence (Appendix D).

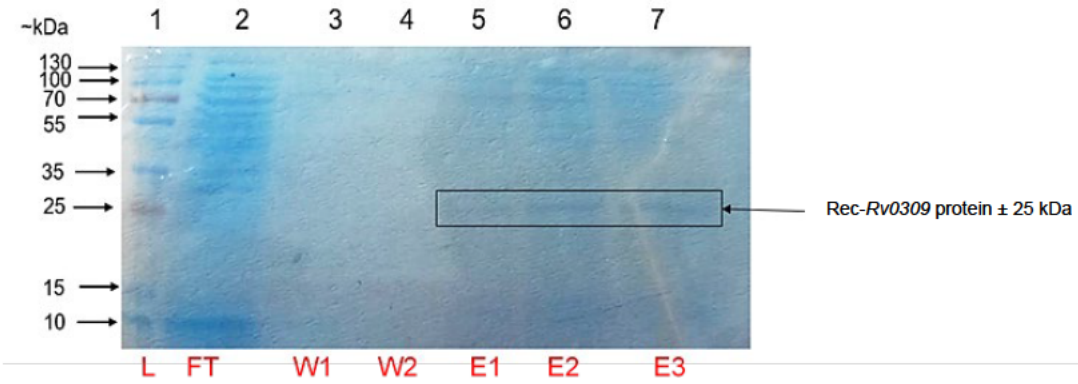

Figure 3.36: SDS-PAGE gel showing purification of recombinant *Rv0309* in pET28a vector using Ni-NTA chromatography. Samples were lysed using B-PER reagent, sonication and purified using Ni-NTA chromatography. Samples were electrophoresed using an 18% reducing Tris-glycine SDS-PAGE gel stained with Coomassie blue. Lane 1: Thermo Scientific PageRuler Plus Prestained Protein Ladder (L), Lane 2: Flow-through (FT), Lane 3: Wash 1 (W1), Lane 4: Wash 2 (W2), Lane 5: Eluent 1 (E1), Lane 6: Eluent 2 (E2), Lane 7: Eluent 3 (E3).

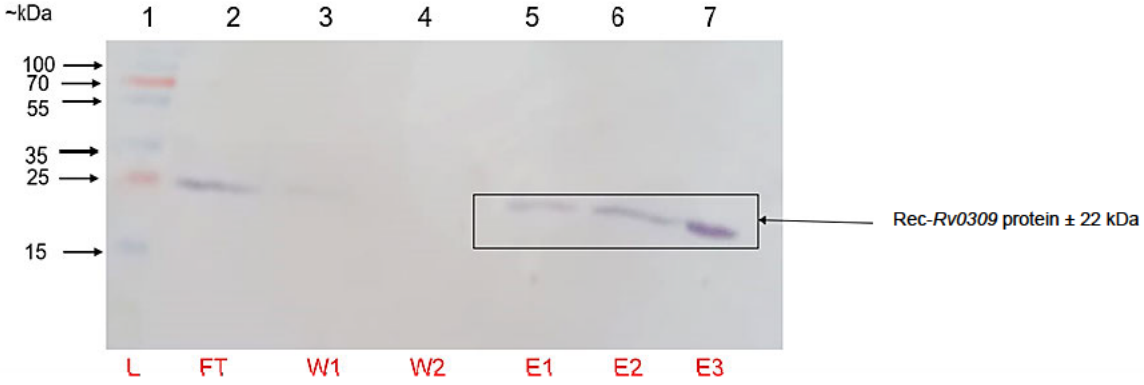

Figure 3.37: Western blot showing purification of recombinant *Rv0309* in pET28a vector using Ni-NTA chromatography. Samples were electrophoresed using an 18% reducing Tris-glycine SDS-PAGE gel. The gel was transferred into nitrocellulose membrane that was incubated overnight with primary antibody (GST-Tag Monoclonal Antibody) and thereafter washed with buffer containing PBST. The membrane was incubated again with secondary antibody (Goat Anti-Mouse IgG Antibody, HRP conjugate). Colour was developed using 3,3′,5,5′-Tetramethylbenzidine (TMB). Lane 1: Thermo Scientific PageRuler Plus Prestained Protein Ladder (L), Lane 2: Flow-through (FT), Lane 3: Wash 1 (W1), Lane 4: Wash 2 (W2), Lane 5: Eluent 1 (E1), Lane 6: Eluent 2 (E2), Lane 7: Eluent 3 (E3).

Purification using ÄKTA purification system

The expressed pellet from 100 mL culture was lysed and sonicated for an extended period and higher setting. The lysate was centrifuged (ThermoFisher Scientific™, Massachusetts, USA), thereafter supernatant collected and loaded onto the Ni-NTA chromatography column (using ÄKTA start™). Elution buffer contained 20 mM NaH_2PO_4, 10 mM NaCl and 500 mM imidazole (pH 7.5). The pellet was lysed using lysozyme, lysis buffer and sonication. The ÄKTA elution profile (Figure 3.38A) revealed that most proteins were released during wash steps, indicating that binding was not optimal. There was a very small peak for eluent samples (Figure 3.38A). The four eluent samples were analysed and target band in the 25 kDa region can be seen. However, other proteins are also present, indicating that a pure target protein was not eluted (Figure 3.38B). A size exclusion experiment was also attempted using the ÄKTA system, however, no peaks were found for eluents (data not provided).

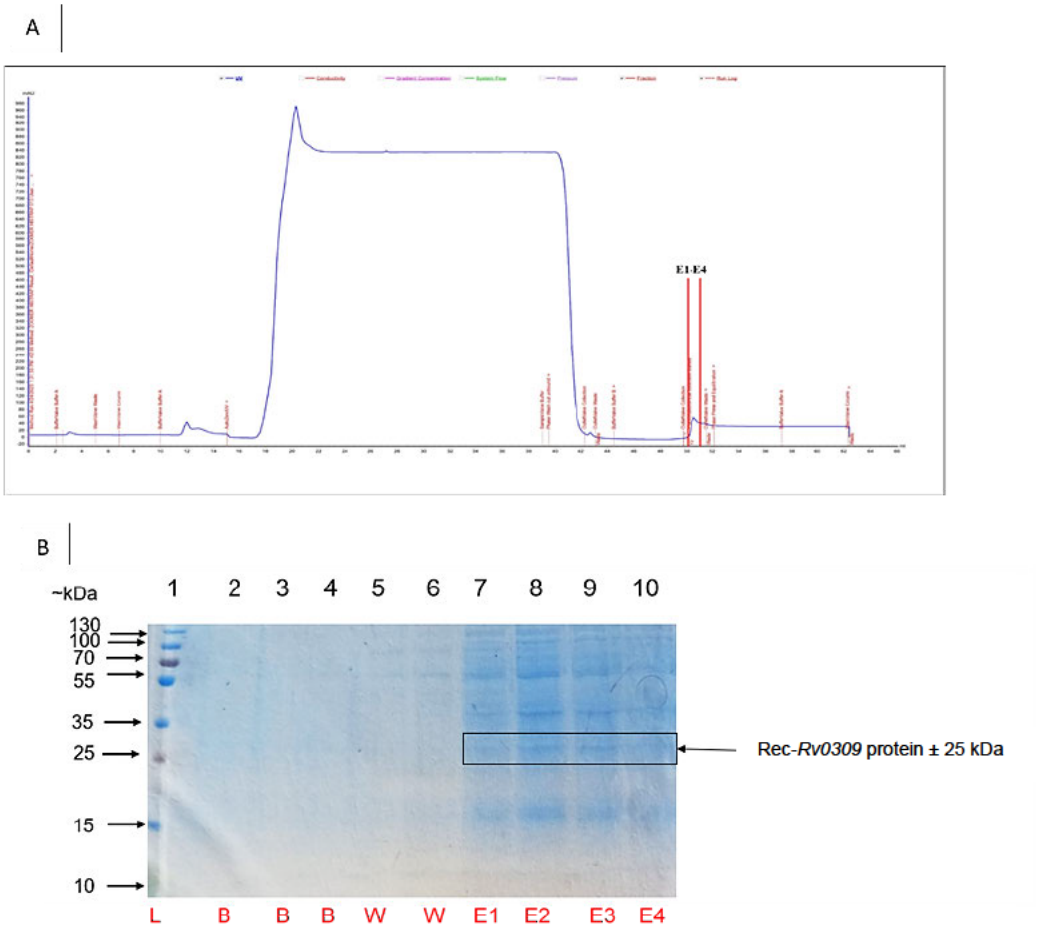

Figure 3.38: SDS-PAGE gel showing purification of recombinant *Rv0309* in pET28a vector using ÄKTA start™. (A) ÄKTA elution profile indicating peaks where eluents were found. (B) Samples were analysed using an 18% reducing Tris-glycine SDS-PAGE gel stained with Coomassie blue. Lane 1: Thermo Scientific Page Ruler Plus Prestained Protein Ladder (L), Lane 2: Blank (B), Lane 3: Blank (B), Lane 4: Blank (B), Lane 5: Wash (W), Lane 6: Wash (W), Lane 7: Eluent 1 (E1), Lane 8: Eluent 2 (E2), Lane 9: Eluent 3 (E3), Lane 10: Eluent 4 (E4).

Lysis of pellet using lysozyme, lysis buffer and sonication with HisPur Cobalt column purification

The expressed pellet was lysed using lysozyme overnight and lysis buffer with sonication the next day. Once centrifuged, the supernatant was used as clear lysate and added to HisPur Cobalt column. Three washes were done along with collection of four eluents after adding elution buffer. The lysis method was unsuccessful as indicated by the absence of a distinct band indicating Rec-protein in the cleared lysate (Lane 2, Figure 3.39). Since clear lysate loaded onto column was not optimal, the eluents retrieved were unsuccessful. The lysis method had to be optimised further. A single, highly concentrated protein band was present between 10-15 kDa, this appeared to be the His-tag.

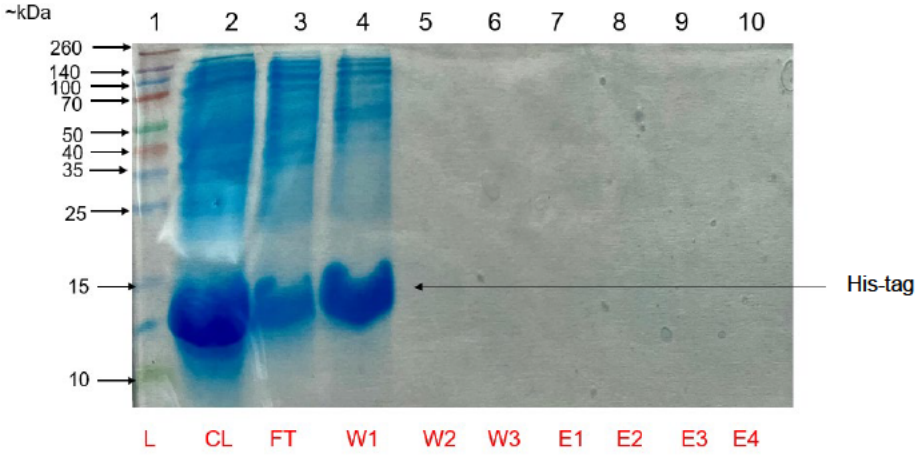

Figure 3.39: SDS-PAGE gel showing purification of recombinant *Rv0309* in pET28a vector using HisPur Cobalt column. Samples were analysed using an 18% reducing Tris-glycine SDS-PAGE gel stained with Coomassie blue. Lane 1: Thermo Scientific Spectra Multicolour Broad Range Protein Ladder (L), Lane 2: Clear lysate (CL), Lane 3: Flow-through (FT), Lane 4: Wash 1 (W1), Lane 5: Wash 2 (W2), Lane 6: Wash 3 (W3), Lane 7: Eluent 1 (E1), Lane 8: Eluent 2 (E2), Lane 9: Eluent 3 (E3), Lane 10: Eluent 4 (E4).

Lysis of pellet using wash buffer and sonication with HisPur Cobalt purification

The protein pellet was lysed using Equilibrium/Wash buffer (containing sodium phosphate, sodium chloride and imidazole) and sonication. Once centrifuged, the supernatant was used as clear lysate and added to column. Three washes were done along with collection of three eluents after adding elution buffer. The total lysate sample was more concentrated than clear lysate sample indicating that some of the protein was retained in the pellet. Although producing a more intense clear lysate band in Figure 3.40, it is clear that the lysate did not bind adequately to column. This is supported by the fact that most of the sample was discharged in the flow-through (Figure 3.40). Very faint bands were seen in eluents (Lanes 8-10). Other proteins were also seen in eluent lanes with a much larger weight (± 65-80 kDa).

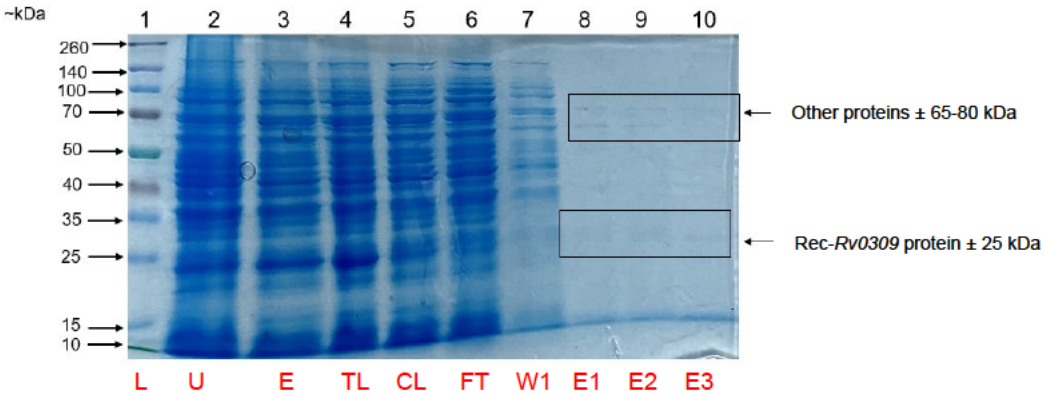

Figure 3.40: SDS-PAGE gel showing purification of recombinant *Rv0309* in pET28a vector using HisPur Cobalt column. Samples were analysed using an 15% reducing Tris-glycine SDS-PAGE gel stained with Coomassie blue. Lane 1: Thermo Scientific Spectra Multicolour Broad Range Protein Ladder (L), Lane 2: Uninduced sample after four hours (U), Lane 3: Expressed pellet after four hours (E), Lane 4: Total lysate (TL), Lane 5: Clear lysate (CL), Lane 6: Flow-through (FT), Lane 7: Wash 1 (W1), Lane 8: Eluent 1 (E1), Lane 9: Eluent 2 (E2), Lane 10: Eluent 3 (E3).

Lysis of pellet using lysis buffer containing SDS and HisPur Cobalt purification

The protein pellet was lysed using sonication and lysis buffer (containing PBS, lysozyme, DTT, PMSF, SDS, Triton X-100). Once centrifuged, the supernatant was used as clear lysate and added to column. Three washes were done along with collection of three eluents after adding elution buffer. The fairly intense clear lysate band (Lane 5, Figure 3.41) indicated that the sample being added to column was of greater concentration as opposed to that in previous experiments. Since the sample was still released in the flow-through step as in previous experiments, this flow-through sample was added back onto column to promote further binding. However, no improvement in binding of Rec-protein to column was observed, since no target bands were seen in eluent lanes (Figure 3.41).

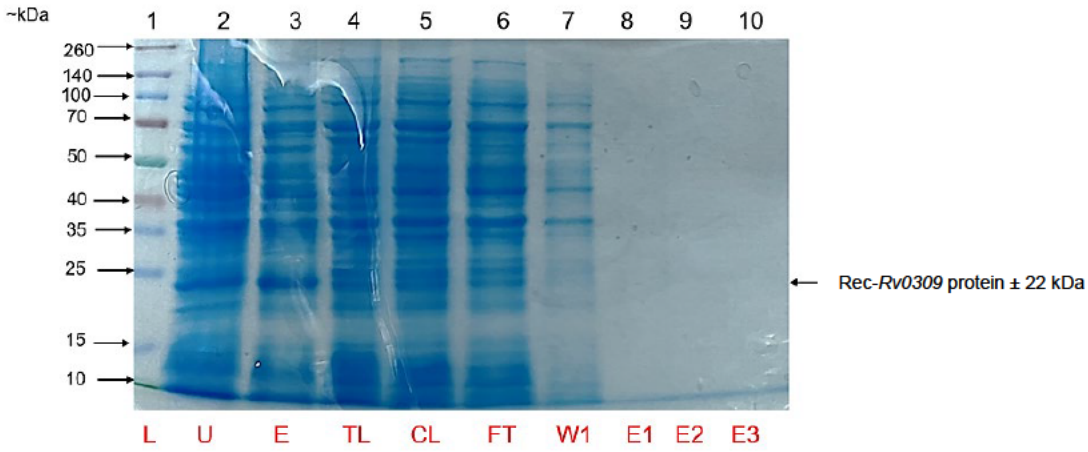

Figure 3.41: SDS-PAGE gel showing purification of recombinant *Rv0309* in pET28a vector using HisPur Cobalt column. Samples were analysed using an 15% reducing Tris-glycine SDS-PAGE gel stained with Coomassie blue. Lane 1: Thermo Scientific Spectra Multicolour Broad Range Protein Ladder (L), Lane 2: Uninduced sample after four hours (U), Lane 3: Expressed pellet after four hours-optimal time (E), Lane 4: Total lysate (TL), Lane 5: Clear lysate (CL), Lane 6: Flow-through (FT), Lane 7: Wash 1 (W1), Lane 8: Eluent 1 (E1), Lane 9: Eluent 2 (E2), Lane 10: Eluent 3 (E3).

Lysis of pellet and purification under denaturing conditions

Protein pellet was lysed using Equilibrium/Wash buffer (containing sodium phosphate, sodium chloride, imidazole and guanidine-hydrochloride) and sonication. Once centrifuged, the supernatant was used as clear lysate and added to column. Three washes (containing guanidine-hydrochloride) were done along with collection of three eluents after adding elution buffer (containing guanidine-hydrochloride). Figure 3.42 shows that uninduced sample and induced samples had similar target bands. The total lysate (Lane 4) migrated oddly, with the lane wider than the others, and the individual bands were difficult to see due to the poor resolution. Eluent lanes showed a few darkened regions indicating presence of proteins in expected and unexpected areas; however, no distinct target bands were present in expected region.

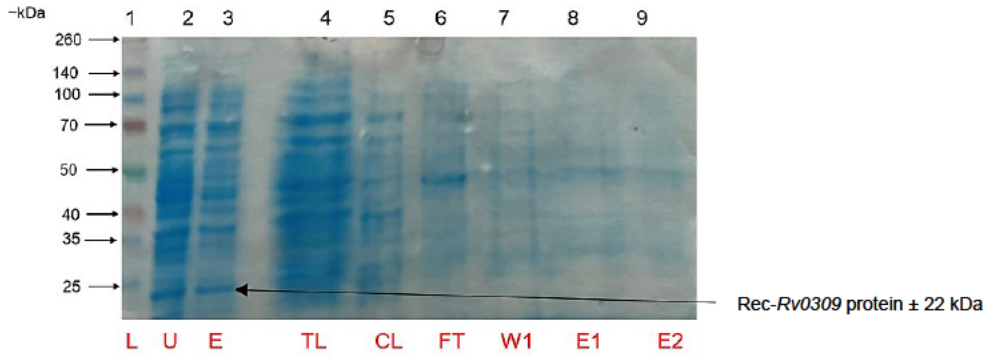

Figure 3.42: SDS-PAGE gel showing purification of fresh recombinant pET28a-*Rv0309* lysate subjected to denaturation. Samples were analysed using an 15% reducing Tris-glycine SDS-PAGE gel stained with Coomassie blue. Lane 1: Thermo Scientific Spectra Multicolour Broad Range Protein Ladder (L), Lane 2: Uninduced sample after four hours (U), Lane 3: Expressed pellet after four hours-optimal time (E), Lane 4: Total lysate (TL), Lane 5: Clear lysate (CL), Lane 6: Flow-through (FT), Lane 7: Wash 1 (W1), Lane 8: Eluent 1 (E1), Lane 9: Eluent 2 (E2).

Purification after adding denaturing agent to stored lysate from a previous experiment

Guanidine-hydrochloride was added to the clear lysate used from the same batch of sample shown in Figure 3.37. Three washes (containing guanidine-hydrochloride) were collected along with three eluents after adding elution buffer (containing guanidine-hydrochloride). (Figure 3.43). The induced sample appears to be similar in intensity to uninduced sample, the clear lysate was very low in concentration (Lane 5), leading to the absence of purified target bands in the eluents.

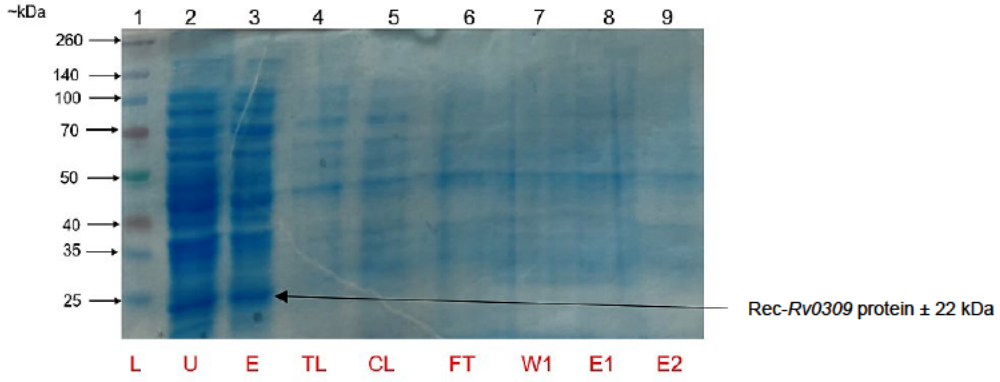

Figure 3.43: SDS-PAGE gel showing purification of stored recombinant pET28a-*Rv0309* lysate subjected to denaturation. Samples were analysed using an 15% reducing Tris-glycine SDS-PAGE gel stained with Coomassie blue. Lane 1: Thermo Scientific Spectra Multicolour Broad Range Protein Ladder (L), Lane 2: Uninduced sample after four hours (U), Lane 3: Expressed pellet after four hours-optimal time (E), Lane 4: Total lysate (TL), Lane 5: Clear lysate (CL), Lane 6: Flow-through (FT), Lane 7: Wash 1 (W1), Lane 8: Eluent 1 (E1), Lane 9: Eluent 2 (E2).

Lysis and purification experiment based on published literature

Once the OD reached ~0.6, LB/Kanamycin-Rec-*Rv0309* cultures were incubated on ice for one hour and induced with 0,25 M IPTG for 4 hours at 25°C. A 50 mL pellet was lysed using sonication buffer (20 mM Tris-HCl pH 7.9, 500 mM NaCl, 5 mM Imidazole, 1 mM PMSF. Lysozyme was added and sample was left on ice for an hour. Thereafter, the sample was passed through a 0.8 mm needle syringe five times and then sonicated. The total lysate was centrifuged (ThermoFisher Scientific™, Massachusetts, USA) and supernatant was collected as clear lysate (soluble protein). The HisTrap (Ni-NTA) resin was equilibrated with equilibration buffer (20 mM Tris-HCl pH 7.9, 500 mM). The sample was added to resin and left overnight at 4°C. The next day, flow-through was collected, and four wash steps were performed as per protocol. Elution was performed using the elution buffer outlined in protocol. Clear lysate was not prominent in expected location (Lane 2, Figure 3.44). Flow-through (Lane 3) and washes contained some of the protein. Three areas had darkened regions indicating protein presence. The eluents looked very similar to wash samples. The gel seems to appear slightly skew as lanes move upwards from left to right. Indistinct, hazy bands can be seen in the expected area as well as at ~34 kDa and at ~45 kDa. No concise intense bands can be seen in eluents, only hazy bands.

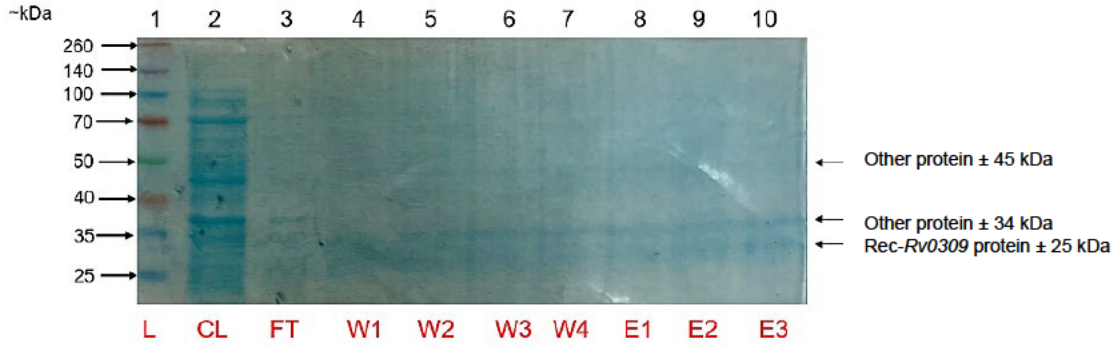

Figure 3.44: SDS-PAGE gel showing purification of recombinant *Rv0309* in pET28a vector using Kumar *et al.*, 2013 protocol as guide. Samples were analysed using an 15% reducing Tris-glycine SDS-PAGE gel stained with Coomassie blue. Lane 1: Thermo Scientific Spectra Multicolour Broad Range Protein Ladder (L), Lane 2: Clear lysate (CL), Lane 3: Flow-through (FT), Lane 4: Wash 1 (W1), Lane 5: Wash 2 (W2), Lane 6: Wash 3 (W3), Lane 7: Wash 4 (W4), Lane 8: Eluent 1 (E1), Lane 9: Eluent 2 (E2), Lane 10: Eluent 3 (E3).

Purification performed at 4°C to improve binding and prevent degradation

Protein pellet was lysed using lysis buffer (containing PBS, lysozyme, DTT, PMSF, SDS, Triton X-100) and sonication. Once centrifuged, the supernatant was used as clear lysate and added to column. The sample was left to bind for 30 minutes on end-over-end rotator. Flow-through was collected and added back onto column for further binding and collected. Purification was performed at 4°C in a walk-in fridge (Figure 3.45). Three washes were done along with collection of three eluents after adding elution buffer. Total lysate sample shows very thin band in expected region. Due to the small target protein concentration in total lysate, the clear lysate band was also low in concentration. Thus, less Rec-protein would have been able to bind to column. Hence, no Rec-protein eluent bands were found.

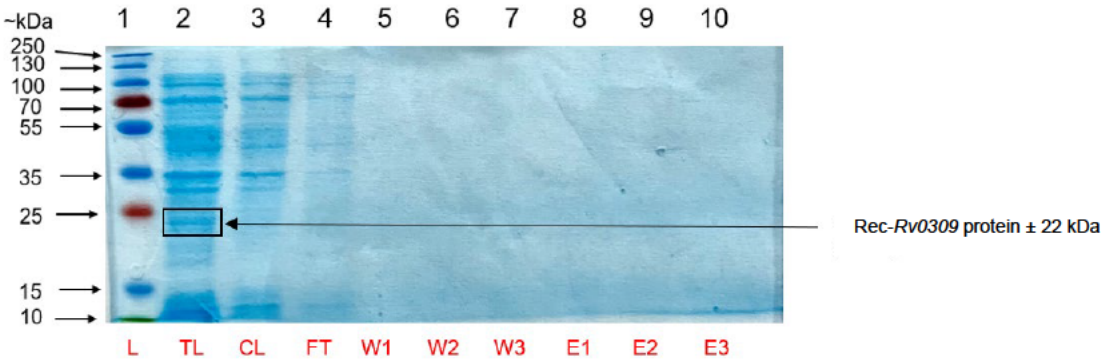

Figure 3.45: SDS-PAGE gel showing purification of recombinant *Rv0309* in pET28a vector using HisPur Cobalt column at 4°C. Samples were analysed using a 18% reducing Tris-glycine SDS-PAGE gel stained with Coomassie blue. Lane 1: Thermo Scientific PageRuler Prestained Protein Ladder (L), Lane 2: Total Lysate (TL), Lane 3: Clear Lysate (CL), Lane 4: Flow-through (FT), Lane 5: Wash 1 (W1), Lane 6: Wash 2 (W2), Lane 7: Wash 3 (W3), Lane 8: Eluent 1 (E1), Lane 9: Eluent 2 (E2), Lane 10: Eluent 3 (E3).

3.2 Bioinformatics

Bioinformatic analysis was conducted to determine reasons for difficulties in the lysis and purification of Rec-proteins. Even though the signal peptide was initially removed as recommended, many challenges were still faced. Academic experts in the field advised that perhaps the protein may be highly hydrophobic. Therefore, hydrophobicity and secondary structure predictions were assessed.

The grand average of hydropathy (GRAVY) analysis of Rv0309 sequence

The GRAVY calculator measures the hydrophobicity or hydrophilicity of a protein and is determined by the sum of hydropathy values of all amino acids divided by the length. The calculated grand average of hydropathy for *Rv0309* was 0.146. The positive value indicates protein is polar and highly hydrophobic in nature.

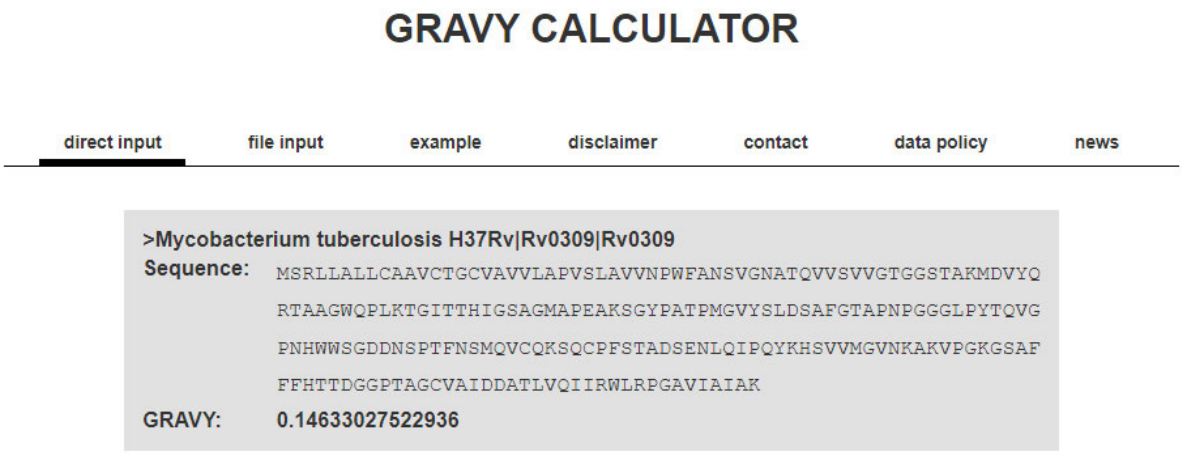

Figure 3.46: GRAVY analysis of *Rv0309* sequence (available at https://www.gravy-calculator.de/).

ThermoFisher Scientific peptide analysis of Rv0309 sequence

The peptide analysis tool offered insight into the hydrophobicity of the sequence when assessing the amino acids found in the peptide. Peptide analysis revealed that *Rv0309* is highly hydrophobic as indicated by the hydrophobicity value 79.11. Synthesis and purification prediction was reported as very difficult. Selected reaction monitoring (SRM)/ multiple selected monitoring (MRM) are techniques used in tandem mass spectrometry and can be valuable tools in biomarker analysis. The SRM/MRM result showed poor compatibility and that it should not be used in SRM/MRM experiments due to unstable elution time and inaccurate quantitation caused by aggregation and insolubility of *Rv0309*.

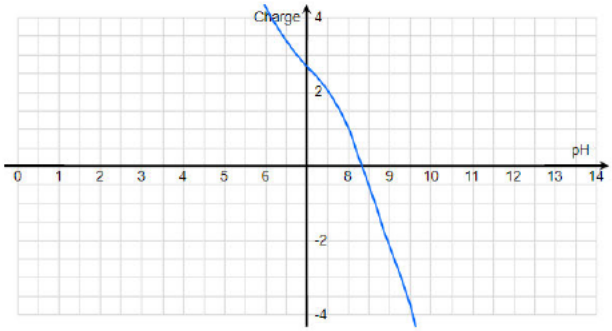

Analyzed sequence

M-S-R-L-L-A-L-L-C-A-A-V-C-T-G-C-V-A-V-V-L-A-P-V-S-L-A-V-V-N-P-W-F-A-N-S-V-G-N-A-T-Q-V-V-S-V-V-G-T-G-G-S-T-A-K-M-D-V-Y-Q-R-T-A-A-G-W-Q-P-L-K-T-G-I-T-T-H-I-G-S-A-G-M-A-P-E-A-K-S-G-Y-P-A-T-P-M-G-V-Y-S-L-D-S-A-F-G-T-A-P-N-P-G-G-G-L-P-Y-T-Q-V-G-P-N-H-W-W-S-G-D-D-N-S-P-T-F-N-S-M-Q-V-C-Q-K-S-Q-C-P-F-S-T-A-D-S-E-N-L-Q-I-P-Q-Y-K-H-S-V-V-M-G-V-N-K-A-K-V-P-G-K-G-S-A-F-F-F-H-T-T-D-G-G-P-T-A-G-C-V-A-I-D-D-A-T-L-V-Q-I-I-R-W-L-R-P-G-A-V-I-A-I-A-K

Sequence length	218
Hydrophobicity	79.11
GRAVY	0.15
MW average	22529.0293 g/mol
MW monoisotopic	22514.2035
Theoretical pI	8.3

⚠ The sequence is longer than 25 amino acids, which may significantly affect the quality of the analysis.

⚠ Some amino acids(Q, E(N-term), C, M, W, N, P, D) are less stable than others and are prone to side reactions. These reactions may occur even under our stringent production conditions. The final peptide yield is the sum of the product and the peptide that has undergone side reactions. Once the sum of the corresponding peaks in analytical HPLC reaches the requested purity, the peptide is shipped. While the total purity stays constant, the ratio of product and byproduct may change over time.

Synthesis/Purification

Difficult — Easy

Synthesis and purification will be challenging, and there is a significant risk that we will not be able to deliver the peptide quantity and purity ordered. If we are successful, though, delivery time may be 2 to 3 times longer than for a standard peptide. Note: If we are not able to deliver the quantity and/or purity ordered, you may cancel the order or receive the product and pay for the quantity and/or purity delivered.

SRM/MRM Compatibility

Bad — Good

This is a very hydrophobic peptide that should not be used in SRM/MRM experiments because of unstable elution time and very inaccurate quantitation caused by aggregation and insolubility.

Figure 3.47: Peptide analysis of *Rv0309* sequence (available at https://www.thermofisher.com/za/en/home/life-science/protein-biology/peptides-proteins/custom-peptide-synthesis-services/peptide-analyzing-tool.html).

The PHYRE 2 software analysis of Rv0309 sequence

Secondary structure and disorder prediction of *Rv0309* was determined using PHYRE2. Figure 3.48 revealed that *Rv0309* is made up of 16% alpha helices, where the largest region at the beginning of sequence appears to be the signal peptide. The sequence contained 27% beta strands and 7% of transmembrane helix. There is also a disordered region that made up 17% of sequence. Alignment coverage analysis revealed similarities with hydrolases.

Figure 3.48: Detailed template information showing secondary structure, disorder prediction and alignment coverage with confidence intervals using PHYRE2 software (available at: http://www.sbg.bio.ic.ac.uk/~phyre2/html/page.cgi?id=index).

CHAPTER 4: DISCUSSION

4.1 Discussion

Tuberculosis (TB) remains a global burden with the high rates of drug resistance, lack of effective rapid point-of-care (POC) tests and timeous initiation of appropriate treatment, as well as an effective vaccine, to reduce TB transmission (World Health Organization [WHO], 2019). Biomarkers can be exploited for their potential in a rapid POC test. Despite many advances, the shortage of biomarkers with high sensitivity and specificity continue to hinder the development of a POC test that can be routinely implemented in clinical settings. *Mycobacterium tuberculosis (*Mtb*) Rv0309* protein has shown promise as a potential biomarker for this purpose. The *Rv0309* gene is localised in the cell wall of Mtb and has been reported to enhance mycobacterial intracellular survival after infection (Peng et al., 2022). This survival has been linked to the inhibition of pro-inflammatory response and decrease in bacterial cell wall permeability. The gene contains highly antigenic sites that may evoke a significant immune response (Reche, 2023). Additional studies have reported the importance of *Rv0309* in biofilm development, Mtb cellular morphology and that the deletion of the gene decreased infecting potential of the mutant strain (Muniram, 2018; Mthembu, 2022).

While published literature has elucidated the structure and biology of *Rv0309* (Kumar et al., 2013; Peng et al., 2022), further downstream analysis on the application and validation of this protein as a target for TB diagnostic and therapeutics have not been reported. This formed the rationale and aim of the present study, to clone, express and purify *Rv0309* in sufficient quantity for future downstream processes to facilitate serodiagnosis, drug or vaccine development.

4.1.1 Truncated Rv0309 gene successfully cloned into pGEX-6P-1 and pET28a vectors

Mycobacterium tuberculosis membrane proteins are notoriously challenging to purify (Bashiri & Baker, 2015). This is due to the hydrophobicity of their sequences and propensity to aggregate. Kumar et al. (2013) noted that purification was challenging for proteins *Rv0309*, *Rv2599* and *Rv3717*, and removing signal peptides was vital in enabling effective purification. A study on cloning, expressing and purifying *Mtb* Rec-proteins found that eight of the fifteen proteins selected were insoluble and were only purified once obtained in soluble form (Utpal et al., 2015). Therefore, in the current study, to facilitate purification, a signal peptide analysis was performed before designing primers for cloning using SignalP 6.0. The analysis (Figure 3.1) revealed that a signal peptide cleavage site existed between positions 15 and 16; hence, the first 15 amino acids were removed. In contrast, 29 amino acids were removed in the study by Kumar et al., 2013, based on the older version of the programme. The advantages of using

a newer programme version include improved algorithms, models and increased training data. SignalP 6.0 can predict additional types of signal peptides and identify their sub-regions left undetected in previous versions (Teufel et al., 2022).

When the truncated *Rv0309* gene was amplified using PCR (Figure 3.2), single bright bands were seen in each lane at the expected region (± 611 bp), indicating successful amplification. Electrophoresis of pGEX-6P-1 and pET28a plasmid DNA (pDNA) (Figure 3.4 and Figure 3.5), revealed various bands representing the expected plasmid conformations. The light smearing found in the pDNA sample lane (Figure 3.5) was suspected to be due to overfilling wells; hence, the overflow onto the gel. Light smearing was also seen in another study showing pDNA samples isolated and restricted using ZymoPURE-EndoZero Midiprep and QIAGEN Midi Kits (Mikhail et al., 2022). A study exploring various methods for plasmid extraction such as alkaline lysis and transposon-aided capture of plasmids (TRACA) showed light smearing in isolated samples (Delaney et al., 2018). These observations suggest that smearing of pDNA samples may be common regardless of kit or method used.

When electrophoresed, restricted sample bands were not sharp and slightly smeared. This can occur if too much enzyme is used, digestion takes longer than necessary, or the enzyme is bound to the sample, affecting band migration (NEB, 2023a; Orange County Biotechnology Education Collaborative, 2023). The restricted insert in Lane 3 (Figure 3.6) for the reaction with pGEX-6P-1 appeared slightly higher than the unrestricted insert in Lane 2. This may have been due to the enzyme still being bound to the sample. Salt concentration can also cause slower migration of a sample. For the restriction reaction with the pET28a vector, the restricted insert was the same size as the unrestricted insert, as expected. Single bands were found for the restricted vectors as expected. Since restriction digestion was successful, samples were quantified and used for ligation reaction.

Ligation with both ratios of insert to vector (3:1 and 5:1) were successful as many colonies were seen and screened positive. Ligation can be attempted with different ratios (ThermoFisher Scientific, 2023a) to improve chances of success. In a previous study, various ratios and associated transformation efficiencies were tested, and the ratio 3:1 was reported to have the highest efficiency (Topcu, 2000). Another study also recommended testing various molar ratios as some inserts are smaller, and higher insert concentrations improved ligation reactions (MacPherson et al., 2022). The ligation mix containing pGEX-6P-1 and insert was transformed directly into *E. coli* BL21 cells as pGEX-6P-1 is a high-copy plasmid. The ligation mix containing pET28a and the insert was first transformed in *E. coli* DH5α cells due to the pET28a plasmid being a low copy plasmid. Once positive transformants were observed, a positive sample was transformed into *E. coli* BL21 cells.

Colony PCR confirmed the presence of insert within the transformed *Rv0309* clones. All colonies screened for *Rv0309*-pGEX-6P-1 showed evidence of the insert, as the bands seen were the same size as the truncated *Rv0309* gene (Figure 3.8). This positive result confirmed the presence of the truncated *Rv0309* gene within the clones. Although colony PCR was successful for most colonies selected in *Rv0309*-pET28a (Figure 3.9), some clones had no insert, which could be due to a self-ligating vector with the presence of selective marker ampicillin (NEB, 2023b). Colony PCR is an efficient tool to confirm clone viability, as expected bands are shown for the *Rv0309* gene. However, the correct size of PCR products does not indicate if any mutations occurred which could potentially affect downstream processing. Therefore, the clones were subjected to plasmid isolation for Sanger sequencing by Inqaba Biotec. The sequence analysis confirmed the clones contained the *Rv0309* gene, which was in-frame, and contained no mutations (Appendix D).

4.1.2 Recombinant Rv0309 proteins successfully expressed using lower temperature, optimal isopropyl ß-D-1-thiogalactopyranoside concentrations and induction times.

Optimisation trials demonstrated that *Rv0309* was optimally expressed in pGEX-6P-1 and pET28a at five and four hours, after induction with 0.5 mM and 0.25 mM IPTG, respectively A lower induction temperature of 25°C was chosen for *Rv0309* expression in both vectors in an effort to reduce inclusion body formation as recommended previously (Sandomenico et al., 2020; Huang et al., 2021; So et al., 2023) as well as follow published literature on *Rv0309* (Kumar et al., 2013). Additionally, Mtb membrane protein production was reported to be higher at a lower temperature compared to expression at 37°C (Grāve et al., 2022). However, *Rv0309* was still found to be in inclusion bodies. Kumar et al. (2013) reported many hurdles to express protein in the soluble form before adopting the strategy of removing signal peptide. On the contrary, *Mycobacterium smegmatis Rv0309* was induced at 45°C in Middlebrook 7H9 (Peng et al., 2022). *Mycobacterium smegmatis* is more resistant to higher temperatures (Smeulders *et al*., 1999; Shires & Steyn, 2001) than Mtb.

4.1.3 Problems encountered during SDS-PAGE and Western blotting

Although the Rec-protein was visualised on gels and confirmed by Western blots, several challenges were encountered during the execution of the experiments. These included low protein concentration, which made the visualisation of bands on gel difficult, unexpected multiple bands, vertical streaking and skewness of gel. The low protein concentration could have occurred through loss when lysis processes were performed. Attempts to increase the protein concentration were made during dialysis by removing most salts and buffer components (Nowakowski et al., 2014) and using Amicon® filters. Concentration plays a

crucial role in maintaining the stability of proteins in solution. Dialysis usually removes additives, such as DTT that stabilises proteins. In the present study, when dialysis was attempted, DTT removal may have contributed to unstable protein in some of the troubleshooting trials. Gel clarity can be improved by the use of freshly prepared reagents or buffers. Fresh running buffer as well other reagents were made numerous times to make up gels. Protein degradation was prevented by storing samples at low temperatures and protease inhibitors were included in lysis buffers. Streaking seen during His-tag denaturing trials may have been caused by unremoved precipitated insoluble material (Kurien & Scofield, 2012). The skewness seen on a gel can be due to various reasons which include, the gel may have had uneven loading volume; however, an equal volume was loaded into each lane hence eliminates this possibility. Inconsistent gel preparation can also cause skewness; however, other gels from the same prepared batch ran normally. Uneven voltage can be another issue, but a constant voltage (90 volts) was used throughout the sample run. The gel buffer pH or concentration may have changed since the buffer is often reused. When a fresh buffer was made, and the gels ran as expected (Bhatt et al., 2022).

The calculated size of GST- and His-tagged *Rv0309* Rec-proteins were ±48 kDa and ±22 kDa, compared to the actual sizes of ±45 kDa and ±25 kDa, respectively, when Rec-proteins were electrophoresed in a gel. The size discrepancy may be due to multiple reasons, such as chemical modifications or amino acid composition. A study reported that the size discrepancy between calculated and observed values of digestive organ expansion factor protein was accounted for by the amino acid composition (Guan et al., 2015). In the present study, the protein size observed may also be higher than calculated size due to post-translational modifications (Shi et al., 2012). Similarly, in another study abnormal migration of cytosolic proteins on SDS-PAGE gel were caused by post-translational modifications (Shi et al., 2012). Post-translational modifications such as glycosylation can add mass to the protein, therefore, slowing protein migration on gel. Membrane and secretory proteins are usually subject to these modifications (Ramazi & Zahiri, 2021). Size discrepancy may also be seen when there is retention of varying degrees of protein secondary structure despite the presence of a denaturant such as SDS in the sample (ThermoFisher Scientific, 2023b).

Western blot analysis confirmed the presence of the target Rec-protein following expression. Specific antibodies against the tagged Rec-protein were employed. The target Rec-protein protein was present in the Western blot containing GST samples; however, other smaller bands were also shown. This may have been due to insufficient blocking, high concentration of sample loaded or high concentration of primary antibody. There were strong signals present for His-tagged protein, with absence of non-specific bands. However, the Western blots after

protein purification demonstrated weak signals for eluent lanes. A likely cause of the weak signals may be the low concentration of protein obtained after purification. As noted above, with SDS-PAGE, the sample may have degraded as samples were left to thaw. When subsequent experiments were performed, precautions were taken to prevent sample degradation, such as maintaining temperature/ storage conditions and ensuring reducing agents were not removed. These improvements are important to ensure the *Rv0309* was above the detection level of the stain for the samples. Additionally, blocking with 0.5% milk for 30 min was reported to be ideal for minimising the loss of antigens from immunoblotting membranes (DenHollander & Befus, 1989).

4.1.4 Lysis and purification challenges contributed to very low yield of purified recombinant Rv0309 protein.

The lysis and purification process presented many challenges despite employing various troubleshooting experiments. Researchers with protein purification expertise provided valuable insight and assistance to overcome these hurdles. Despite this, a few significant problems could not be resolved. The total lysate and clear lysate bands were less concentrated than expected, indicating that the lysis method was not optimal. Hence, many trials were performed to improve the lysis of the Rec-protein. During purification, most of the lysed protein was released in the flow-through step before washes, indicating that the protein was not binding to the columns effectively. When a small amount of the protein appeared to bind to the column, there was co-elution of the target with other proteins.

4.1.4.1 *Rv0309*-pGEX-6P-1 lysis and purification trials

An initial attempt involved increasing the volume of culture to increase the concentration of the sample due to the larger pellet size obtained. However, it was later discovered that the protein was present in inclusion bodies. Hence, the focus shifted to solubilising inclusion bodies for purification. Dialysis and concentration of samples using Amicon® filters did not yield any significant difference, as unconcentrated samples exhibited similar band intensity and size on gels. Loss of protein despite using Amicon® filters may occur due to protein precipitation, leading to obstruction of the filter. Reduced volumes of lysis buffer, Triton X-100 and solubilisation buffer were adopted to increase concentration whilst avoiding dilution of the sample. Different temperatures were also tested during freeze-thaw steps and pellet storage before lysis, but these variations did not yield significant changes. A key observation was made when a supernatant previously discarded, was collected and analysed during insoluble protein preparation. Interestingly, the band intensity was higher in this supernatant compared to the pellet, prompting a purification attempt. However, the results showed little to no elution

of the target Rec-protein, most of the Rec-protein was again released in the before-wash steps, confirming that the protein did not bind to the column.

In an effort to improve the binding of the protein to the column, binding time was increased from two hours to four hours and then six hours. Increasing the binding time seemed to improve the amount of protein adhering to the agarose, as seen by more noticeable eluent bands. However, the bands were still not as intense as desired due to most of the protein still being released in the before-wash samples. Overnight binding at 4°C appeared to improve the target eluent band; however, there was co-elution with other proteins (for His-tagged protein), or the protein was not released from the agarose (for GST-tagged protein). Sonication of an expressed pellet is a common troubleshooting suggestion (Moore et al., 2016). The negative control sample that was not subject to sonication was much fainter than other lysed samples indicating lysis was not optimal without sonication. Notably, longer sonication times seemed to intensify the protein band, with optimal results achieved when combining mechanical and chemical lysis. Other studies support a combination of mechanical and chemical methods to increase lysis efficiency (Harrison, 1991; Anand et al., 2007; Balasundaram et al., 2009; Shehadul Islam et al., 2017). Although the lysate appeared more intense, purification was still unsuccessful.

To verify the functionality of a column, purification was attempted with expressed pGEX-6P-1. Purification confirmed that the GST-tag could bind and elute effectively. Affinity tags have been reported to maintain the solubility of an insoluble protein (LaVallie et al., 1993; Zhang et al., 1998; Wingfield, 2015); hence, it is also unlikely that a tag would inhibit the protein's ability to bind to the column. The protein's isoelectric point (pI) was considered, where the pH of buffers was adjusted (Wingfield, 2015). However, this did not impact purification significantly as an affinity column was used and designed to bind GST-lagged protein. Collectively, the troubleshooting findings suggested that the GST-tag in the Rec-protein was being folded in such a way, that made it inaccessible to binding sites on the column. Substitution of DTT for β-mercaptoethanol in lysis buffer showed that the latter reagent did not specifically interfere with the Rec-protein stability or conformation.

Various purification methods were explored, such as batch, gravity-flow columns, ÄKTA purification system, ion-exchange chromatography and size exclusion. Previous studies demonstrated optimal protein recovery using these methods (Werner et al., 1994; Batas & Chaudhuri, 1996; Li et al., 2002; Kweon et al., 2004). However, in the present study, irrespective of the method, this study's results consistently demonstrated that the protein did not bind effectively to the purification column and was released in the before-wash/wash steps before elution, and often with other proteins.

A zwitterionic detergent, CHAPS, solubilises and stabilises membrane proteins. Sarkosyl serves a similar purpose and was meant to maintain solubility, particularly when purification occurs under denaturing conditions. When the original lysis buffer containing PBS, Triton X-100, Lysozyme, PMSF, DTT and EDTA was used as wash buffer and sarkosyl added to elution buffer, the pure Rec-protein was shown in eluent lanes. The use of sarkosyl during purification was also reported (Schlager et al., 2012; Massiah et al., 2016). Schlager et al. (2012) reported high affinity binding and elution profiles when using sarkosyl whilst Massiah et al. (2016) reported that although sarkosyl is very effective in solubilising insoluble protein, it can be difficult to purify as sarkosyl molecules encapsulate the protein along with tag regions thus preventing binding. In the current study, trials with both CHAPS and Triton X-100 in the wash buffer and sarkosyl in the elution buffer showed promising results. Although the concentration was low, purified Rec-protein was obtained but these results were not reproducible. Similarly, the trial using lysis buffer as wash buffer and sarkosyl in elution buffer showed Rec-protein in eluents; however, results were not reproducible.

4.1.4.2 *Rv0309*-pET28a lysis and purification trials

Due to the lack of success with the GST-tagged Rec-protein, the cloning was repeated in pET28a, containing a His-tag, which is smaller than the GST-tag. The bacterial protein extraction reagent (B-PER) reagent was initially used as a lysis buffer for the His-tagged *Rv0309*. The advantages of this mild detergent include solubilisation without excessive denaturation, efficiency as reagent offers one-step cell lysis, suitability for any scale of protein extraction and compatibility with protease inhibitors and can be used for both His-tag and GST-tag purification. However, purification was unsuccessful. Various purification methods were attempted for His-tag, such as ÄKTA purification using Ni-NTA and HisPur Cobalt cartridges, Ni-NTA beads, Ni-NTA agarose in gravity flow column, size exclusion chromatography and HisPur Cobalt agarose in gravity flow columns. An improved clear lysate band intensity was obtained with a harsher sonication mode. Denaturing trials were performed using the methods outlined in ThermoFisher Scientific manufacturer's sheet with guanidine hydrochloride, and those recommended by our expert research consultants. A strong denaturing agent such as guanidine hydrochloride or urea should be able to completely solubilise inclusion bodies and expose the tag to the Ni-NTA matrix (Humbert, 2019). To determine whether the His-tag was being hidden during folding, denaturing trials can be done or moving the affinity tag to the opposite terminus (Bornhorst & Falke, 2000). In the current study, denaturing trials reflected that Rec-protein had better binding compared to the GST-tagged protein. However, this also promoted non-specific proteins binding to the column, and co-elution during the elution steps. As suggested in other studies, attempts were made to lyse

the sample on ice and perform purification in a 4°C walk-in fridge (Wingfield, 2015). Working at 4°C helps keep proteins stable and prevents degradation, and lower temperatures can also assist and maintain solubility. Despite these efforts, purification remained unsuccessful.

Kumar et al. (2013) reported that although Rec-proteins were cloned, expressed and purified, challenges with the purification of proteins were encountered and removal of the signal peptide assisted greatly. However, attempts using their lysis and purification method failed to reproduce their results. The Rec-protein seemed to still be in the pellet as clear lysate band was not as concentrated as expected. In another study, (Peng et al., 2022) reported purifying the protein using *Mycobacterium smegmatis Rv0309* gene as opposed to Mtb H37Rv used in Kumar et al. (2013) and the present study. Since the two previous studies did not show the flow-through or wash samples in their results, the binding efficiencies could not be compared to the data obtained in the current study.

Another observation during the purification trials was that the large-scale expressed pellet did not reflect the same band intensity obtained during the optimised small-scale expression. The reason for this may be oxygen and nutrient limitations that can affect growth and productivity (Krause et al., 2016). The band size and intensity of the uninduced and expressed pellets from the large-scale expression were very similar at the optimal time point. The *E. coli* BL21 cells have a baseline expression of target protein without the presence of IPTG. Significantly higher membrane protein yield was found in the absence of IPTG in a study (Zhang et al., 2015). Alternatively, the similar growth in uninduced samples and expressed samples could suggest a leaky expression and this would be a challenge if protein was toxic to the cells (Kato, 2020). Another observation made was that expressed pellet samples often looked less intense than optimisation experiments. This may be due to storage of pellet; however, fresh pellets were made often and pellet stored for long periods were not used in experiments.

Partial, minor success was demonstrated when His-tagged Rec-protein was present in the eluent, but had co-eluted with other proteins. The other proteins on the gel varied in size, but most appeared larger than the target. The Western blot reflected the target protein in the expected location with no other bands seen in eluent lanes. When the target protein band found in the eluent was excised and sequenced using peptide mass fingerprinting, there was a 98% match with the reference sequence, with the size correlating to the calculated size. However, the concentration was low and lacked the purity required for future downstream processing.

Multiple studies have demonstrated the presence of purified proteins, but in combination with other proteins. A study to isolate and purify antigens secreted by Mtb strain C for diagnostic purposes revealed the presence of purified target proteins, along with various protein bands

in SDS-PAGE (Khosrobeygi et al., 2021). However, the Western blot displayed only one band between 30 kDa and 41 kDa. Despite the co-elution of other proteins with the target, Khosrobeygi et al. (2021) concluded that the Mtb culture filtrate antigens could be used for diagnostic purposes. Similarly, *Rv1131* together with multiple bands in the eluent were present after purification; however, one band was seen on the Western blot (Eniyan & Bajpai, 2015). Conventional purification systems produced limited success with soluble MPT51 (*Rv3803c*) as there were very low yields and some contamination; however, when the Rec-protein was overexpressed, optimal results were found (Ramalingam et al., 2004).

The Mtb PE_PGRS45 (*Rv2615c*) protein was successfully purified using the pMAL-c5x vector (Xu et al., 2021). However, the purified protein contained other bands, which were removed during Factor Xa digestion, resulting in a single-banded Rec-protein used for an ELISA assay. The vector, pMAL-c5x, contained maltose-binding protein as a fusion partner. In another study, an additional protein band was observed together with *Rv3874* and *Rv3875* protein eluents. Purification was repeated using eluent samples resulting in eluents of single Rec-proteins with high concentration (Hanif et al., 2010) and the additional bands were absent (Hanif et al., 2010). The intensity of the initial eluent and eluent after performing purification again was similar, indicating these proteins bound well to the column, and protein was not lost as opposed to the present study.

4.1.5 Bioinformatics

The grand average of hydropathicity (GRAVY) value of *Rv0309* was 0.146, indicating strong lipophilicity, similar to published literature (Peng et al., 2022). The ThermoFisher Scientific peptide analysis revealed that the hydrophobicity of the protein was very high at 79.11%. The hydrophobicity analysis of the *Rv0309* sequence, revealed that *Rv0309* has continuous hydrophobic regions, which suggests that the protein folds in a way that inhibits binding and aggregates easily (Mitraki et al., 1991; Singh et al., 2015). As a last resort, the peptide synthesis company GenScript was approached to synthesise an *Rv0309* peptide to enable downstream work. Based on GenScript team's experience, the success rate of synthesis below 80 amino acids is predicted to be generally high. However, since the peptide in the present study is approximately 2.5X greater in length at 202 amino acids long, the success rate of peptide synthesis was predicted to be very low. Additionally, GenScript noted that aggregation would occur easily, making it difficult for amino acid condensation, thus increasing the difficulty of production. Thus, the company was unable to comply with the request. The secondary structure of *Rv0309* produced by PHYRE2 software showed that 27% of the sequence is comprised of beta strands. Beta strands can form beta sheets that have the ability to form a hydrophobic core on either side of sheet (Cheng et al., 2013). Kumar et al. (2013)

reported that *Rv0309* contained 47% beta sheets using Dichroweb analysis of circular dichroism. Amino acids in beta sheets are often hydrophobic. There is presence of alpha helices in the signal peptide region at the beginning of the sequence and towards the end of the sequence. Alpha helices are generally made up of exposed hydrophobic residues (Skipper, 2005) with an embedded hydrophilic region. Similarities were found between *Rv0309* and hydrolases. This may be due to *Rv0309* encoding Ldt which has shown hydrolase activity in *Enterococcus faecalis* bacterial cell wall components as well as cell wall cross-linking (Magnet et al., 2007). Cell wall hydrolases are key for the growth and separation of bacterial cells (Wyckoff et al., 2012) and can serve as multifunctional proteins that possess adhesin and virulence properties (Vermassen et al., 2019). Hydrolase activity has also been shown in MTP, lpqL, Ag85 complex, MPT51, Fba, PrcB, SahH and *Rv3717* (Maharajh et al., 2023).

4.2 Limitations of study

Limitations of this study include the expression system not being optimal to facilitate the lysis and purification of *Rv0309*. Additionally, the high levels of hydrophobicity found within sequence contributed to poor lysis and purification.

4.3 Conclusions

While cloning and large-scale expression of the recombinant *Rv0309* protein were successfully undertaken, Rec-protein was confirmed by Western blotting and sequencing, the purification still posed major challenges despite numerous troubleshooting experiments. Although there was some success with pure protein being obtained during the study, the concentration was low and results were not reproducible. The main problems were sub-optimal lysis of the Rec-protein and ineffective binding to the purification column. Therefore, the *Rv0309* protein could not be purified in sufficient quantity for downstream applications. The insights gained from the lysis, purification and bioinformatic analysis of *Rv0309* in this study contribute to the understanding of membrane protein biochemistry and the intricacies associated with Mtb protein purification.

4.4 Recommendations

Since *Rv0309* peptide analysis revealed high levels of synthesis difficulty and high hydrophobicity, one can consider expression of the protein in a different host such as yeast, baculovirus, or cell-free expression systems. A strategy to prevent inclusion body formation

can be co-expression with chaperones; however, a study reported that the strategy did not improve solubility (Choi & Geletu, 2018). This report is also supported by other studies reporting the inconsistencies regarding use of co-expression molecular chaperones (Makrides, 1996; Sørensen & Mortensen, 2005). However, cloning in a vector such as pMAL, that contains a molecular chaperone for effective protein production has shown great success in other studies (Bach et al., 2001; Hu et al., 2011; Xu et al., 2021). The highest epitope region of *Rv0309* could be synthesised and fused to an immunogenic chaperone protein. A study compared induction using IPTG and lactose and results showed that lactose was able to produce more soluble protein during expression as opposed to IPTG that produced more inclusion bodies (Wurm et al., 2016). Similarly, another study explored autoinduction using lactose and glucose and was successful in obtaining the induction level required (Tahara et al., 2021). A combination of fusion strategy and nanotechnology may be promising (Mahmoodi et al., 2019). Since using CHAPS and sarkosyl showed promising results in the study, methods making use of these reagents can be explored further to improve yield, even though much is washed out. Purification can also be attempted using an unconventional technique such as the teabag method (Hering et al., 2020). These trials should aim to decrease the chances of aggregation and incorrect folding. Once *Rv0309* has been purified sufficiently, studies can be performed to assess *Rv0309* as a biomarker or for potential drug discovery. These strategies can be applied to other membrane proteins or microbes that are challenging to purify.

REFERENCES

Abdool Karim, Q., & Baxter, C. (2022). COVID-19: Impact on the HIV and tuberculosis response, service delivery, and research in South Africa. *Current HIV/AIDS Reports*, *19*(1), 46-53. https://doi.org/10.1007/s11904-021-00588-5

Al-Saeedi, M., & Al-Hajoj, S. (2017). Diversity and evolution of drug resistance mechanisms in *Mycobacterium tuberculosis*. *Infection and Drug Resistance*, *10*, 333-342. https://doi.org/10.2147/idr.S144446

Alderwick, L. J., Birch, H. L., Mishra, A. K., Eggeling, L., & Besra, G. S. (2007). Structure, function and biosynthesis of the *Mycobacterium tuberculosis* cell wall: arabinogalactan and lipoarabinomannan assembly with a view to discovering new drug targets. *Biochemical Society Transactions*, *35*(5), 1325-1328. https://doi.org/10.1042/bst0351325

Alderwick, L. J., Harrison, J., Lloyd, G. S., & Birch, H. L. (2015). The Mycobacterial cell wall-peptidoglycan and arabinogalactan. *Cold Spring Harbor Perspective in Medicine*, *5*(8), a021113. https://doi.org/10.1101/cshperspect.a021113

Alene, K. A., Wangdi, K., & Clements, A. C. A. (2020). Impact of the COVID-19 pandemic on tuberculosis control: an overview. *Tropical Medicine and Infectious Disease*, *5*(3). https://doi.org/10.3390/tropicalmed5030123

Algood, H.M., Chan, J., & Flynn, J.L. (2003). Chemokines and tuberculosis. *Cytokine & growth factor reviews*, 14(6), 467-477. https://doi.org/10.1016/s1359-6101(03)00054-6

Anand, H., Balasundaram, B., Pandit, A., & Harrison, S. (2007). The effect of chemical pre-treatment combined with mechanical disruption on the extent of disruption and release of intracellular protein from *E. coli*. *Biochemical Engineering Journal*, *35*(2), 166-173. https://doi.org/10.1016/j.bej.2007.01.011

Andrea, P., Christopher, F., Anna, V., Karin, W., & Katherine, F. (2013). Xpert MTB/RIF for diagnosis of tuberculosis and drug-resistant tuberculosis: a cost and affordability analysis. *European Respiratory Journal*, *42*(3), 708. https://doi.org/10.1183/09031936.00147912

Asano, M., Nakane, A., & Minagawa, T. (1993). Endogenous gamma interferon is essential in granuloma formation induced by glycolipid-containing mycolic acid in mice. *Infection and Immunity*, *61*(7), 2872-2878. https://doi.org/10.1128/iai.61.7.2872-2878.1993

Asmar, S., & Drancourt, M. (2015). Rapid culture-based diagnosis of pulmonary tuberculosis in developed and developing countries. *Frontiers in Microbiology*, *6*, 1184. https://doi.org/10.3389/fmicb.2015.01184

Bach, H., Mazor, Y., Shaky, S., Shoham-Lev, A., Berdichevsky, Y., Gutnick, D. L., & Benhar, I. (2001). *Escherichia coli* maltose-binding protein as a molecular chaperone for recombinant intracellular cytoplasmic single-chain antibodies. *Journal of Molecular Biology*, *312*(1), 79-93. https://doi.org/10.1006/jmbi.2001.4914

Bagcchi, S. (2023). WHO's global tuberculosis report 2022. *The Lancet Microbe*, *4*(1), e20. https://doi.org/10.1016/S2666-5247(22)00359-7

Balasundaram, B., Harrison, S., & Bracewell, D. G. (2009). Advances in product release strategies and impact on bioprocess design. *Trends in Biotechnology*, *27*(8), 477-485. https://doi.org/10.1016/j.tibtech.2009.04.004

Bansal-Mutalik, R., & Nikaido, H. (2014). Mycobacterial outer membrane is a lipid bilayer and the inner membrane is unusually rich in diacyl phosphatidylinositol dimannosides. *Proceedings of the National Academy of Sciences*, *111*(13), 4958-4963. https://doi.org/10.1073/pnas.1403078111

Barberis, I., Bragazzi, N. L., Galluzzo, L., & Martini, M. (2017). The history of tuberculosis: from the first historical records to the isolation of Koch's bacillus. *Journal of Preventative Medicine and Hygiene*, *58*(1), E9-e12.

Bashiri, G., & Baker, E. N. (2015). Production of recombinant proteins in *Mycobacterium smegmatis* for structural and functional studies. *Protein Science*, *24*(1), 1-10. https://doi.org/10.1002/pro.2584

Batas, B., & Chaudhuri, J. B. (1996). Protein refolding at high concentration using size-exclusion chromatography. *Biotechnology and Bioengineering*, *50*(1), 16-23.

Belisle, J. T., Vissa, V. D., Sievert, T., Takayama, K., Brennan, P. J., & Besra, G. S. (1997). Role of the major antigen of *Mycobacterium tuberculosis* in cell wall biogenesis. *Science*, *276*(5317), 1420-1422. https://doi.org/10.1126/science.276.5317.1420

Berry, C., du Cros, P., Fielding, K., Gajewski, S., Kazounis, E., McHugh, T. D., Merle, C., Motta, I., Moore, D. A. J., & Nyang'wa, B. T. (2022). TB-PRACTECAL: study protocol for a randomised, controlled, open-label, phase II-III trial to evaluate the safety and efficacy of regimens containing bedaquiline and pretomanid for the treatment of adult patients with pulmonary multidrug-resistant tuberculosis. *Trials*, *23*(1), 484. https://doi.org/10.1186/s13063-022-06331-8

Bhatt, M., Rai, V., Kumar, A., Kiran, Yadav, A. K., Rajak, K. K., Gupta, V., Chander, V., & Avasthe, R. K. (2022). SDS-PAGE and Western Blotting: basic principles and protocol. *Protocols for the Diagnosis of Pig Viral Diseases* (pp. 313-328). Springer US. https://doi.org/10.1007/978-1-0716-2043-4_23

Bisht, D., & Meena, L. S. (2019). Adhesion molecules facilitate host-pathogen interaction & mediate *Mycobacterium tuberculosis* pathogenesis. *Indian Journal of Medical Research*, *150*(1), 23-32. https://doi.org/10.4103/ijmr.IJMR_2055_16

Bornhorst, J. A., & Falke, J. J. (2000). Purification of proteins using polyhistidine affinity tags. *Methods in Enzymology*, *326*, 245-254. https://doi.org/10.1016/s0076-6879(00)26058-8

Brennan, M. J., Delogu, G., Chen, Y., Bardarov, S., Kriakov, J., Alavi, M., & Jacobs, W. R., Jr. (2001). Evidence that mycobacterial PE_PGRS proteins are cell surface constituents that influence interactions with other cells. *Infection and Immunity*, *69*(12), 7326-7333. https://doi.org/10.1128/iai.69.12.7326-7333.2001

Brennan, P. J. (2003). Structure, function, and biogenesis of the cell wall of *Mycobacterium tuberculosis*. *Tuberculosis (Edinburgh, Scotland)*, *83*(1-3), 91-97. https://doi.org/10.1016/s1472-9792(02)00089-6

Brown-Elliott, B. A., Simmer, P. J., Trovato, A., Hyle, E. P., Droz, S., Buckwalter, S. P., Borroni, E., Branda, J. A., Iana, E., Mariottini, A., Nelson, J., Matteelli, A., Toney, N. C., Scarparo, C., de Man, T. J. B., Vasireddy, R., Gandhi, R. T., Wengenack, N. L., Cirillo, D. M., Wallace, R.J., Tortoli, E. (2018). *Mycobacterium decipiens* sp. nov., a new species closely related to the *Mycobacterium tuberculosis* complex. *International Journal of Systemic and Evolutionary Microbiology*, *68*(11), 3557-3562. https://doi.org/10.1099/ijsem.0.003031

Caulfield, A. J., & Wengenack, N. L. (2016). Diagnosis of active tuberculosis disease: From microscopy to molecular techniques. *Journal of Clinical Tuberculosis and Other Mycobacterial Diseases*, *4*, 33-43. https://doi.org/10.1016/j.jctube.2016.05.005.

CDC, Centers for Disease Control and Prevention. (2020). Latent TB infection and TB disease. https://www.cdc.gov/tb/topic/basics/tbinfectiondisease.htm

Chakaya, J., Petersen, E., Nantanda, R., Mungai, B. N., Migliori, G. B., Amanullah, F., Lungu, P., Ntoumi, F., Kumarasamy, N., Maeurer, M., & Zumla, A. (2022). The WHO global tuberculosis 2021 report – not so good news and turning the tide back to End TB. *International Journal of Infectious Diseases*, *124*, S26-S29. https://doi.org/https:/doi.org/10.1016/j.ijid.2022.03.011

Cheng, P. N., Pham, J. D., & Nowick, J. S. (2013). The supramolecular chemistry of β-sheets. *Journal of the American Chemical Society*, *135*(15), 5477-5492. https://doi.org/10.1021/ja3088407

Choi, T. J., & Geletu, T. T. (2018). High level expression and purification of recombinant flounder growth hormone in *E. coli*. *Journal of Genetic Engineering and Biotechnology*, *16*(2), 347-355. https://doi.org/10.1016/j.jgeb.2018.03.006

Churchyard, G., Kim, P., Shah, N. S., Rustomjee, R., Gandhi, N., Mathema, B., Dowdy, D., Kasmar, A., & Cardenas, V. (2017). What we know about tuberculosis transmission: an overview. *The Journal of Infectious Diseases*, *216*(suppl_6), S629-S635. https://doi.org/10.1093/infdis/jix362

Cilloni, L., Fu, H., Vesga, J. F., Dowdy, D., Pretorius, C., Ahmedov, S., Nair, S. A., Mosneaga, A., Masini, E., Sahu, S., & Arinaminpathy, N. (2020). The potential impact of the COVID-19 pandemic on the tuberculosis epidemic a modelling analysis. *EClinicalMedicine*, *28*, 100603. https://doi.org/10.1016/j.eclinm.2020.100603

Correale, S., Ruggiero, A., Capparelli, R., Pedone, E., Berisio, R. (2013). Structures of free and inhibited forms of the L, D-transpeptidase LdtMt1 from *Mycobacterium tuberculosis*. *Acta Crystallographica*. *69.* 1697-706. https://doi.org/10.1107/S0907444913013085.

Cotton, M. F., Madhi, S. A., Luabeya, A. K., Tameris, M., Hesseling, A. C., Shenje, J., Schoeman, E., Hatherill, M., Desai, S., Kapse, D., Brückner, S., Koen, A., Jose, L., Moultrie, A., Bhikha, S., Walzl, G., Gutschmidt, A., Kotze, L. A., Allies, D. L., Loxton, A.D., Kulkarni, P. S. (2022). Safety and immunogenicity of VPM1002 versus BCG in South African newborn babies: a randomised, phase 2 non-inferiority double-blind controlled trial. *Lancet Infectious Diseases*, *22*(10), 1472-1483. https://doi.org/10.1016/s1473-3099(22)00222-5

De Maio, F., Squeglia, F., Goletti, D., & Delogu, G. (2019). The mycobacterial HBHA protein: a promising biomarker for tuberculosis. *Current Medicinal Chemistry*, *26*(11), 2051-2060. https://doi.org/10.2174/0929867325666181029165805

Delaney, S., Murphy, R., & Walsh, F. (2018). A comparison of methods for the extraction of plasmids capable of conferring antibiotic resistance in a human pathogen from complex broiler cecal samples [original research]. *Frontiers in Microbiology*, *9*. https://doi.org/10.3389/fmicb.2018.01731

Delogu, G., & Brennan, M. J. (1999). Functional domains present in the mycobacterial hemagglutinin, HBHA. *Journal of Bacteriology*, *181*(24), 7464-7469. https://doi.org/10.1128/jb.181.24.7464-7469.1999

Deng, Y., Duan, Y. F., Gao, S. P., & Wang, J. M. (2021). Comparison of LAMP, GeneXpert, mycobacterial culture, smear microscopy, TSPOT.TB, TBAg/PHA Ratio for diagnosis of pulmonary tuberculosis. *Current Medical Science*, *41*(5), 1023-1028. https://doi.org/10.1007/s11596-021-2404-4

DenHollander, N., & Befus, D. (1989). Loss of antigens from immunoblotting membranes. *Journal of Immunological Methods*, *122*(1), 129-135. https://doi.org/10.1016/0022-1759(89)90343-8

Dersch, P., & Isberg, R. R. (2000). An immunoglobulin superfamily-like domain unique to the Yersinia pseudotuberculosis invasin protein is required for stimulation of bacterial uptake via integrin receptors. *Infection and Immunity*, *68*(5), 2930-2938. https://doi.org/10.1128/iai.68.5.2930-2938.2000

Desikan, P. (2013). Sputum smear microscopy in tuberculosis: is it still relevant? *Indian Journal of Medical Research*, *137*(3), 442-444.

Desikan, P., Panwalkar, N., Mirza, S. B., Chaturvedi, A., Ansari, K., Varathe, R., Chourey, M., Kumar, P., & Pandey, M. (2017). Line probe assay for detection of *Mycobacterium tuberculosis* complex: an experience from central India. *Indian Journal of Medical Research*, *145*(1), 70-73. https://doi.org/10.4103/ijmr.IJMR_831_14

Di Carlo, E., Forni, G., Lollini, P., Colombo, M. P., Modesti, A., & Musiani, P. (2001). The intriguing role of polymorphonuclear neutrophils in antitumor reactions. *Blood*, *97*(2), 339-345. https://doi.org/10.1182/blood.v97.2.339

Dirix, V., Dauby, N., Hites, M., Watelet, E., Van Praet, A., Godefroid, A., Petit, E., Singh, M., Locht, C., Mascart, F., & Corbière, V. (2022). Optimal detection of latent *Mycobacterium tuberculosis* infection by combined heparin-binding hemagglutinin (HBHA) and early secreted antigenic target 6 (ESAT-6) whole-blood interferon gamma release assays. *Journal of Clinical Microbiology*, *60*(5), e0244321. https://doi.org/10.1128/jcm.02443-21

Dubnau, E., & Smith, I. (2003). *Mycobacterium tuberculosis* gene expression in macrophages. *Microbes and Infection*, *5*(7), 629-637. https://doi.org/10.1016/s1286-4579(03)00090-x

Dunn, J. J., Starke, J. R., & Revell, P. A. (2016). Laboratory diagnosis of *Mycobacterium tuberculosis* infection and disease in children. *Journal of Clinical Microbiology*, *54*(6), 1434-1441. https://doi.org/10.1128/jcm.03043-15

Dzobo, K., & Dandara, C. (2023). The extracellular matrix: its composition, function, remodeling, and role in tumorigenesis. Biomimetics. *8*(2). 146. https://doi.org/10.3390/biomimetics8020146.

Ejalu, D. L., Irioko, A., Kirabo, R., Mukose, A. D., Ekirapa, E., Kagaayi, J., & Namutundu, J. (2022). Cost-effectiveness of GeneXpert Omni compared with GeneXpert MTB/Rif for point-of-care diagnosis of tuberculosis in a low-resource, high-burden setting in Eastern Uganda: a cost-effectiveness analysis based on decision analytical modelling. *British Medical Journal Open*, *12*(8), e059823. https://doi.org/10.1136/bmjopen-2021-059823

Eniyan, K., & Bajpai, U. (2015). Cloning, expression, purification and bioinformatic analysis of 2–methylcitrate synthase from *Mycobacterium tuberculosis*. *Asian Pacific Journal of*

Tropical Medicine, *8*(1), 19-23. https://doi.org/https:/doi.org/10.1016/S1995-7645(14)60181-4

Fang, Z., Schubert, W.D., van Pittus, N.C.G. (2016). Expression and production of soluble *Mycobacterium tuberculosis* H37Rv mycosin-3. *Biochemistry and Biophysics Reports, 5*, 448-5808. https://doi.org/10.1016/j.bbrep.2016.02.005

Faujdar, J., Gupta, P., Natrajan, M., Das, R., Chauhan, D. S., Katoch, V. M., & Gupta, U. D. (2011). *Mycobacterium indicus pranii* as stand-alone or adjunct immunotherapeutic in treatment of experimental animal tuberculosis. *Indian Journal of Medical Research*, *134*(5), 696-703. https://doi.org/10.4103/0971-5916.90999

Forrellad, M. A., Klepp, L. I., Gioffré, A., Sabio y García, J., Morbidoni, H. R., de la Paz Santangelo, M., Cataldi, A. A., & Bigi, F. (2013). Virulence factors of the *Mycobacterium tuberculosis* complex. *Virulence*, *4*(1), 3-66. *https://doi.org/10.4161/viru.22329*

Francis, D. M., & Page, R. (2010). Strategies to optimize protein expression in *E. coli. Current Protocols in Protein Science*, *61*(1), 5.24.21-25.24.29. https://doi.org/https:/doi.org/10.1002/0471140864.ps0524s61

Fratti, R. A., Chua, J., Vergne, I., & Deretic, V. (2003). *Mycobacterium tuberculosis* glycosylated phosphatidylinositol causes phagosome maturation arrest. *Proceedings of the Nationall Academy of Sciences*, *100*(9), 5437-5442. https://doi.org/10.1073/pnas.0737613100

Garcia-Prats, A. J., Svensson, E. M., Winckler, J., Draper, H. R., Fairlie, L., van der Laan, L. E., Masenya, M., Schaaf, H. S., Wiesner, L., Norman, J., Aarnoutse, R. E., Karlsson, M. O., Denti, P., & Hesseling, A. C. (2021). Pharmacokinetics and safety of high-dose rifampicin in children with TB: the Opti-Rif trial. *Journal of Antimicrobial Chemotherapy*, *76*(12), 3237-3246. https://doi.org/10.1093/jac/dkab336

Gill, C., Dolan, L., Piggott, L., & McLaughlin, A. (2022). New developments in tuberculosis diagnosis and treatment. *Breathe*, *18*(1), 210149. https://doi.org/10.1183/20734735.0149-2021

Goffin, C., & Ghuysen, J. M. (2002). Biochemistry and comparative genomics of SxxK superfamily acyltransferases offer a clue to the mycobacterial paradox: presence of penicillin-susceptible target proteins versus lack of efficiency of penicillin as therapeutic agent. *Microbiology and Molecular Biology Reviews*, *66*(4), 702-738. https://doi.org/10.1128/mmbr.66.4.702-738.2002

Gong, W., Liang, Y., & Wu, X. (2018). The current status, challenges, and future developments of new tuberculosis vaccines. *Human Vaccine & Immunotherapeutics*, *14*(7), 1697-1716. https://doi.org/10.1080/21645515.2018.1458806

Gopalaswamy, R., Kumar, N., Vashistha, H., Rajendran, P., Kayesth, J., Peravali, C. J., Kashyap, S., Ghosh, S., Yumo, H., Moore, M., Anand, S., Ramachandran, R., Alavadi, U., Saini, S., & Shanmugam, S. (2023). Comprehensive assessment of invalid and indeterminate results in Truenat MTB-RIF testing across sites under the national TB elimination program of India [original research]. *Frontiers in Public Health*, *11*. https://doi.org/10.3389/fpubh.2023.1255756

Gopalaswamy, R., & Subbian, S. (2022). An update on tuberculosis vaccines. *Methods in Molecular Biology*, *2410*, 387-409. https://doi.org/10.1007/978-1-0716-1884-4_20

Govender, V. S., Ramsugit, S., & Pillay, M. (2014). *Mycobacterium tuberculosis* adhesins: potential biomarkers as anti-tuberculosis therapeutic and diagnostic targets. *Microbiology*, *160*(9), 1821-1831. https://doi.org/10.1099/mic.0.082206-0

Grāve, K., Bennett, M. D., & Högbom, M. (2022). High-throughput strategy for identification of *Mycobacterium tuberculosis* membrane protein expression conditions using folding reporter GFP. *Protein Expression and Purification*, *198*, 106132. https://doi.org/https:/doi.org/10.1016/j.pep.2022.106132

Greenfield, N. J. (2006). Using circular dichroism spectra to estimate protein secondary structure. *Nature Protocols*, *1*(6), 2876-2890. https://doi.org/10.1038/nprot.2006.202

Guan, Y., Zhu, Q., Huang, D., Zhao, S., Jan Lo, L., & Peng, J. (2015). An equation to estimate the difference between theoretically predicted and SDS PAGE-displayed molecular weights for an acidic peptide. *Scientific Reports*, *5*, 13370. https://doi.org/10.1038/srep13370

Günther, G. (2014). Multidrug-resistant and extensively drug-resistant tuberculosis: a review of current concepts and future challenges. Journal of *Clinical Medicine*, *14*(3), 279-285. https://doi.org/10.7861/clinmedicine.14-3-279

Gupta, R., Lavollay, M., Mainardi, J. L., Arthur, M., Bishai, W. R., & Lamichhane, G. (2010). The *Mycobacterium tuberculosis* protein LdtMt2 is a nonclassical transpeptidase required for virulence and resistance to amoxicillin. *Nature Medicine*, *16*(4), 466-469. https://doi.org/10.1038/nm.2120

Haley, C. A., Macias, P., Jasuja, S., Jones, B. A., Rowlinson, M. C., Jaimon, R., Onderko, P., Darnall, E., Gomez, M. E., Peloquin, C., Ashkin, D., & Goswami, N. D. (2021). Novel 6-month treatment for drug-resistant tuberculosis, United States. *Emerging Infectious Diseases*, *27*(1), 332-334. https://doi.org/10.3201/eid2701.203766

Hanif, S. N. M., Al-Attiyah, R., & Mustafa, A. S. (2010). Molecular cloning, expression, purification and immunological characterization of three low-molecular weight proteins encoded by genes in genomic regions of difference of *Mycobacterium tuberculosis*.

Scandinavian Journal of Immunology, *71*(5), 353-361. https://doi.org/https:/doi.org/10.1111/j.1365-3083.2010.02388.x

Harrison, S. T. (1991). Bacterial cell disruption: a key unit operation in the recovery of intracellular products. *Biotechnology Advances*, *9*(2), 217-240. https://doi.org/10.1016/0734-9750(91)90005-g

Hashmi, A. A., Naz, S., Yaqeen, S. R., Ahmed, O., Ali, S. I., Irfan, M., Kamal, A., & Faridi, N. (2020). Utility of the GeneXpert *Mycobacterium tuberculosis/*Rifampin (MTB/RIF) assay on paraffin-embedded biopsy tissue samples for detecting tuberculosis: comparison with histopathology. *Cureus*, *12*(12), e12048. https://doi.org/10.7759/cureus.12048

Hatherill, M., & Cobelens, F. (2022). Infant BCG vaccination is beneficial, but not sufficient. *The Lancet Global Health*, *10*(9), e1220-e1221. https://doi.org/10.1016/S2214-109X(22)00325-4

He, X. Y., Li, J., Hao, J., Chen, H. B., Zhao, Y. Z., Huang, X. Y., He, K., Xiao, L., Ye, L. P., Qu, Y. M., & Ge, L. H. (2011). Assessment of five antigens from *Mycobacterium tuberculosis* for serodiagnosis of tuberculosis. *Clinical and Vaccine Immunology*, *18*(4), 565-570. https://doi.org/10.1128/cvi.00507-10

Hering, J., Missel, J. W., Zhang, L., Gunnarsson, A., Castaldo, M., Pedersen, P. A., Ek, M., Gourdon, P., & Snijder, H. J. (2020). The rapid “teabag” method for high-end purification of membrane proteins. *Scientific Reports*, *10*(1), 16167. https://doi.org/10.1038/s41598-020-73285-9

Houben, R. M., & Dodd, P. J. (2016). The global burden of latent tuberculosis infection: a re-estimation using mathematical modelling. *Public Library of Science Medicine*, *13*(10), e1002152. https://doi.org/10.1371/journal.pmed.1002152

Hu, J., Qin, H., Gao, F. P., & Cross, T. A. (2011). A systematic assessment of mature MBP in membrane protein production: overexpression, membrane targeting and purification. *Protein Expression and Purification*, *80*(1), 34-40. https:/doi.org/10.1016/j.pep.2011.06.001

Huang, C.-J., Peng, H.-L., Patel, A. K., Singhania, R. R., Dong, C.-D., & Cheng, C.-Y. (2021). Effects of lower temperature on expression and biochemical characteristics of HCV NS3 antigen recombinant protein. *Catalysts*, *11*(11), 1297. https://www.mdpi.com/2073-4344/11/11/1297

Huang, Y., Ai, L., Wang, X., Sun, Z., & Wang, F. (2022). Review and updates on the diagnosis of tuberculosis. *Journal of Clinical Medicine*, *11*(19). https://doi.org/10.3390/jcm11195826

Humbert, M. V. (2019). Cloning, expression, and purification of recombinant *Neisseria gonorrhoeae* proteins. *Methods in Molecular Biology*, *1997*, 233-266. https://doi.org/10.1007/978-1-4939-9496-0_15

Jacobo-Delgado, Y. M., Rodríguez-Carlos, A., Serrano, C. J., & Rivas-Santiago, B. (2023). *Mycobacterium tuberculosis* cell-wall and antimicrobial peptides: a mission impossible? [review]. *Frontiers in Immunology*, *14*. https://doi.org/10.3389/fimmu.2023.1194923

Jenum, S., Tonby, K., Rueegg, C.S., Rühwald, M., Kristiansen, M.P., Bang, P., Olsen, I.C., Sellæg, K., Røstad, K., Mustafa, T., Taskén, K., Kvale, D., Mortensen, R., & Dyrhol-Riise, A.M. (2021). A Phase I/II randomized trial of H56:IC31 vaccination and adjunctive cyclooxygenase-2-inhibitor treatment in tuberculosis patients. *Nature communications*, 12 (1), 6774. https://doi.org/10.1038/s41467-021-27029-6

Jiang, Y., Liu, H., Wang, X., Xiao, S., Li, M., Li, G., Zhao, L., Zhao, X., Dou, X., & Wan, K. (2017). Genetic diversity of immune-related antigens in Region of Difference 2 of *Mycobacterium tuberculosis* strains. *Tuberculosis*, *104*, 1-7. https://doi.org/10.1016/j.tube.2016.05.002

Jnawali, H. N., & Ryoo, S. (2013). First– and second–line drugs and drug resistance. *Tuberculosis* (pp. Ch. 10). https://doi.org/10.5772/54960

Kartmann, B., Stenger, S., & Niederweis, M. (1999). Porins in the cell wall of *Mycobacterium tuberculosis*. *Journal of Bacteriology*, *181*(20), 6543-6546. https://doi.org/10.1128/jb.181.20.6543-6546.1999

Katelaris, A. L., Jackson, C., Southern, J., Gupta, R. K., Drobniewski, F., Lalvani, A., Lipman, M., Mangtani, P., & Abubakar, I. (2020). Effectiveness of BCG vaccination against *Mycobacterium tuberculosis* infection in adults: a cross-sectional analysis of a UK-based cohort. *The Journal of Infectious Diseases*, *221*(1), 146-155. https://doi.org/10.1093/infdis/jiz430

Kato, Y. (2020). Extremely low leakage expression systems using dual transcriptional-translational control for toxic protein production. *International Journal of Molecular Science*, *21*(3). https://doi.org/10.3390/ijms21030705

Khosrobeygi, M., Mosavari, N., Salehi, M., Mojgani, N., & Akbari, M. (2021). Isolation and purification of low molecular weight proteins from culture filtrate of *Mycobacterium tuberculosis* Strain C. *Archives of Razi Institute*, *76*(2), 273-281. https://doi.org/10.22092/ari.2020.127691.1390

Kiazyk, S., & Ball, T. B. (2017). Latent tuberculosis infection: an overview. *Canada Communicable Disease Report*, *43*(3-4), 62-66. https://doi.org/10.14745/ccdr.v43i34a01

Kim, S., de Los Reyes, V. A., & Jung, E. (2020). Country-specific intervention strategies for top three TB burden countries using mathematical model. *Public Library of Science One*, *15*(4), e0230964. https://doi.org/10.1371/journal.pone.0230964

Kline, K. A., Fälker, S., Dahlberg, S., Normark, S., & Henriques-Normark, B. (2009). Bacterial adhesins in host-microbe interactions. *Cell Host Microbe*, *5*(6), 580-592. https://doi.org/10.1016/j.chom.2009.05.011

Klopper, M., Warren, R. M., Hayes, C., Gey van Pittius, N. C., Streicher, E. M., Müller, B., Sirgel, F. A., Chabula-Nxiweni, M., Hoosain, E., Coetzee, G., David van Helden, P., Victor, T. C., & Trollip, A. P. (2013). Emergence and spread of extensively and totally drug-resistant tuberculosis, South Africa. *Emerging Infectious Diseases*, *19*(3), 449-455. https://doi.org/10.3201/eid1903.120246

Krause, M., Neubauer, A., & Neubauer, P. (2016). The fed-batch principle for the molecular biology lab: controlled nutrient diets in ready-made media improve production of recombinant proteins in *Escherichia coli. Microbial Cell Factories*, *15*(1), 110. https://doi.org/10.1186/s12934-016-0513-8

Kular, J. K., Basu, S., & Sharma, R. I. (2014). The extracellular matrix: Structure, composition, age-related differences, tools for analysis and applications for tissue engineering. *Journal of Tissue Engineering*, *5*, 2041731414557112. https://doi.org/10.1177/2041731414557112

Kumar, S., Puniya, B. L., Parween, S., Nahar, P., & Ramachandran, S. (2013). Identification of novel adhesins of *M. tuberculosis* H37Rv using integrated approach of multiple computational algorithms and experimental analysis. *Public Library of Science One*, *8*(7), e69790. https://doi.org/10.1371/journal.pone.0069790

Kurien, B. T., & Scofield, R. H. (2012). Common artifacts and mistakes made in electrophoresis. *Methods in Molecular Biology*, *869*, 633-640. https://doi.org/10.1007/978-1-61779-821-4_58

Kweon, D. H., Lee, D. H., Han, N. S., & Seo, J. H. (2004). Solid-phase refolding of cyclodextrin glycosyltransferase adsorbed on cation-exchange resin. *Biotechnology progress*, *20*(1), 277-283. https://doi.org/10.1021/bp0341895

Larsen, M. H., Biermann, K., Tandberg, S., Hsu, T., & Jacobs, J., William R. (2007). Genetic Manipulation of *Mycobacterium tuberculosis*. *Current Protocols in Microbiology*, *6*(1), 11-21. https://doi.org/https:/doi.org/10.1002/9780471729259.mc10a02s6

LaVallie, E. R., DiBlasio, E. A., Kovacic, S., Grant, K. L., Schendel, P. F., & McCoy, J. M. (1993). A thioredoxin gene fusion expression system that circumvents inclusion body formation in the *E. coli* cytoplasm. *Biotechnology*, *11*(2), 187-193. https://doi.org/10.1038/nbt0293-187

Lavollay, M., Fourgeaud, M., Herrmann, J. L., Dubost, L., Marie, A., Gutmann, L., Arthur, M., & Mainardi, J. L. (2011). The peptidoglycan of *Mycobacterium abscessus* is predominantly cross-linked by L,D-transpeptidases. *Journal of Bacteriology*, *193*(3), 778-782. https://doi.org/10.1128/jb.00606-10

Lawn, S. D. (2015). Advances in diagnostic assays for tuberculosis. *Cold Spring Harbor Perspectives in Medicine*, *5*(12), a017806. https://doi.org/10.1101/cshperspect.a017806

Lawn, S. D., Mwaba, P., Bates, M., Piatek, A., Alexander, H., Marais, B. J., Cuevas, L. E., McHugh, T. D., Zijenah, L., Kapata, N., Abubakar, I., McNerney, R., Hoelscher, M., Memish, Z. A., Migliori, G. B., Kim, P., Maeurer, M., Schito, M., & Zumla, A. (2013). Advances in tuberculosis diagnostics: the Xpert MTB/RIF assay and future prospects for a point-of-care test. *Lancet Infectious Diseases*, *13*(4), 349-361. https://doi.org/10.1016/s1473-3099(13)70008-2

Lebina, L., et, & al. (2021). *A cluster randomized trial of targeted universal testing for TB in clinics.* Conference on Retroviruses and Opportunistic Infections.

Li, J., Lu, J., Wang, G., Zhao, A., & Xu, M. (2022). Past, present and future of Bacillus Calmette-Guérin vaccine use in China. *Vaccines (Basel)*, *10*(7). https://doi.org/10.3390/vaccines10071157

Li, M., Zhang, G., & Su, Z. (2002). Dual gradient ion-exchange chromatography improved refolding yield of lysozyme. *Journal of Chromatography A*, *959*(1-2), 113-120. https://doi.org/10.1016/s0021-9673(02)00462-4

Long, R., Divangahi, M., & Schwartzman, K. (2022) Chapter 2: Transmission and pathogenesis of tuberculosis. *Canadian Journal of Respiratory, Critical Care, and Sleep Medicine*, *6*(1), 22-32. https://doi.org/10.1080/24745332.2022.2035540

Lu, P., Wu, K., Zhou, H., Yu, H., Yuan, J., Dong, L., Liu, Q., Ding, X., Lu, W., Yang, H., Zhu, L., & Martinez, L. (2023). Evaluation of ESAT6-CFP10 skin test for *Mycobacterium tuberculosis* infection among persons living with HIV in China. *Journal of Clinical Microbiology*, *61*(4), e0181622. https://doi.org/10.1128/jcm.01816-22

Luca, S., & Mihaescu, T. (2013). History of BCG vaccine. *Maedica*, *8*(1), 53-58.

Maartens, G., Decloedt, E., & Cohen, K. (2009). Effectiveness and safety of antiretrovirals with rifampicin: crucial issues for high-burden countries. *Antiviral Therapy*, *14*(8), 1039-1043. https://doi.org/10.3851/imp1455

MacPherson, K., Malhi, J., Haroon, N., & Musa, A. (2022). Cloning optimization for substrate-induced gene expression technology. *Undergraduate Journal of Experimental Microbiology and Immunology*, *27*, 1-12.

Magnet, S., Bellais, S., Dubost, L., Fourgeaud, M., Mainardi, J. L., Petit-Frère, S., Marie, A., Mengin-Lecreulx, D., Arthur, M., & Gutmann, L. (2007). Identification of the L,D-transpeptidases responsible for attachment of the Braun lipoprotein to Escherichia coli peptidoglycan. *Journal of Bacteriology*, *189*(10), 3927-3931. https://doi.org/10.1128/jb.00084-07

Maharajh, R., Pillay, M., & Senzani, S. (2023). A computational method for the prediction and functional analysis of potential *Mycobacterium tuberculosis* adhesin-related proteins. *Expert Review of Proteomics*, 1-11. https://doi.org/10.1080/14789450.2023.2275678

Mahmoodi, S., Pourhassan-Moghaddam, M., Wood, D. W., Majdi, H., & Zarghami, N. (2019). Current affinity approaches for purification of recombinant proteins. *Cogent Biology*, *5*(1), 1665406. https://doi.org/10.1080/23312025.2019.1665406

Mäkinen, J., Marttila, H. J., Marjamäki, M., Viljanen, M. K., & Soini, H. (2006). Comparison of two commercially available DNA line probe assays for detection of multidrug-resistant *Mycobacterium tuberculosis*. *Journal of Clinical Microbiology*, *44*(2), 350-352. https://doi.org/10.1128/jcm.44.2.350-352.2006

Makrides, S. C. (1996). Strategies for achieving high-level expression of genes in *Escherichia coli. Microbiological Reviews*, *60*(3), 512-538. https://doi.org/10.1128/mr.60.3.512-538.1996

Martín, C., Marinova, D., Aguiló, N., & Gonzalo-Asensio, J. (2021). MTBVAC, a live TB vaccine poised to initiate efficacy trials 100 years after BCG. *Vaccine*, *39*(50), 7277-7285. https://doi.org/10.1016/j.vaccine.2021.06.049

Martinez, L., Cords, O., Liu, Q., Acuna-Villaorduna, C., Bonnet, M., Fox, G. J., Carvalho, A. C. C., Chan, P.-C., Croda, J., Hill, P. C., Lopez-Varela, E., Donkor, S., Fielding, K., Graham, S. M., Espinal, M. A., Kampmann, B., Reingold, A., Huerga, H., Villalba, J. A., Grandjean, L., Sotgiu, G., Egere, U., Singh, S., Zhu, L., Lienhardt, C., Denholm, J., Seddon, J.A., Whalen, C.C., Garcia-Basteiro, A.L., Triasih, R., Chen, C., Singh, J., Huang, L., Sharma, S., Hannoun, D., del Corral, H., Mandalakas, A.M., Malone, L.L., Ling, D., Kritski, A., Stein, C.M., Vashishtha, R., Boulahbal, F., Fang, C., Boom, W.H., Netto, E.M., Lemos, A.C., Hesseling, A.C., Kay, A., Jones-López, E.C., Horsburgh, C.R., Lange, C., Andrews, J. R. (2022). Infant BCG vaccination and risk of pulmonary and extrapulmonary tuberculosis throughout the life course: a systematic review and individual participant data meta-analysis. *The Lancet Global Health*, *10*(9), e1307-e1316. https://doi.org/10.1016/S2214-109X(22)00283-2

Massiah, M. A., Wright, K. M., & Du, H. (2016). Obtaining soluble folded proteins from inclusion bodies using sarkosyl, Triton X-100, and CHAPS: application to LB and M9 minimal

media. *Current Protocols in Protein Science*, *84*, 6.13.11-16.13.24. https://doi.org/10.1002/0471140864.ps0613s84

Mathebula, U., Emerson, C., Agizew, T., Pals, S., Boyd, R., Mathoma, A., Basotli, J., Rankgoane-Pono, G., Serumola, C., Date, A., Auld, A. F., & Finlay, A. (2020). Improving sputum collection processes to increase tuberculosis case finding among HIV-positive persons in Botswana. *Public Health Action*, *10*(1), 11-16. https://doi.org/10.5588/pha.19.0051

Mazurek, G. H., Jereb, J., Vernon, A., LoBue, P., Goldberg, S., & Castro, K. (2010). Updated guidelines for using interferon gamma release assays to detect *Mycobacterium tuberculosis* infection. *Morbidity and Mortality Weekly Recommendations and Reports*, *59*, 1-25. https://stacks.cdc.gov/view/cdc/5670

Meena, L. S., & Rajni. (2010). Survival mechanisms of pathogenic *Mycobacterium tuberculosis* H37Rv. *Federation of European Biochemical Societies Journal*, *277*(11), 2416-2427. https://doi.org/10.1111/j.1742-4658.2010.07666.x

Mikhail, B., Dmitrijs, M., & Ivan, M. (2022). A new device-mediated miniprep method. *Applied Microbiology and Biotechnology Express*, *12*(1), 21. https://doi.org/10.1186/s13568-022-01360-7

Mitraki, A., Fane, B., Haase-Pettingell, C., Sturtevant, J., & King, J. (1991). Global suppression of protein folding defects and inclusion body formation. *Science*, *253*(5015), 54-58. https://doi.org/10.1126/science.1648264

Monde, N., Munyeme, M., Chongwe, G., Wensman, J. J., Zulu, M., Siziya, S., Tembo, R., Siame, K. K., Shambaba, O., & Malama, S. (2023). First and second-Line anti-tuberculosis drug-resistance patterns in pulmonary tuberculosis patients in Zambia. *Antibiotics*, *12*(1). https://doi.org/10.3390/antibiotics12010166

Moore, S. M., Hess, S. M., & Jorgenson, J. W. (2016). Extraction, enrichment, solubilization, and digestion techniques for membrane proteomics. *Journal of Proteome Research*, *15*(4), 1243-1252. https://doi.org/10.1021/acs.jproteome.5b01122

Morè, N., Martorana, A. M., Biboy, J., Otten, C., Winkle, M., Serrano, C. K. G., Montón Silva, A., Atkinson, L., Yau, H., Breukink, E., den Blaauwen, T., Vollmer, W., & Polissi, A. (2019). Peptidoglycan remodeling enables *Escherichia coli* to survive severe outer membrane assembly defect. *mBio Journal*, *10*(1). https://doi.org/10.1128/mBio.02729-18

Morrison, H., & McShane, H. (2021). Local pulmonary immunological biomarkers in tuberculosis. *Frontiers in Immunology*, *12*, 640916. https://doi.org/10.3389/fimmu.2021.640916

Mthembu, J. N. (2022). *The role of specific adhesins in the regulation of other adhesin genes associated with Mycobacterium tuberculosis pathogenicity.* [Master's dissertation]. University of KwaZulu-Natal, Durban, South Africa.

Muniram, S. (2018). *Mycobacterium tuberculosis L, D-Transpeptidase promotes in-vitro growth, biofilm production and septum formation during cell division.* [Master's dissertation]. University of KwaZulu-Natal, Durban, South Africa.

Mustafa, A. S. (2012). What's new in the development of tuberculosis vaccines. *Medical Principles and Practice*, *21*(3), 195-196. https://doi.org/10.1159/000337919

Ndzi, E. N., Nkenfou, C. N., Gwom, L. C., Fainguem, N., Fokam, J., & Pefura, Y. (2016). The pros and cons of the QuantiFERON test for the diagnosis of tuberculosis, prediction of disease progression, and treatment monitoring. *International Journal of Mycobacteriology*, *5*(2), 177-184. https:/doi.org/10.1016/j.ijmyco.2016.02.005

NEB, New England Biolabs. (2023a). FAQ: Why do the bands smear after SfaNI digestion when running an average agarose gel? https://www.neb.com/en/faqs/2011/06/21/why-do-the-bands-smear-after-sfani-digestion-when-running-an-agarose-gel#

NEB, New England Biolabs. (2023b). Troubleshooting Guide for Cloning. https://www.neb.com/en/tools-and-resources/troubleshooting-guides/troubleshooting-guide-for-cloning

Nowakowski, A.B., Wobig, W.J., & Petering, D.H. (2014) Native SDS-PAGE: high resolution electrophoresis separation of proteins with retention of native properties including bound metal ions. *Metallomics: Integrated Biometal Science*, 6(5), 1068-1078. https://doi.org/10.1039/c4mt00033a

Orange County Biotechnology Education Collaborative, O. B. E. (2023). Restriction digest with gel electrophoresis. https://bio.libretexts.org/Bookshelves/Biotechnology/Lab_Manual

Pai, M., Kasaeva, T., & Swaminathan, S. (2022). Covid-19's devastating effect on tuberculosis care — a path to recovery. *New England Journal of Medicine*, *386*(16), 1490-1493. https://doi.org/10.1056/NEJMp2118145

Peng, Y., Zhu, X., Gao, L., Wang, J., Liu, H., Zhu, T., Zhu, Y., Tang, X., Hu, C., Chen, X., Chen, H., Chen, Y., & Guo, A. (2022). *Mycobacterium tuberculosis Rv0309* dampens the inflammatory response and enhances mycobacterial survival. *Frontiers in Immunology*, *13*, 829410. https://doi.org/10.3389/fimmu.2022.829410

Percival, S. L., Emanuel, C., Cutting, K. F., & Williams, D. W. (2012). Microbiology of the skin and the role of biofilms in infection. *International Wound Journal*, *9*(1), 14-32. https://doi.org/10.1111/j.1742-481X.2011.00836.x

Phunpae, P., Chanwong, S., Tayapiwatana, C., Apiratmateekul, N., Makeudom, A., & Kasinrerk, W. (2013). Rapid diagnosis of tuberculosis by identification of Antigen 85 in

mycobacterial culture system. *Diagnostic Microbiology and Infectious Disease*, *78*. https://doi.org/10.1016/j.diagmicrobio.2013.11.028

Pinxteren, L. A. H. v., Ravn, P., Agger, E. M., Pollock, J., & Andersen, P. (2000). Diagnosis of tuberculosis based on the two specific antigens ESAT-6 and CFP-10. *Clinical Diagnostic Laboratory Immunology*, *7*(2), 155-160. https://doi.org/doi:10.1128/cdli.7.2.155-160.2000

Pooran, A., Theron, G., Zijenah, L., Chanda, D., Clowes, P., Mwenge, L., Mutenherwa, F., Lecesse, P., Metcalfe, J., Sohn, H., Hoelscher, M., Pym, A., Peter, J., Dowdy, D., & Dheda, K. (2019). Point of care Xpert MTB/RIF versus smear microscopy for tuberculosis diagnosis in southern African primary care clinics: a multicentre economic evaluation. *Lancet Global Health*, *7*(6), e798-e807. https://doi.org/10.1016/s2214-109x(19)30164-0

Quan, W., Shasha, G., Xiaolin, W., Quanfang, D., Ning, X., Hui, L., Jie, Z., & Qiang, S. (2022). Global prevalence, treatment and outcome of tuberculosis and COVID-19 coinfection: a systematic review and meta-analysis. *British Medical Journal Open*, *12*(6), e059396. https://doi.org/10.1136/bmjopen-2021-059396

Rabinowitz, P., & Conti, L. (2010). Zoonoses. *Human-Animal Medicine*, 105-298.

Rajni, & Meena, L. S. (2010). Guanosine triphosphatases as novel therapeutic targets in tuberculosis. *International Journal of Infectious Diseases*, *14*(8), e682-687. https://doi.org/10.1016/j.ijid.2009.11.016

Rajni, & Meena, L. S. (2011). Unique characteristic features of *Mycobacterium tuberculosis* in relation to immune system. *American Journal of Immunology*, *7*(1). https://doi.org/10.3844/ajisp.2011.1.8

Ramalingam, B., Baulard, A. R., Locht, C., Narayanan, P. R., & Raja, A. (2004). Cloning, expression, and purification of the 27kDa (MPT51, Rv3803c) protein of *Mycobacterium tuberculosis*. *Protein Expression and Purification*, *36*(1), 53-60. https://doi.org/https:/doi.org/10.1016/j.pep.2004.01.016

Ramazi, S., & Zahiri, J. (2021). Posttranslational modifications in proteins: resources, tools and prediction methods. *Database*, *2021*. https://doi.org/10.1093/database/baab012

Ramsugit, S., & Pillay, M. (2016). Identification of *Mycobacterium tuberculosis* adherence-mediating components: a review of key methods to confirm adhesin function. *Iran Journal of Basic Medical Science*, *19*(6), 579-584.

Reche, P. (2023). *Predicting Antigenic Peptides*. http://imed.med.ucm.es/Tools/antigenic.html#Introduction

Rojas Echenique, J. I., Kryazhimskiy, S., Nguyen Ba, A. N., & Desai, M. M. (2019). Modular epistasis and the compensatory evolution of gene deletion mutants. *Public Library of Science*, *15*(2), e1007958. https://doi.org/10.1371/journal.pgen.1007958

Sahdev, S., Khattar, S. K., & Saini, K. S. (2008). Production of active eukaryotic proteins through bacterial expression systems: a review of the existing biotechnology strategies. *Molecular and Cell Biochemistry*, *307*(1-2), 249-264. https://doi.org/10.1007/s11010-007-9603-6

Sahu, S., Ditiu, L., Sachdeva, K. S., & Zumla, A. (2021). Recovering from the impact of the Covid-19 pandemic and accelerating to achieving the United Nations general assembly tuberculosis targets. *International Journal of Infectious Diseases*, *113 Suppl 1*, S100-s103. https://doi.org/10.1016/j.ijid.2021.02.078

Sambrook, J., & Russell, D. W. (2001). *Molecular Cloning: A Laboratory Manual.* Cold Spring Harbor Laboratory Press.

San-Miguel, T., Pérez-Bermúdez, P., & Gavidia, I. (2013). Production of soluble eukaryotic recombinant proteins in *E. coli* is favoured in early log-phase cultures induced at low temperature. *Springerplus*, *2*(1), 89. https://doi.org/10.1186/2193-1801-2-89

Sanders, A. N., Wright, L. F., & Pavelka, M. S. (2014). Genetic characterization of mycobacterial L,D-transpeptidases. *Microbiology*, *160*(Pt 8), 1795-1806. https://doi.org/10.1099/mic.0.078980-0

Sandomenico, A., Sivaccumar, J. P., & Ruvo, M. (2020). Evolution of *Escherichia coli* expression system in producing antibody recombinant fragments. *International Journal Of Molecular Sciences*, *21*(17), 6324.

Saramago, S., Magalhães, J., & Pinheiro, M. (2021). Tuberculosis vaccines: an update of recent and ongoing clinical trials. *Applied Sciences*, *11*(19).

Schlager, B., Straessle, A., & Hafen, E. (2012). Use of anionic denaturing detergents to purify insoluble proteins after overexpression. *BioMed Central Biotechnology*, *12*(1), 95. https://doi.org/10.1186/1472-6750-12-95

Seung, K. J., Keshavjee, S., & Rich, M. L. (2015). Multidrug-resistant tuberculosis and extensively drug-resistant tuberculosis. *Cold Spring Harbor Perspectives in Medicine*, *5*(9), a017863. https://doi.org/10.1101/cshperspect.a017863

Shahrear, S., & Islam, A. B. M. M. K. (2023). Modeling of MT. P495, an mRNA-based vaccine against the phosphate-binding protein PstS1 of *Mycobacterium tuberculosis*. *Molecular Diversity*, *27*(4), 1613-1632. https://doi.org/10.1007/s11030-022-10515-4

Sharma, S. K., Katoch, K., Sarin, R., Balambal, R., Kumar Jain, N., Patel, N., Murthy, K. J. R., Singla, N., Saha, P. K., Khanna, A., Singh, U., Kumar, S., Sengupta, A., Banavaliker, J. N., Chauhan, D. S., Sachan, S., Wasim, M., Tripathi, S., Dutt, N., Jain, N., Joshi, N.,

Penmesta, S.R.R., Gaddam, S., Gupta, S., Khamar, B., Dey, B., Mitra, D.K., Arora, S.K., Bhaskar, S., Rani, R. (2017). Efficacy and safety of *Mycobacterium indicus pranii* as an adjunct therapy in Category II pulmonary tuberculosis in a randomized trial. *Science Reports*, *7*(1), 3354. https://doi.org/10.1038/s41598-017-03514-1

Shehadul Islam, M., Aryasomayajula, A., & Selvaganapathy, P. R. (2017). A review on macroscale and microscale cell lysis methods. *Micromachines, 8*(3), 83. https://doi.org/10.3390/mi8030083

Shi, Y., Mowery, R. A., Ashley, J., Hentz, M., Ramirez, A. J., Bilgicer, B., Slunt-Brown, H., Borchelt, D. R., & Shaw, B. F. (2012). Abnormal SDS-PAGE migration of cytosolic proteins can identify domains and mechanisms that control surfactant binding. *Protein Science*, *21*(8), 1197-1209. https://doi.org/10.1002/pro.2107

Shibabaw, A., Gelaw, B., Gebreyes, W., Robinson, R., Wang, S. H., & Tessema, B. (2020). The burden of pre-extensively and extensively drug-resistant tuberculosis among MDR-TB patients in the Amhara region, Ethiopia. *Public Library of Science One*, *15*(2), e0229040. https://doi.org/10.1371/journal.pone.0229040

Shingadia, D. (2012). Tuberculosis in childhood. *Therapeutic Advances in Respiratory Disease*, *6*(3), 161-171. https://doi.org/10.1177/1753465812436662

Shires, K., & Steyn, L. (2001). The cold-shock stress response in *Mycobacterium smegmatis* induces the expression of a histone-like protein. *Molecular Microbiology*, *39*(4), 994-1009. https://doi.org/10.1046/j.1365-2958.2001.02291.x.

Singh, A., Upadhyay, V., Upadhyay, A. K., Singh, S. M., & Panda, A. K. (2015). Protein recovery from inclusion bodies of *Escherichia coli* using mild solubilization process. *Microbial Cell Factories*, *14*(1), 41. https://10.1186/s12934-015-0222-8

Singh, R., Dwivedi, S. P., Gaharwar, U. S., Meena, R., Rajamani, P., & Prasad, T. (2020). Recent updates on drug resistance in *Mycobacterium tuberculosis*. *Journal of Applied Microbiology*, *128*(6), 1547-1567. https://doi.org/10.1186/s12934-015-0222-8

Skipper, L. (2005). PROTEINS | Overview. *Encyclopedia of Analytical Science (Second Edition)* (pp. 344-352). https:/doi.org/10.1016/B0-12-369397-7/00493-3

Smeulders, M.J., Keer, J., Speight, R.A., & Williams, H.D. (1999). Adaptation of *Mycobacterium smegmatis* to stationary phase. *Journal of Bacteriology*, *181*(1), 270-283. https://doi.org/10.1128/JB.181.1.270-283.1999

Smith, I. (2003) *Mycobacterium tuberculosis* pathogenesis and molecular determinants of virulence. *Clinical Microbiology Reviews*, *16*(3), 463-496. https://doi.org/10.1128/CMR.16.3.463-496.2003

So, K.-K., Le, N. M. T., Nguyen, N.-L., & Kim, D.-H. (2023). Improving expression and assembly of difficult-to-express heterologous proteins in *Saccharomyces cerevisiae* by

culturing at a sub-physiological temperature. *Microbial Cell Factories*, *22*(1), 55. https://doi.org/10.1186/s12934-023-02065-7

Sohn, H., Kasaie, P., Kendall, E., Gomez, G. B., Vassall, A., Pai, M., & Dowdy, D. (2019). Informing decision-making for universal access to quality tuberculosis diagnosis in India: an economic-epidemiological model. *BioMed Central Medicine*, *17*(1), 155. https://doi.org/10.1186/s12916-019-1384-8

Sørensen, H. P., & Mortensen, K. K. (2005). Advanced genetic strategies for recombinant protein expression in *Escherichia coli. Journal of Biotechnology*, *115*(2), 113-128. https://doi.org/10.1016/j.jbiotec.2004.08.004

Sreeramareddy, C. T., Panduru, K. V., Menten, J., & Van den Ende, J. (2009). Time delays in diagnosis of pulmonary tuberculosis: a systematic review of literature. *BioMed Central Infectious Diseases*, *9*, 91. https://doi.org/10.1186/1471-2334-9-91

Sriruan, C., Kasinrerk, W., Intorasoot, S., Butr-Indr, B., Netirat, N., Khantipongse, J., & Phunpae, P. (2022). Identification and monitoring of *Mycobacterium tuberculosis* growth in liquid culture by antigen 85 detection. *Journal of Associated Medical Sciences*, *55*(3), 96-104. https://he01.tci-thaijo.org/index.php/bulletinAMS/article/view/255554

Stankeviciute, G., Miguel, A. V., Radkov, A., Chou, S., Huang, K. C., & Klein, E. A. (2019). Differential modes of crosslinking establish spatially distinct regions of peptidoglycan in *Caulobacter crescentus*. *Molecular Microbiology*, *111*(4), 995-1008. https://doi.org/10.1111/mmi.14199

Sterling, T. R., Njie, G., Zenner, D., Cohn, D. L., Reves, R., Ahmed, A., Menzies, D., Horsburgh, C. R., Crane, C. M., Burgos, M., LoBue, P., Winston, C. A., & Belknap, R. (2020). Guidelines for the treatment of latent tuberculosis infection: recommendations from the national tuberculosis controllers association and CDC, 2020. *American Journal of Transplantation*, *20*(4), 1196-1206. https://doi.org/https:/doi.org/10.1111/ajt.15841

Stop TB Partnership. (2022). *TB Vaccine Pipeline*. Working Group on New TB Vaccines. Updated 2 November 2022, from https://newtbvaccines.org/tb-vaccine-pipeline/.

Tahara, N., Tachibana, I., Takeo, K., Yamashita, S., Shimada, A., Hashimoto, M., Ohno, S., Yokogawa, T., Nakagawa, T., Suzuki, F., & Ebihara, A. (2021). Boosting auto-induction of recombinant proteins in *Escherichia coli* with glucose and lactose additives. *Protein and Peptide Letters*, *28*(10), 1180-1190. https://doi.org/10.2174/0929866528666210805120715

Teufel, F., Almagro Armenteros, J. J., Johansen, A. R., Gíslason, M. H., Pihl, S. I., Tsirigos, K. D., Winther, O., Brunak, S., von Heijne, G., & Nielsen, H. (2022). SignalP 6.0

predicts all five types of signal peptides using protein language models. *Nature Biotechnology*, *40*(7), 1023-1025. https://doi.org/10.1038/s41587-021-01156-3

ThermoFisher Scientific, T. S. (2023a). Optimize your DNA ligations.

Thermofisher Scientific, T. S. (2023b). Overview of protein electrophoresis.

Tiberi, S., Muñoz-Torrico, M., Duarte, R., Dalcolmo, M., D'Ambrosio, L., & Migliori, G. B. (2018). New drugs and perspectives for new anti-tuberculosis regimens. *Pulmonology*, *24*(2), 86-98. https://doi.org/10.1016/j.rppnen.2017.10.009

Tietze, K. J. (2012). Chapter 5 - Review of laboratory and diagnostic tests. *Clinical Skills for Pharmacists (Third Edition)* (pp. 86-122). https:/doi.org/10.1016/B978-0-323-07738-5.10005-5

Tkachuk, A. P., Bykonia, E. N., Popova, L. I., Kleymenov, D. A., Semashko, M. A., Chulanov, V. P., Fitilev, S. B., Maksimov, S. L., Smolyarchuk, E. A., Manuylov, V. A., Vasina, D. V., Gushchin, V. A., & Gintsburg, A. L. (2020). Safety and immunogenicity of the GamTBvac, the recombinant subunit tuberculosis vaccine candidate: A phase II, multi-center, double-blind, randomized, placebo-controlled study. *Vaccines*, *8*(4).

Topcu, Z. (2000). An optimized recipe for cloning of the polymerase chain reaction-amplified DNA inserts into plasmid vectors. *Acta Biochimica Polonica*, *47*(3), 841-846. https://doi.org/10.3390/vaccines8040652

Torres-Sangiao, E., Holban, A. M., & Gestal, M. C. (2016). Advanced nanobiomaterials: vaccines, diagnosis and treatment of infectious diseases. *Molecules*, *21*(7). https://doi.org/10.3390/molecules21070867

Trunz, B. B., Fine, P., & Dye, C. (2006). Effect of BCG vaccination on childhood tuberculous meningitis and miliary tuberculosis worldwide: a meta-analysis and assessment of cost-effectiveness. *Lancet*, *367*(9517), 1173-1180. https://doi.org/10.1016/s0140-6736(06)68507-3

Ugarte-Gil, C., Elkington, P. T., Gotuzzo, E., Friedland, J. S., & Moore, D. A. J. (2015). Induced sputum is safe and well-tolerated for TB diagnosis in a resource-poor primary healthcare setting. *American Journal of Tropical Medicine and Hygiene*, *92*(3), 633-635. https://doi.org/10.4269/ajtmh.14-0583

United Kingdom Research and Innovation (2023). Common heartburn drugs could speed up tuberculosis treatment. Available at: www.ukri.org. Accessed: 5 March 2023.

Utpal, A., Tyagi, A., Kumar, A., Gaurav, A., Singh, A., Tiwari, A., Singh, A., Kalha, B., Bhatt, B., Yadav, B., Tuli, D., Rohira, H., Bhatt, H., Kumari, K., Vashistha, K., Singh, K., Nisaa, K., Kumar, M., Sharma, N., & Bajpai, U. (2015). Building a repository of potential drug targets in *Mycobacterium tuberculosis* by crowdsourcing. *ResearchGate*, *1*, 1-15.

Van Der Meeren, O., Hatherill, M., Nduba, V., Wilkinson, R. J., Muyoyeta, M., Van Brakel, E., Ayles, H. M., Henostroza, G., Thienemann, F., Scriba, T. J., Diacon, A., Blatner, G. L., Demoitié, M. A., Tameris, M., Malahleha, M., Innes, J. C., Hellström, E., Martinson, N., Singh, T., Akite, E.J., Azam, A.K., Bollaerts, A., Ginsberg, A.M., Evans, T.G., Gillard, P., Tait, D. R. (2018). Phase 2b controlled trial of M72/AS01(E) vaccine to prevent tuberculosis. *New England Journal of Medicine*, *379*(17), 1621-1634. https://doi.org/10.1056/NEJMoa1803484

Vasina, J. A., & Baneyx, F. (1996). Recombinant protein expression at low temperatures under the transcriptional control of the major *Escherichia coli* cold shock promoter cspA. *Applied Environmental Microbiology*, *62*(4), 1444-1447. https://doi.org/10.1128/aem.62.4.1444-1447.1996

Velayati, A. A., Farnia, P., & Masjedi, M. R. (2013). Totally drug-resistant tuberculosis (TDR-TB): A debate on global health communities. *International Journal of Mycobacteriology*, *2*(2), 71-72. https://doi.org/10.1016/j.ijmyco.2013.04.005

Verma, N., Arora, V., Awasthi, R., Chan, Y., Jha, N. K., Thapa, K., Jawaid, T., Kamal, M., Gupta, G., Liu, G., Paudel, K. R., Hansbro, P. M., George Oliver, B. G., Singh, S. K., Chellappan, D. K., Dureja, H., & Dua, K. (2022). Recent developments, challenges and future prospects in advanced drug delivery systems in the management of tuberculosis. *Journal of Drug Delivery Science and Technology*, *75*, 103690. https://doi.org/https:/doi.org/10.1016/j.jddst.2022.103690

Vermassen, A., Leroy, S., Talon, R., Provot, C., Popowska, M., & Desvaux, M. (2019). Cell wall hydrolases in bacteria: insight on the diversity of cell wall amidases, glycosidases and peptidases toward peptidoglycan. *Frontiers in Microbiology*, *10*, 331. https://doi.org/10.3389/fmicb.2019.00331

Vinod, V., Vijayrajratnam, S., Vasudevan, A. K., & Biswas, R. (2020). The cell surface adhesins of *Mycobacterium tuberculosis*. *Microbiological Research*, *232*, 126392. https://doi.org/10.1016/j.micres.2019.126392

Voskuil, M. I., Bartek, I. L., Visconti, K., & Schoolnik, G. K. (2011). The response of *Mycobacterium tuberculosis* to reactive oxygen and nitrogen species. *Frontiers in Microbiology*, *2*, 105. https://doi.org/10.3389/fmicb.2011.00105

Walzl, G., Ronacher, K., Djoba Siawaya, J. F., & Dockrell, H. M. (2008). Biomarkers for TB treatment response: challenges and future strategies. *Journal of Infection*, *57*(2), 103-109. https://doi.org/10.1016/j.jinf.2008.06.007

Werner, M. H., Clore, G. M., Gronenborn, A. M., Kondoh, A., & Fisher, R. J. (1994). Refolding proteins by gel filtration chromatography. *Federation of European Biochemical Societies Letters*, *345*(2-3), 125-130.

World Health Organization. (2017) WHO Global Tuberculosis Report 2016. Accessed on 20 January 2020. https://who.int/publications/i/item/9789241565394

World Health Organization. (2019) WHO Global Tuberculosis Report 2018. Accessed on 20 January 2020. https://who.int/publications/i/item/9789241565646

World Health Organization. (2020) WHO Global Tuberculosis Report 2019. Accessed 7 February 2021. Available at: https://who.int/publications/i/item/9789241565714

World Health Organization. (2021a) WHO Global Tuberculosis Report 2020. Accessed 1 February 2022. Available at: https://who.int/publications/i/item/9789240013131

World Health Organization (2021b). WHO announces updated definitions of extensively drug-resistant tuberculosis. Accessed 28 April 2022. Available at: https://who.int/news/item/27-01-2021-who-announces-updated-definitions-of-extensively-drug-resistant-tuberculosis

World Health Organization. (2022) WHO Global Tuberculosis Report 2021. Accessed 2 February 2023. Available at: https://who.int/publications/i/item/9789240037021.

World Health Organization (2023) Tuberculosis Fact Sheet. Accessed 7 November 2023. Available at: https://www.who.int/news-room/fact-sheets/detail/tuberculosis

Wingfield, P. T. (2015). Overview of the purification of recombinant proteins. *Current Protocols in Protein Science*, *80*, 6.1.1-6.1.35. https://doi.org/10.1002/0471140864.ps0601s80

Woldemeskel, S. A., & Goley, E. D. (2017). Shapeshifting to survive: Shape determination and regulation in *Caulobacter crescentus*. *Trends in Microbiology*, *25*(8), 673-687. https://doi.org/10.1016/j.tim.2017.03.006

Wurm, D. J., Veiter, L., Ulonska, S., Eggenreich, B., Herwig, C., & Spadiut, O. (2016). The *E. coli* pET expression system revisited—mechanistic correlation between glucose and lactose uptake. *Applied Microbiology and Biotechnology*, *100*(20), 8721-8729. https://doi.org/10.1007/s00253-016-7620-7

Wyckoff, T. J., Taylor, J. A., & Salama, N. R. (2012). Beyond growth: novel functions for bacterial cell wall hydrolases. *Trends in Microbiology*, *20*(11), 540-547. https://doi.org/10.1016/j.tim.2012.08.003

Xu, T., Li, M., Wang, C., Yuan, M., Chang, X., Qian, Z., Li, B., Sun, M., & Wang, H. (2021). Codon optimization, soluble expression and purification of PE_PGRS45 gene from *Mycobacterium tuberculosis* and preparation of its polyclonal antibody protein. *Journal of Microbiology and Biotechnology*, *31*(11), 1583-1590. https://doi.org/10.4014/jmb.2106.06006

Yimer, S. A., Bjune, G. A., & Holm-Hansen, C. (2014). Time to first consultation, diagnosis and treatment of TB among patients attending a referral hospital in Northwest,

Ethiopia. *BioMed Central Infectious Diseases*, *14*, 19. https://doi.org/10.1186/1471-2334-14-19

Zhang, Y., Olsen, D. R., Nguyen, K. B., Olson, P. S., Rhodes, E. T., & Mascarenhas, D. (1998). Expression of eukaryotic proteins in soluble form in *Escherichia coli. Protein Expression and Purification*, *12*(2), 159-165. https://doi.org/10.1006/prep.1997.0834

Zhang, Z., Kuipers, G., Niemiec, Ł., Baumgarten, T., Slotboom, D. J., de Gier, J. W., & Hjelm, A. (2015). High-level production of membrane proteins in *E. coli* BL21(DE3) by omitting the inducer IPTG. *Microbial Cell Factories*, *14*, 142. https://doi.org/10.1186/s12934-015-0328-z

Zheng, W., LaCourse, S. M., Song, B., Singh, D. K., Khanna, M., Olivo, J., Stern, J., Escudero, J. N., Vergara, C., Zhang, F., Li, S., Wang, S., Cranmer, L. M., Huang, Z., Bojanowski, C. M., Bao, D., Njuguna, I., Xiao, Y., Wamalwa, D. C., Nguyen, D.T., Yang, L., Maleche-Obimbo, E., Nguyen, N., Zhang, L., Phan, H., Fan, J., Ning, B., Li, C., Lyon, C.J., Graviss, E.A., John-Stewart, G., Mitchell, C.D., Ramsay, A.J., Kaushal, D., Liang, R., Pérez-Then, E., Hu, T. Y. (2022). Diagnosis of paediatric tuberculosis by optically detecting two virulence factors on extracellular vesicles in blood samples. *Nature Biomedical Engineering*, *6*(8), 979-991. https://doi.org/10.1038/s41551-022-00922-1

Zumla, A., Chakaya, J., Centis, R., D'Ambrosio, L., Mwaba, P., Bates, M., Kapata, N., Nyirenda, T., Chanda, D., Mfinanga, S., Hoelscher, M., Maeurer, M., & Migliori, G. B. (2015). Tuberculosis treatment and management- an update on treatment regimens, trials, new drugs, and adjunct therapies. *Lancet Respiratory Medicine*, *3*(3), 220-234. https://doi.org/10.1016/s2213-2600(15)00063-6

Zumla, A., Chakaya, J., Khan, M., Fatima, R., Wejse, C., Al-Abri, S., Fox, G. J., Nachega, J., Kapata, N., Knipper, M., Orcutt, M., Goscé, L., Abubakar, I., Nagu, T. J., Mugusi, F., Gordon, A. K., Shanmugam, S., Bachmann, N. L., Lam, C., Sintchenko, V., Rudolf, F., Amanullah, F., Kock, R., Haider, N., Lipman, M., King, M., Maeurer, M., Goletti, D., Petrone, L., Yaqoob, A., Tiberi, S., Ditiu, L., Sahu, S., Marais, B., Issayeva, A.M., Petersen, E. (2021). World tuberculosis day 2021 theme - 'The Clock is Ticking' - and the world is running out of time to deliver the United Nations general assembly commitments to end TB due to the COVID-19 pandemic. *International Journal of Infectious Diseases*, *113* (1), S1-s6. https://doi.org/10.1016/j.ijid.2021.03.046

APPENDIX A: ETHICS APPROVAL

Biomedical Research Ethics Committee (BREC) approved protocol.

UNIVERSITY OF KWAZULU-NATAL
INYUVESI YAKWAZULU-NATALI

26 July 2021

Miss Nikita Deyal (217012710)
School of Lab Med & Medical Sc
Medical School

Dear Miss Deyal,

Protocol reference number: BREC/00002801/2021
Project title: Expression, purification and evaluation of the Rv0309 adhesin recombinant protein for the detection of tuberculosis.
Degree: MMedSc

EXPEDITED APPLICATION: APPROVAL LETTER

A sub-committee of the Biomedical Research Ethics Committee has considered and noted your application.

The conditions have been met and the study is given full ethics approval and may begin as from 26 July 2021. Please ensure that outstanding site permissions are obtained and forwarded to BREC for approval before commencing research at a site.

This approval is subject to national and UKZN lockdown regulations, see (http://research.ukzn.ac.za/Libraries/BREC/BREC_Lockdown_Level_4_Guidelines.sflb.ashx). Based on feedback from some sites, we urge PIs to show sensitivity and exercise appropriate consideration at sites where personnel and service users appear stressed or overloaded.

This approval is valid for one year from 26 July 2021. To ensure uninterrupted approval of this study beyond the approval expiry date, an application for recertification must be submitted to BREC on the appropriate BREC form 2-3 months before the expiry date.

Any amendments to this study, unless urgently required to ensure safety of participants, must be approved by BREC prior to implementation.

Your acceptance of this approval denotes your compliance with South African National Research Ethics Guidelines (2015), South African National Good Clinical Practice Guidelines (2020) (if applicable) and with UKZN BREC ethics requirements as contained in the UKZN BREC Terms of Reference and Standard Operating Procedures, all available at http://research.ukzn.ac.za/Research-Ethics/Biomedical-Research-Ethics.aspx.

BREC is registered with the South African National Health Research Ethics Council (REC-290408-009). BREC has US Office for Human Research Protections (OHRP) Federal-wide Assurance (FWA 678).

The sub-committee's decision will be noted by a full Committee at its next meeting taking place on 10 August 2021.

Yours sincerely,

[redacted]

Prof D Wassenaar
Chair: Biomedical Research Ethics Committee

Biomedical Research Ethics Committee
Chair: Professor D R Wassenaar
UKZN Research Ethics Office Westville Campus, Govan Mbeki Building
Postal Address: Private Bag X54001, Durban 4000
Email: BREC@ukzn.ac.za
Website: http://research.ukzn.ac.za/Research-Ethics/Biomedical-Research-Ethics.aspx

Amendments to protocol were approved by BREC.

UNIVERSITY OF KWAZULU-NATAL
INYUVESI YAKWAZULU-NATALI

06 November 2023

Miss Nikita Deyal (217012710)
School of Laboratory Medicine & Medical Science
Medical School

Dear Miss Deyal,

Protocol reference number: BREC/00002801/2021
Project title: Expression, purification and evaluation of the Rv0309 adhesin recombinant protein for the detection of tuberculosis.
Degree: MMedSc
Amended title: Cloning, Expression and Purification of Mycobacterium tuberculosis Rv0309 adhesin protein.

We wish to advise you that your application for amendments listed below received on 01 November 2023 for the above study has been noted and approved by a subcommittee of the Biomedical Research Ethics Committee.

Amendments noted and approved:

1. Amended title: Cloning, Expression and Purification of Mycobacterium tuberculosis Rv0309 adhesin protein.
2. Amended aim: To clone, express and purify Mtb Rv0309 adhesin protein.
3. Amended Research Question: Can the Rv0309 protein be cloned, expressed and purified for future evaluation as a biomarker?
4. The study will be performed in the Discipline of Medical Microbiology, at UKZN Medical School.
5. No ELISA assays or statistical analysis will be done.

The committee will be notified of the above approval at its next meeting to be held on 14 November 2023.

Yours sincerely

[redacted]

Ms. A Marimuthu
(for) Prof T Hardcastle
Acting Deputy Chair: Biomedical Research Ethics Committee

APPENDIX B: MEDIA, REAGENTS AND SOLUTIONS

MEDIA

LB- Ampicillin Media Plates

2.5 g Sodium Chloride

2.5 g Tryptone (Pancreatic Digest Powder)

1.75 g Yeast Extract

5.0 g Bacteriological Agar

200-250 mL dH_2O

1. Weigh out the above ingredients and add to a bottle.
2. Add 100 mL of dH_2O and mix gently until ingredients are dissolved.
3. Top up the volume to 250 mL with dH_2O.
4. Autoclave and cool in a 55°C water bath.
5. Introduce 250 µL of thawed ampicillin (100 mg/mL) to cooling media and swirl.
6. Dispense 15-20 mL into each petri dish (90 mm)

LB- Ampicillin Broth

2.5 g Sodium Chloride

2.5 g Tryptone (Pancreatic Digest Powder)

1.75 g Yeast Extract

200-250 mL dH_2O

1. Weigh out the above ingredients and add to a bottle.
2. Add 100 mL of dH_2O and mix gently until ingredients are dissolved.
3. Top up the volume to 250 mL with dH_2O.
4. Autoclave and cool in a 55°C water bath.
5. Introduce 250 µL of thawed ampicillin (100 mg/mL) to cooling media and swirl.
6. Store at 4°C.

LB- Kanamycin Media Plates

2.5 g Sodium Chloride

2.5 g Tryptone (Pancreatic Digest Powder)

1.75 g Yeast Extract

5.0 g Bacteriological Agar

200-250 mL dH_2O

1. Weigh out the above ingredients and add to a bottle.
2. Add 100 mL of dH_2O and mix gently until ingredients are dissolved.
3. Top up the volume to 250 mL with dH_2O.
4. Autoclave and cool in a 55°C water bath.
5. Introduce 250 µL of thawed kanamycin (50 mg/mL) to cooling media and swirl.
6. Dispense 15-20 mL into each petri dish (90 mm).

LB- Kanamycin Broth

2.5 g Sodium Chloride

2.5 g Tryptone (Pancreatic Digest Powder)

1.75 g Yeast Extract

200-250 mL dH_2O

1. Weigh out the above ingredients and add to a bottle.
2. Add 100 mL of dH_2O and mix gently until ingredients are dissolved.
3. Top up the volume to 250 mL with dH_2O.
4. Autoclave and cool in a 55°C water bath.
5. Introduce 250 µL of thawed kanamycin (50 mg/mL) to cooling media and swirl.
6. Store at 4°C.

*50x TAE buffer (*For 1 L)

242.2 g Trizma base

57.1 mL glacial acetic acid

100 mL 0.5 M EDTA, pH 8

dH_20

1. Dissolve 242.2 g Trizma base in around 600 mL of dH_2O
2. Slowly add 57.1 mL glacial acetic acid
3. Add 100 mL 0.5 M EDTA, pH 8
4. Bring up the volume to 1 L with ddH2O

1 x TAE buffer

20 mL 50 x TAE buffer, pH 8.0-8.3

980 mL dH2O

1. Add the above solution to a 1 L bottle and gently invert.

1 X Phosphate Buffered Saline (PBS) Buffer

PBS tablet

500 mL dH2O

1. Add one PBS tablet to 500 mL of dH2O water.
2. Autoclave the solution.
3. Store at 4°C.

PBS-Lysis Buffer

90 mL 1 x PBS Buffer

1 mL PMSF

5 mL Triton X-100

0.1 mL 50 mM DTT

0.2 mL 0.5 M EDTA

1 mL Lysozyme

1. Add PBS, Triton X-100, DTT and EDTA to a bottle.
2. Place in the water bath until contents are dissolved.
3. Add PMSF and lysozyme and gently swirl.

50 mM Tris, 150 mM NaCl

1.51 g Trizma base

2.19 g NaCl

250 ml dH_2O

1. Dissolve the Trizma base and NaCl in 200 mL dH_2O.
2. Adjust the pH to 8.5 using 6 N HCl and top up the volume to 250 mL using dH_2O.
3. Store at 4°C.

Reduced Glutathione Elution Buffer

0.03 g Reduced glutathione

10 mL Tris-NaCl

1. Dissolve the reduced glutathione in Tris-NaCl.
2. Adjust pH to 8.0 using 1 M NaOH.

Towbin Transfer Buffer

80 mL dH_2O

0.24 g Trizma base

1.44 g Glycine

20 mL Methanol

1. Mix the above ingredients and adjust pH to 8.3 using 6 N HCl.
2. Store at 4°C.

1 X Electrode Buffer

3 g Trizma base

14.4 g Glycine

1 g SDS

1 L dH_2O

1. Dissolve above ingredients in 1L dH_2O.
2. Store at 22°C.

PBS with Tween20 (PBST)

100 mL 1 x PBS

100 µL Tween20

1. Mix the above ingredients together and store at 4°C.

Solubilisation Buffer

50 mL Tris-NaCl, pH 8.0

39 µl β-mercaptoethanol

12.02 g Urea crystals

1. Add the above ingredients into a bottle and heat until dissolved.

5 % blocking buffer (Western blot)

30 mL PBST

1.5 g Skim Milk Powder (Spar)

1. Dissolve the skim milk powder in PBST and use immediately.

REAGENTS

6 N HCl

9.854 mL 37% hydrochloric acid (HCl)

dH_2O

1. Slowly add the HCl to 5 mL of dH_2O and then adjust the volume to 20 mL using dH_2O.

1 M Sodium Hydroxide (NaOH)

3.99 g NaOH pellets

100 mL dH_2O

1. Slowly add the pellets to the dH_2O. Store at 22°C.

0.5 M Ethylenediaminetetraacetic acid (EDTA)

9.3 g EDTA.$2H_2O$

50 mL dH_2O

~1 g NaOH pellets

1. Add the EDTA.$2H_2O$ to 30 mL of dH_2O and add few NaOH pellets.
2. Place bottle on a magnetic stirrer.
3. Adjust pH to 8.0 using NaOH pellets and top up volume to 50 mL with dH_2O.
4. Store at room temperature.

50 mM Calcium Chloride ($CaCl_2$)

3.67 g $CaCl_2$ di-hydrous

500 mL dH_2O

1. Dissolve CaCl2 in dH_2O and autoclave.
2. Store at 4°C.

50 mM $CaCl_2$ -15 % glycerol

2.775 g $CaCl_2$ di-hydrous

75 mL glycerol

400-500 mL dH_2O

1. Dissolve CaCl2 in 300 mL dH_2O
2. Gradually add the glycerol.
3. Top up the volume to 500 mL with dH_2O
4. Store at 4°C.

1.0 M Tris, pH 8.8 (a stock buffer for separating gels)

For 250 mL

30.25 g Trizma base

250 mL dH_20

HCl

1. Dissolve 30.25 g Trizma base in around 200 mL of dH_2O
2. Adjust the pH to 8.8 with concentrated HCl
3. Bring up the volume to 250 mL with dH_2O

Note: Make sure to let the solution cool down to room temperature before making the final pH adjustment.

1.5 M Tris, pH 6.8 (a stock buffer for stacking gels)

For 250 mL

45.38 g

250 mL dH_20

HCl

1. Dissolve 45.38 g Trizma base in around 200 mL of dH_2O

2. Adjust the pH to 6.8 with concentrated HCl
3. Bring up the volume to 250 mL with dH_2O

Note: Make sure to let the solution cool down to room temperature before making the final pH adjustment.

Coomassie Blue stain

0.5 g Brilliant Blue G Pure (Sigma)

125 mL Methanol

25 mL Acetic Acid

1. Add all ingredients to a bottle and top up with dH_2O to 500 mL.
2. Store at room temperature.

Destaining solution

500 mL dH_2O

400 mL methanol

100 mL acetic acid

1. Add methanol and acetic acid to water in a fume hood.
2. Store at room temperature.

10% Ammonium persulphate (APS)

0.10 g APS

dH_20

1. Add the APS into a microcentrifuge tube and dissolve in 1 mL dH_2O.

30% Bis-acrylamide

14.6 g acrylamide

0.4 g N'-N'-Bis-methylene-acrylamide (Bio-Rad)

50 mL dH_2O

1. Dissolve all ingredients in 20 mL dH_2O by placing on a heated magnetic stirrer
2. Bring volume up to 50 mL

3. Store in the dark at 4°C.

10% SDS-PAGE Resolving gel

7.9 mL dH_2O

6.7 mL 30% Bis-acrylamide

5 mL 1.5 M Tris-HCl, pH 8.8

200 µL 10% SDS

200 µL 10% APS

8 µL TEMED

1. Add the above ingredients carefully in the same order to a beaker.
2. Swirl and dispense into pre-clamped SDS-PAGE plates
3. Wait 30-40 minutes for polymerization

15% SDS-PAGE Resolving gel

4.6 mL dH_2O

10 mL 30% Bis-acrylamide

5 mL 1.5 M Tris-HCl, pH 8.8

200 µL 10% SDS

200 µL 10% APS

8 µL TEMED

1. Add the above ingredients carefully in the same order to a beaker.
2. Swirl and dispense into pre-clamped SDS-PAGE plates
3. Wait 30-40 minutes for polymerization

18% SDS-PAGE Resolving gel

3.1 mL dH_2O

14.4 mL 30% Bis-acrylamide

6 mL 1.5 M Tris-HCl, pH 8.8

240 µL 10% SDS

240 µL 10% APS

24 µL TEMED

1. Add the above ingredients carefully in the same order to a beaker.
2. Swirl and dispense into pre-clamped SDS-PAGE plates
3. Wait 30-40 minutes for polymerization

5% SDS-PAGE stacking gel

5.5 mL dH_2O

1.3 mL 30% Bis-acrylamide

1 mL 1.0 M Tris-HCl, pH 6.8

80 µL 10% SDS

80 µL 10% APS

4 µL TEMED

1. Add the ingredients in the same order carefully to a beaker.
2. Swirl and dispense into pre-clamped SDS-PAGE plates and create a layer of Isopropanol.
3. Wait 15 minutes for polymerization

1% Triton X-100

200 µL Triton X-100

20 mL dH_2O

1. Add Triton X-100 to dH_2O and heat until dissolved.

1 M Isopropyl β-D-1 thiogalactopyranoside (IPTG)

238 mg IPTG

1 mL dH_2O

1. Add IPTG to 900 µL dH_2O and wait for the contents to dissolve
2. Top up to 1 mL.
3. Store at -20°C.

1 M Imidazole

50 mL dH_2O water

3.43 g Imidazole

1. Add Imidazole to water and ensure contents are dissolved before storing.

Lysozyme (100 mg/mL)

10 mg Lysozyme (Sigma)

1 mL dH_2O

1. Dissolve the lysozyme in dH_2O.

Store at 22°C.

10% Sodium dodecyl sulphate (SDS)

2.5 g SDS

1. Dissolve SDS in 15 ml of dH_2O by placing in water bath and then top up with dH_2O to 25 mL.

APPENDIX C: CALCULATIONS

Ligation Calculation

In order to calculate volume of insert required in ligation reaction, the *in silico* ligation calculator was used (available at https://nebiocalculator.neb.com/#!/ligation).

The following values were entered into fields:

For Rv0309-pGEX-6P-1:

1:3

Vector size in base pairs = 4984 bp

Vector amount in nanograms = 50 ng

Insert size in base pairs = 611 bp

Enter molar ratio vector (1) and insert (3) ratio

The result calculated was: 18.39 ng insert DNA to 50 ng of vector DNA

Thereafter, the calculated result was divided by nanodrop reading of insert sample. This result was amount added in ligation reaction.

Volume of insert = 18.39/ 76 = 0.24 µL

In order to get volume of vector required in ligation reaction, 50 ng was divided by nanodrop reading of vector sample.

Volume of vector = 50/ 78 = 0.64 µL

1:5

Vector size in base pairs = 4984 bp

Vector amount in nanograms = 50 ng

Insert size in base pairs = 611 bp

Enter molar ratio vector (1) and insert (5) ratio

The result calculated was: 30.65 ng insert DNA to 50 ng of vector DNA

Thereafter, the calculated result was divided by nanodrop reading of insert sample. This result was amount added in ligation reaction.

Volume of insert = 30.65/ 78.5 = 0.39 µL

For Rv0309-pET28a:

1:3

Vector size in base pairs = 5369 bp

Vector amount in nanograms = 50 ng

Insert size in base pairs = 611 bp

Enter molar ratio vector (1) and insert (3) ratio

The result calculated was: 17.07 ng insert DNA to 50 ng of vector DNA

Thereafter, the calculated result was divided by nanodrop reading of insert sample. This result was amount added in ligation reaction.

Volume of insert = 17.07/ 24 = 0.7 µL

In order to get volume of vector required in ligation reaction, 50 ng was divided by nanodrop reading of vector sample.

Volume of vector = 50/ 34.2 = 1.46 µL

1:5

Vector size in base pairs = 5369 bp

Vector amount in nanograms = 50 ng

Insert size in base pairs = 611 bp

Enter molar ratio vector (1) and insert (5) ratio

The result calculated was: 28.45 ng insert DNA to 50 ng of vector DNA

Thereafter, the calculated result was divided by nanodrop reading of insert sample. This result was amount added in ligation reaction.

Volume of insert = 28.45/ 24.5 = 1.16 µL

IPTG volumes for induction (0.25; 0.5, 0.75 and 1 mM)

For 10 mL culture

$C_1V_1 = C_2V_2$

(1000 mM) (V_1) = (**0.25 mM**) (10 mL)

V_1= 0.0025 mL

V_1= 2.5 µL

$C_1V_1 = C_2V_2$

(1000 mM) (V_1) = (**0.5 mM**) (10 mL)

V_1= 0.005 mL

V_1= 5 µL

$C_1V_1 = C_2V_2$

(1000 mM) (V_1) = (**0.75 mM**) (10 mL)

V_1= 0.0075 mL

V_1= 7.5 µL

$C_1V_1 = C_2V_2$

(1000 mM) (V1) = (**1 mM**) (10 mL)

V_1= 0.01 mL

V_1= 10 µL

For 20 mL culture

$C_1V_1 = C_2V_2$

(1000 mM) (V_1) = (**0.25 mM**) (20 mL)

V_1= 0.005 mL

V_1= 5 µL

$C_1V_1 = C_2V_2$

(1000 mM) (V_1) = (**0.5 mM**) (20 mL)

V_1= 0.01 mL

V_1= 10 µL

$C_1V_1 = C_2V_2$

(1000 mM) (V_1) = (**0.75 mM**) (20 mL)

V_1= 0.015 mL

V_1= 15 µL

$C_1V_1 = C_2V_2$

(1000 mM) (V1) = (**1 mM**) (20 mL)

V_1= 0.02 mL

V_1= 20 µL

<u>For 50 mL culture</u>

$C_1V_1 = C_2V_2$

(1000 mM) (V_1) = (**0.25 mM**) (50 mL)

V_1= 0.0125 mL

V_1= 12.5 µL

$C_1V_1 = C_2V_2$

(1000 mM) (V_1) = (**0.5 mM**) (50 mL)

V_1= 0.025 mL

V_1= 25 µL

$C_1V_1 = C_2V_2$

(1000 mM) (V_1) = (**0.75 mM**) (50 mL)

V_1= 0.0375 mL

V_1= 37.5 µL

$C_1V_1 = C_2V_2$

(1000 mM) (V1) = (**1 mM**) (50 mL)

V_1= 0.05 mL

V_1= 50 µL

<u>For 1000 mL (1 Litre) culture</u>

$C_1V_1 = C_2V_2$

(1000 mM) (V_1) = (**0.25 mM**) (1000 mL)

V_1= 0.25 mL

V_1= 250 µL

$C_1V_1 = C_2V_2$

(1000 mM) (V_1) = (**0.5 mM**) (1000 mL)

V_1= 0.5 mL

V_1= 500 µL

$C_1V_1 = C_2V_2$

(1000 mM) (V_1) = (**0.75 mM**) (1000 mL)

V_1= 0.75 mL

V_1= 750 µL

$C_1V_1 = C_2V_2$

(1000 mM) (V1) = (**1 mM**) (1000 mL)

V_1= 1 mL

V_1= 1000 µL

APPENDIX D: SEQUENCING DATA

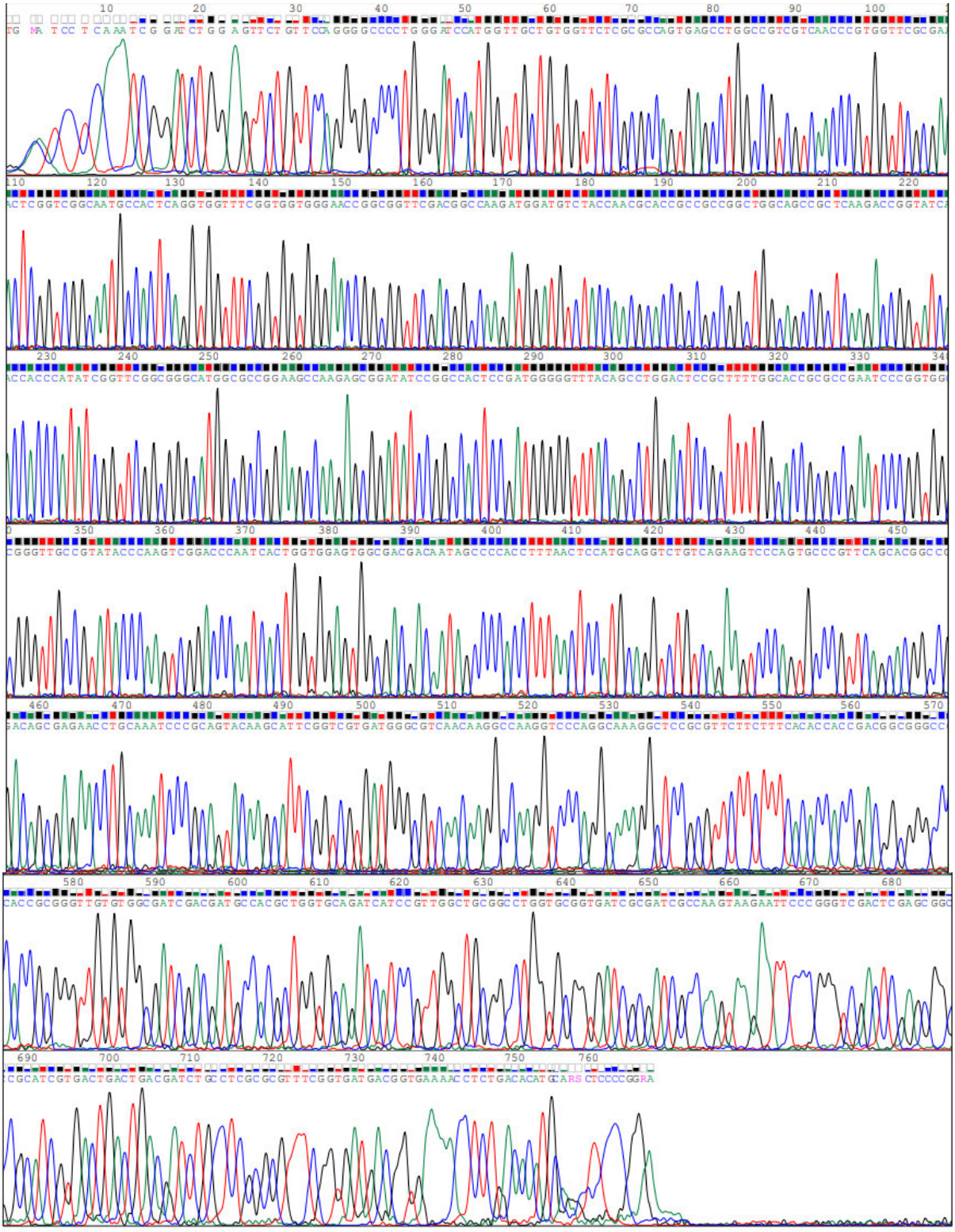

Figure A1: Snippet of chromatogram of pGEX 5' of pGEX-6P-1-*Rv0309* clone using Chromas software.

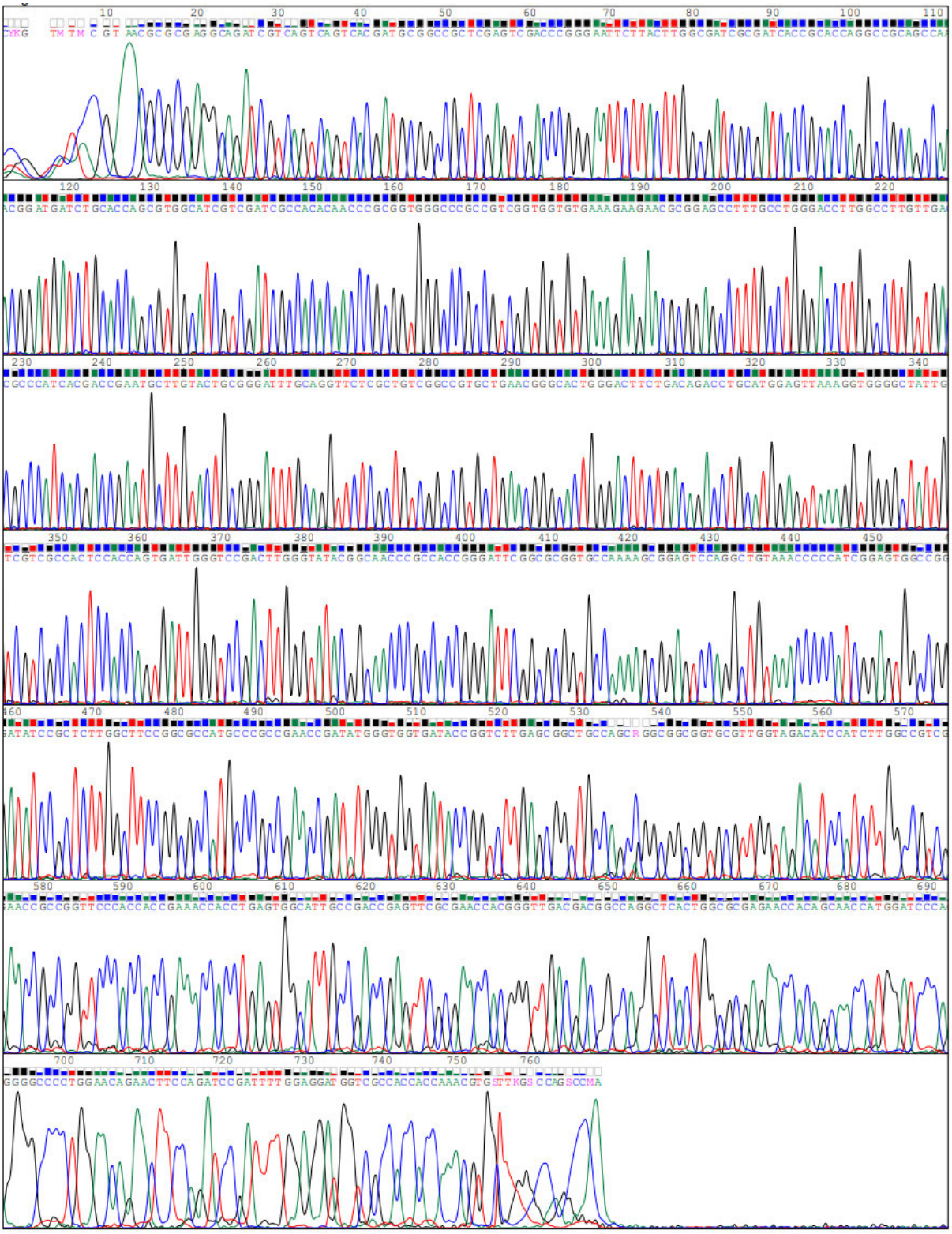

Figure A2: Snippet of chromatogram of pGEX 3' of pGEX-6P-1-*Rv0309* clone using Chromas software.

Figure A3: *Rv0309*-pGEX-6P-1 BioEdit Sequence Alignment

pGEXRv0309 refers to consensus sequence of pure pDNA sample submitted.

Mtb Rv0309 refers to expected sequence of Rv0309 based on Mycobrowser.

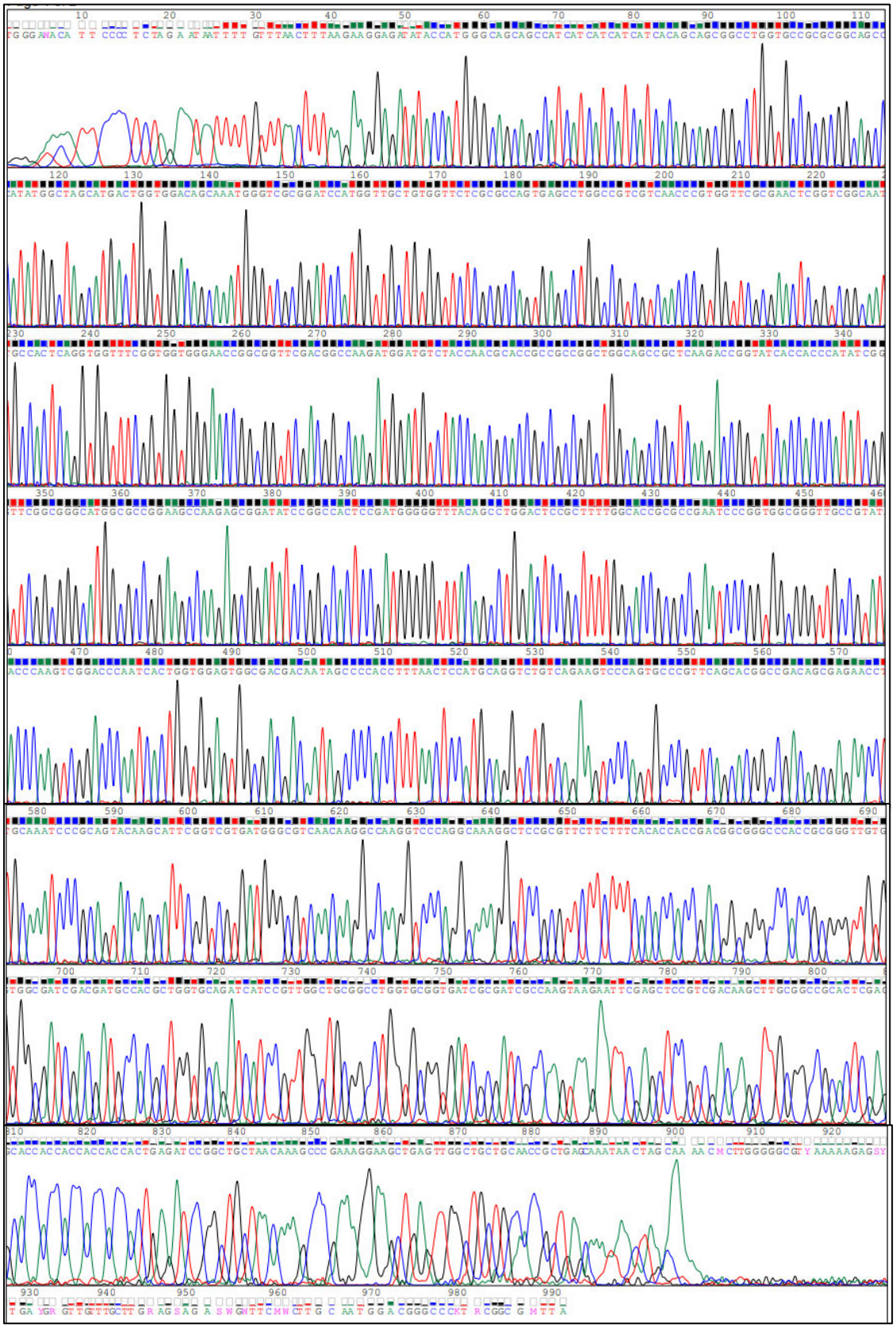

Figure A4: Snippet of chromatogram of pET T7 of pET28a-*Rv0309* clone using Chromas software.

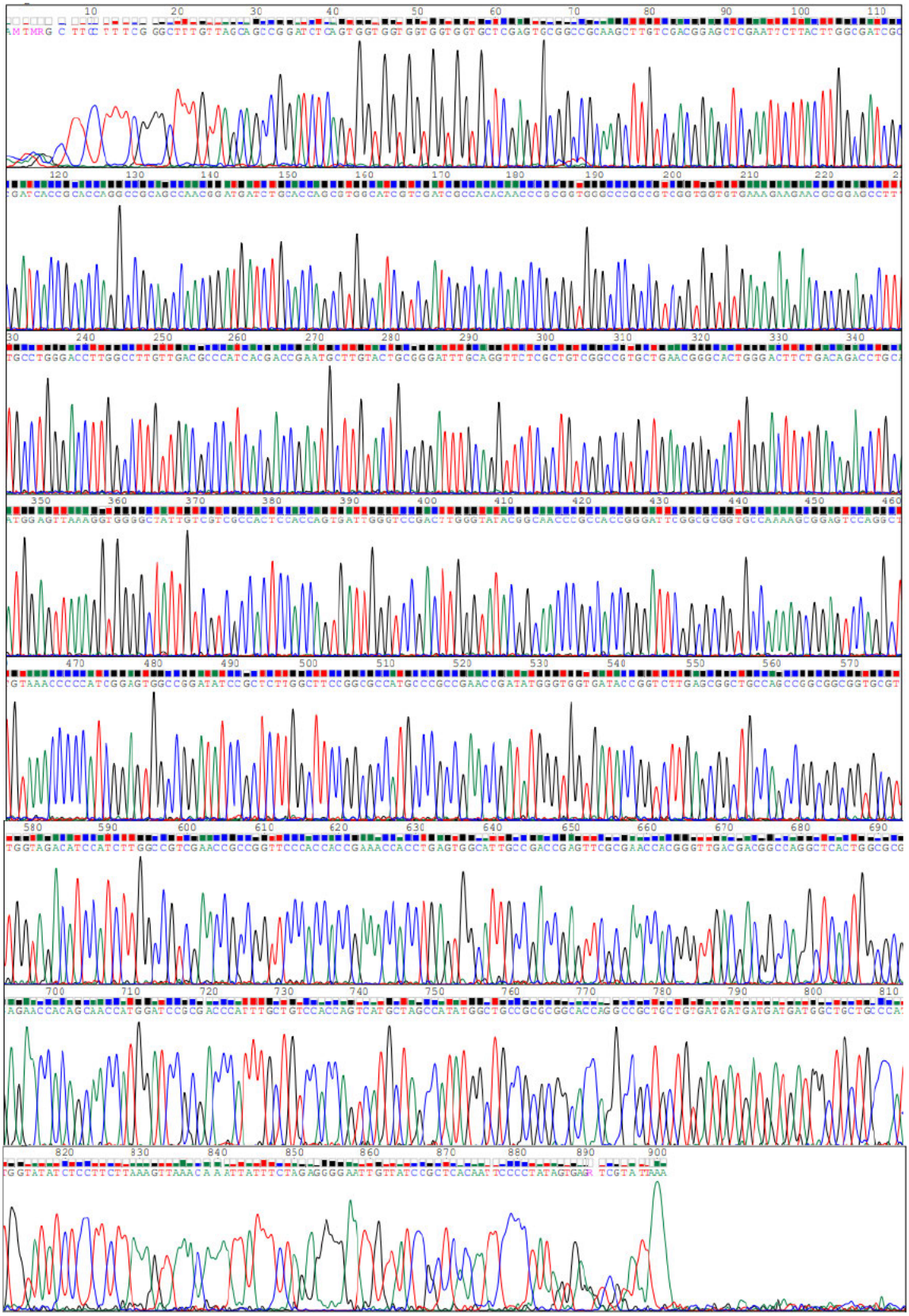

Figure A5: Snippet of chromatogram of pET Terminator of pET28a-*Rv0309* clone using Chromas software.

Figure A6: *Rv0309*-pET28a BioEdit Sequence Alignment

pETRv0309 refers to consensus sequence of pure pDNA sample submitted.

Mtb Rv0309 refers to expected sequence of Rv0309 based on Mycobrowser.

Rv0309 Amino Acid – S6 sequence

GSMVAVVLAPVSLAVVNPWFANSVGNATQVVSVVGTGGSTA
KMDVYQRTAAGWQPLKTGITTHIGSAGMAPEAKSGYPATPM
GVYSLDSAFGTAPNPGGGLPYTQVGPNHWWSGDDNSPTFN
SMQVCQKSQCPFSTADSENLQIPQYKHSVVMGVNKAKVPGK
GSAFFFHTTDGGPTAGCVAIDDATLVQIIRWLRPGAVIAIAK-
EF

Unused	Total	%Cov	%Cov(50)	%Cov(95)	Accession	Peptides(95%)
22,36	22,36	98,070002	98,0700016	98,0700016	Rv0309	22

Figure A7: Results obtained from Passively Eluting Proteins from Polyacrylamide gels as Intact species for Mass Spectrometry (PEPPI-MS) analysis at Council for Scientific and Industrial Research (CSIR).

APPENDIX E: SUMMARY OF LYSIS AND PURIFICATION TROUBLE-SHOOTING

Table A1: Summary of lysis and purification troubleshooting for GST and His-tagged proteins.

Lysis / Purification troubleshooting – GST tagged protein	Lysis / Purification troubleshooting – HIS tagged protein
➢ ↑ volume of protein pellet.	➢ Bacterial Protein Extraction Reagent (B-PER reagent) used as lysis buffer.
➢ Insoluble protein preparation : Phosphate-buffered saline (PBS) lysis buffer, freeze-thaw method, Triton X-100 addition, solubilisation buffer, dialysis.	➢ Sonicated using harsher condition.
➢ Volumes of lysis buffer, Triton X-100 and solubilisation buffer halved.	➢ Tris-NaCl, KCl, Glycerol, PMSF, Triton X-100 added to pellet and left overnight. Freeze-Thaw step included the next day.
➢ Tested different storage temperatures and temperatures during insoluble protein preparation.	➢ Lysozyme added to pellet and left overnight. Tris-NaCl, KCl, Glycerol, PMSF, Triton X-100 added the next day.
➢ Supernatant that was originally discarded in insoluble protein preparation was stored and concentrated using Amikon filters.	➢ Equilibrium/Wash buffer (containing sodium phosphate, sodium chloride and imidazole used as lysis buffer.
➢ Column binding time ↑ from 2, 4, and 6 hours to overnight.	➢ PBS, lysozyme, DTT, phenylmethylsulfonyl fluoride (PMSF), Sodium lauryl sulfate (SDS), Triton X-100 added to pellet as lysis buffer.
➢ Introduced sonication and optimized condition.	➢ Equilibrium/Wash buffer (containing sodium phosphate, sodium chloride and imidazole with an addition Guanidine hydrochloride to test under denaturing conditions.
➢ Tested whether both chemical and mechanical lysis is best for protein or if only one presents optimal results.	➢ Lysozyme added to pellet and left overnight. Tris, KCl, Glycerol, PMSF, Triton X-100 added the next day along with Guanidine hydrochloride.
➢ Purified vector on its own to see if column is functional.	➢ Attempted method based on previously published paper (Kumar et al., 2013)
➢ Adjusted pH of buffers based on pI of protein.	➢ Performed different purification methods : ÄKTA™ purification using Ni-Nta cartridge, ÄKTA™ purification using HisPur Cobalt cartridge, Ni-Nta beads, Ni-Nta agarose, Size Exclusion Chromatography, HisPur Cobalt agarose using gravity flow columns.
➢ Substituted Dithiothreitol (DTT) for β-mercaptoethanol.	➢ Performed purification process in 4°C walk-in fridge.
➢ Performed different purification methods : ÄKTA purification, Ion-Exchange Chromatography, Size-exclusion and gravity flow column.	➢ Peptide Mass Fingerprinting to sequence protein and determine mass.
➢ Included 3-((3-cholamidopropyl) dimethylammonio)-1-propanesulfonate (CHAPS) in lysis buffer and sarkosyl in elution buffer.	
➢ Used lysis buffer as wash buffer and added sarkosyl in elution buffer.	

APPENDIX F: TURNITIN REPORT

CLONING, EXPRESSION AND PURIFICATION OF MYCOBACTERIUM TUBERCULOSIS RV0309 ADHESIN PROTEIN.

ORIGINALITY REPORT

13%	5%	4%	12%
SIMILARITY INDEX	INTERNET SOURCES	PUBLICATIONS	STUDENT PAPERS

PRIMARY SOURCES

1	Submitted to University of KwaZulu-Natal Student Paper	10%
2	JOO Y. KIM. "Zinc finger-containing glycine-rich RNA-binding protein in *Oryza sativa* has an RNA chaperone activity under cold stress conditions", Plant Cell & Environment, 02/2010 Publication	1%
3	researchspace.ukzn.ac.za Internet Source	1%
4	apps.who.int Internet Source	1%
5	Submitted to Monash University Sunway Campus Malaysia Sdn Bhd Student Paper	1%
6	www.nature.com Internet Source	1%